Universität für Bodenkultur Wien

MINI COLUMN FUNCTION AND PREDICTION TO LARGE SCALE

Department für Biotechnologie

Institut für angewandte Mikrobiologie

Leiterin: Reingard Grabherr, Univ.Prof. Dipl.-Ing. Dr.nat.techn.

Betreuer: Alois Jungbauer, Univ.Prof. Dipl. -Ing. Dr.nat.techn.

Dissertation

zur Erlangung des Doktorgrades

an der Universität für Bodenkultur Wien

Eingereicht von

Susanne Schweiger, Dipl.-Ing. BSc

Wien, Februar 2018

Acknowledgements

First of all, I want to thank my supervisor and mentor Alois Jungbauer for his motivation, positive thinking no matter what and all his ideas, but also for giving me the freedom to pursue my own ideas, to learn how to work independently and to encouraging me to a stay abroad.

I am thankful to my acib project team, including Astrid Dürauer, Rupert Tscheließnig, Christian Jungreuthmayer, Dmytro Iurashev and Theresa Scharl-Hirsch for their input and support during my thesis.

I am grateful for Eva Berger´s help with the experimental work in the last months of my project. Without her additional hands and mind, I would not have accomplished as many results.

Next, I want to thank our company partner Atoll/Repligen in Weingarten, especially Tim Schröder for enabling this project, for believing in me, for the fast approvals and for the off-work talks about life.

I also want to thank Christine Gebski and Jamie Peyser from Repligen in the US for their support in enabling the experiments on the very large scale columns and Alan Chan for his help in enabling all my wishes regarding experimental design and his understanding for all the additional experiments I wanted to do.

Many thanks to the whole downstream processing group, especially the "5th floor gangstas" Mark Dürkop, Stephan Hinterberger, Alexander Matlschweiger, Patricia Pereira Aguilar and Tobias Schneider, for all their scientific input, the discussions and their mental support in difficult phases.

I want to thank my family for their supporting and encouraging me during my studies and my whole life.

Finally, I want to thank Gottfried Eilenberger for being there when I need him, for his understanding, for listening, for his chemical advice and for being just the way he his.

Zusammenfassung

Vorgepackte präparative Chromatographiesäulen werden immer häufiger in der Entwicklung und Herstellung Biopharmazeutika verwendet. Sie ermöglichen flexible Anpassungen an Marktanforderungen und Outsourcing von aufwändigen Packprozessen und Validierungen. Allerdings muss eine ausreichende Packungsqualität für den beabsichtigten Gebrauch und die Skalierbarkeit vom Labor- zum Produktionsmaßstab gezeigt werden, um die Vergleichbarkeit von Ergebnissen und einen nahtlosen Datentransfer gewährleisten zu können. In dieser Dissertation wurden gleiche Packungsqualitäten für vorgepackte Säulen über einen Zeitraum von 10 Jahren beobachtet. Die Variation in der Packung zwischen vorgepackten Chromatographiesäulen wurde als 10-15 % für das zweite zentrale Peak-Moment quantifiziert, was bestätigt, dass die Schwankung in der Packungsqualität ausreichend niedrig ist. Die Effizienz von vorgepackten Säulen war gleich oder besser als jene von selbst gepackten Säulen. Die Skalierbarkeit der Packungsqualität von vorgepackten Säulen, die mit unterschiedlichen Medien gepackt waren, wurde für nicht zurückgehaltene Azetonpulse nachgewiesen. Scale-up Vorhersagen sind mit Hilfe von empirischen Gleichungen möglich. Darüber hinaus wurde die Skalierbarkeit von vorgepackten Säulen für Proteintrennungen vom 1 mL Labor- zum 57 L Produktionsmaßstab bewiesen. Normalisierte Durchbruchskurven überlagerten sich gut und ergaben gleiche Gleichgewichts- und dynamische Bindungskapazitäten über alle Säulengrößen. Auch Stufengradienten für die Trennung von drei Modellproteinen konnten erfolgreich skaliert werden. Es konnte gezeigt werden, dass der Einfluss von Extra-Säulen Effekten, wie zum Beispiel des Mixers, für genaue Skalierungsvorhersagen berücksichtigt werden muss. Zusammenfassend sind vorgepackte Chromatographiesäulen aufgrund ihrer konsistenten Ergebnisse über die Zeit, verschiedene Medienarten und unterschiedliche Größenmaßstäbe geeignet, konventionelle selbst gepackte Säulen zu ersetzen.

Abstract

Pre-packed preparative chromatography columns are increasing in popularity for the development and manufacturing of biopharmaceuticals. They allow for flexible adaptations to market demands and outsourcing of the laborious packing and validation processes. Nonetheless, sufficient packing quality for the intended use and scalability from laboratory to process scale columns needs to be demonstrated in order to ensure comparable experimental output and easy transfer of data. In this doctoral thesis, equal packing qualities were observed for pre-packed columns over a time span of 10 years, convincingly demonstrating that reproducible packings can be achieved over long time periods. Packing quality mainly impacts the second central peak moment, which is a measure for peak width. The column-to-column variation was quantified as 10-15 % for the second peak moment confirming that the variation in packing quality is sufficiently low. The performance of pre-packed columns was compared to that of conventional self-packed columns and found to be equal or superior. Scalability of the packing quality of pre-packed columns packed with different media was shown for non-retained acetone pulses. Empirical equations allowing scale-up predictions were developed. Moreover, scalability of pre-packed columns was demonstrated for protein separations from 1 mL laboratory to 57 L production scale. Normalized breakthrough curves overlaid well and equal equilibrium and dynamic binding capacities were calculated for all scales. Step gradient protein separations of three model proteins were successfully scaled-up. All studies confirmed the importance of extra column effects, such as the influence of the mixer of the chromatography system for reliable scale up predictions. It can be concluded that pre-packed chromatography columns are suitable in replacing conventional self-packed columns due to their consistent performance over time, different media types and different scales.

Table of Contents

1 Introduction

1.1 New paradigms in biomanufacturing

1.1.1 Disposables

The biopharmaceutical industry is increasingly using disposables throughout the production process [1,2]. Their main advantages are flexibility, rapid change over times and elimination of cleaning validations. These attributes make disposables especially interesting for the production of toxic or pathogenic compounds as well as for the prevention of cross-contamination between different products produced in the same facility. Contract manufacturing organizations in particular prefer the use of disposables due to their flexibility and the ability to directly allocate the costs to a customer. Disposables facilitate the transition to scalable multi-product facilities for on-demand production of biopharmaceuticals. This can also be important for orphan drugs or in the emerging field of personalized medicine [3]. Major challenges for disposables, which still have to be overcome are the limited scale, the lack of standardization between disposable systems of different suppliers, the availability of suitable disposable sensors, the dependency on suppliers and the evaluation of leachables and extractables from the materials [4–8]. Leachables can significantly deteriorate proliferation of mammalian cell lines [9]. Before the sale of a pharmaceutical product the absence of leachables has to be proven. Leachables present in early stages of the process can be removed by subsequent purification steps [6]. However, for late stage process steps such as late chromatography steps including disposable columns this might not be possible.

The use of disposables in upstream processing is already common with one fully disposable upstream process licensed by Shire [10]. In downstream processing, disposables are less commonly used. The most frequently used disposables in downstream processing are filters and membrane chromatography columns [3–5]. Additionally, also single use tangential flow filtration systems like the Cadence or Allegro systems from Pall are available on the market [11]. However, the biopharmaceutical industry is increasingly focused on the development of fully disposable processes [12]. As a result, the sales of disposable packed bed chromatography columns is expected to rise in the future. With the ÄKTA Ready chromatography skid even a chromatography system with a fully disposable fluid path is on the market now [13].

1.1.2 Pre-packed chromatography columns

In recent years, pre-packed preparative chromatography columns have increased in popularity for process development but also for large scale production of biopharmaceuticals [14]. Numerous advantages have convinced users to change from the self-packed to the pre-packed column format. The major benefit is that the laborious and time intensive process of column packing can be outsourced to specialized companies [15]. Column packing is often considered an art rather than science since it is influenced by many variables, such as the packing method used [16,17], the properties of the chromatography medium [18–20], the column hardware [21–24], the packing solution [24] or the slurry concentration [18,24]. In addition, pre-packed columns are already pre-qualified by the suppliers and are expected to be of equal packing quality between different media and column sizes. This is for example essential in resin screening studies or for continuous chromatography. Packing and packing validation accounts for 5-10 % of all preparation work in downstream processing [8]. Pre-packed columns can be supplied with Good Manufacturing Practice (GMP) certification and can be produced in clean rooms if required. Pre-packed columns are available at different scales ranging from columns in the 96-well format which can be operated by pipetting robots up to production scale columns with up to 60 cm inner diameter (ID). Pre-packed columns fall under the wide term of disposables, since the column hardware is not intended to be re-packed with a different medium after usage [6]. Instead, the whole columns are discarded if they are not needed further. However, due to the high costs of the packed medium, packed columns are often used for several cycles with cleaning steps in between and are not discarded after one purification run [5,13]. This is done for columns used in the production of material for clinical trials of phases I and II. In larger scales, for example in clinical phase III or for manufacturing runs, sometimes even the whole pre-packed columns are discarded after one batch.

Pre-packed chromatography columns are available from many suppliers (e.g. GE Healthcare, Pall Life Sciences, Pierce, MilliporeSigma, BioRad, Life Technologies). The most popular supplier for pre-packed columns is GE Healthcare with a market share of 55 % in 2014 [25]. However, they only pack their own media. Repligen is the second largest supplier with a market share of 31 %. After their acquisition of Atoll GmbH in 2016, they now offer the widest range of columns with volumes from 50 µl up to 85 L, covering more than six orders or magnitude. In contrast to many other manufacturers, they also pack columns with media from other suppliers. Their column platform consists of RoboColumns, PipetColumns, CentriColumns, MiniChrom, ValiChrom and large scale OPUS columns. RoboColumns, PipetColumns and CentriColumns are available in a 96-well format. While RoboColumn are designed for usage with robotic liquid handling systems (pipetting robots), Pipet columns can

be used with positive liquid displacement pipets and CentriColumns are operated with a centrifuge. It is not possible to keep constant fluid flow in all of these three column types since they are only operated with a limited reservoir of fluid. Linear gradients can only be simulated by very small increments of step gradients. MiniChrom, ValiChrom and regular OPUS columns are designed for operation with regular chromatography workstations or skids which apply a constant flow to the column. MiniChrom columns are designed as disposable columns made of polypropylene and are available only at pre-defined column lengths. In contrast, the walls of ValiChrom columns are made of glass and the column bed height can be chosen freely by the customer. MiniChrom and ValiChrom columns are designed for process development and scale-down studies. OPUS columns are designed for manufacturing and are available at customer-defined lengths.

Pre-packed columns operable with pipetting robots are routinely used for high throughput screening. There are numerous studies available showing that their performance is comparable to that of small laboratory scale self- and pre-packed columns [26–29]. However, customers are reluctant to use pre-packed columns at scales larger than laboratory scale since there are no studies showing sufficient packing quality for their intended use or scalability between different column volumes.

1.2 Column qualification

In all scales, whether small scale or production scale, chromatography columns are tested before use to check their packing quality and to identify defects in order to ensure run reproducibility. The results of these qualifications are highly dependent on the experimental set-up and the method of peak analysis. Columns are typically qualified with pulses of small non-interacting solutes with a high diffusivity since their retention is not mediated by mass transfer and therefore the structure of the packed bed itself will have a higher influence on the peak profile than for retained solutes [30,31]. Consequently, small solutes enable the detection of flow non-uniformities due to improper packing. The testing solute [21] and the injected sample amount [32] have an impact on the shape of the resulting peak and therefore must be kept constant for comparative studies.

1.2.1 Quality parameters

Packing quality is evaluated in terms of peak retention, peak width and peak shape. These parameters are equivalent to the first, second and third statistical moment of a peak. Moments are often preferred since they do not assume symmetrical peak shape but describe the peak directly. The zero-th moment (M_0) is the area under the peak and is calculated by

$$M_0 = \int_0^\infty C(t)\, dt \tag{1}$$

where *C(t)* is the solute concentration as a function of time *t* at the column outlet.

The first moment (M_1) is an indicator for peak retention and is calculated by

$$M_1 = \frac{\int_0^\infty t * C(t)\, dt}{M_0} \tag{2}$$

The second central moment (M_2) is a measure for the variance (width) of a peak and the third central moment (M_3) describes the shape of a peak. They can be calculated by

$$M_n = \frac{\int_0^\infty (t - M_1)^n * C(t)\, dt}{M_0} \tag{3}$$

where *n* is the *n*th statistical moment. The degree of asymmetry can be described by the peak skewness, which was calculated by

$$Skew = \frac{M_3}{M_2{}^{3/2}} \tag{4}$$

The peak skewness is negative for fronting peaks, zero for symmetrical peaks, and positive for tailing peaks. Other typical column quality parameters are “height equivalent to a theoretical plate” HETP (*H*) and peak asymmetry (*As*) [30], which are calculated by

$$H = \frac{M_2 * L}{M_1^2} \tag{5}$$

where M_2 is the second statistical moment and *L* is the column length. The HETP of a column is also referred to as column efficiency. For comparison of columns packed with different media and tested at different velocities, the reduced HETP (*h*) is used, which is calculated by

$$h = \frac{H}{d_p} \tag{6}$$

where d_p is the particle diameter of the medium. The peak asymmetry describes the deviation of the peak shape from ideal symmetrical shape and is commonly calculated at 10 % peak height with

$$As = \frac{b}{a} \tag{7}$$

where *b* is the width from peak maximum to the rear part of the peak and *a* is the width from the front part of the peak to the peak maximum. It was suggested that the peak skewness is used instead of the asymmetry factor to describe peak shape [33].

Another quality parameter of the packing is its density. Packing density describes how tightly the beads are packed inside the column and is commonly described by the extra particle porosity (void fraction) ε. It is determined by injection of a large non-interacting molecule, which cannot penetrate the pores of the chromatography beads, such as blue dextran [34] or poly(vinyl pyrrolidone) [35]. It therefore elutes at the void volume of the column. The extra particle porosity is then calculated from the peak profile by

$$\varepsilon = \frac{V_R - V_{ex}}{V_C} \tag{8}$$

where V_R is the retention volume, V_{ex} is the extra column volume and V_C is the column volume. Alternatively, the extra particle porosity of the packed bed can be calculated for non-compressible rigid spherical beads from the pressure drop over the column (ΔP) using the Kozeny-Carman equation

$$\Delta P = 150 \frac{(1-\varepsilon)^2}{\varepsilon^3} \frac{\eta u L}{d_p^2} \tag{9}$$

where η is the mobile phase viscosity and u is the superficial velocity of the mobile phase. However, this is not the case for compressible beads, which are frequently used in preparative chromatography [36]. A model was developed to describe the pressure flow relationship, which assumes a linear relationship between bed compression and relative flow velocity [37]. According to this model there is a linear relationship between the pressure drop and the flow rate as long as the mobile phase velocity during operation of the column is smaller than the packing velocity u_0. If the mobile phase velocity exceeds the packing velocity, the bed will compress resulting in a non-linear relationship between the column pressure and the flow rate (Figure 1). Moreover, the initial bed height L_0 will decrease to the actual bed height L and consequently also the initial extra particle porosity ε_0 will decrease to a final extra particle porosity ε. The slope of the pressure flow curve becomes infinite at the critical velocity. Depending on the compressibility of the medium, the pressure flow curve may also change with the column diameter. The higher the column diameter, the more the pressure-flow curves shift to the left, which means the maximum flow velocity will be lower for columns with a larger diameter.

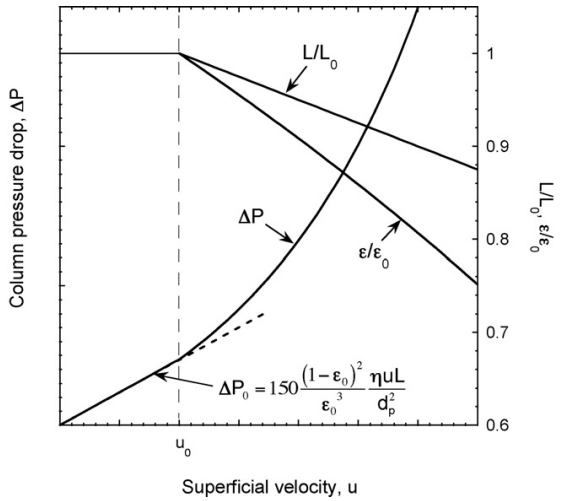

Figure 1 Change of the pressure drop, bed height and extra particle porosity with superficial velocity for compressible media [37].

Even if a stable bed has formed after packing, the extra particle porosity can vary up to 15 % depending on the packing parameters [38]. Despite packing density being a measure for the physical structure of the packed bed, there is no correlation between the packing density and the column performance [39].

1.2.2 Peak analysis

The peak moments, HETP and asymmetry are quality parameters which are obtained from the detector response over a time, the so called chromatographic peak. However, peak analysis is blurred by noise and baseline drift [40–44]. An increase in random noise leads to an increase in the calculated moments, which is particularly pronounced for higher moments and tailing peaks [45].The method for determination of the peak start and end point is crucial since it adds additional variation to the results, especially when peaks are detected automatically [46]. The higher the threshold level (the percentage of the peak height at which peak analysis start and ends) the lower the resulting moments. This effect gets also increases for higher moments and tailing peaks [45]. Recently, it has been shown, that proper baseline correction and setting of the integration intervals allows the determination of higher moments with a good accuracy [47]. Depending on the peak analysis method, the relative standard deviation of the first moment is approximately 0.07 %, while it is in a range of 3.7-15 % for the second moment and 15-73 % for the third moment [48].

The two most commonly used peak analysis methods are direct numerical integration and peak fitting to a predefined function (Figure 2). The exponentially modified Gaussian (EMG) distribution [49,50] is the most popular function for peak fitting and provides robust results [51], especially for peaks with high experimental noise. The EMG was derived by convolution of a Gaussian peak with an exponential decay function. However, there is no physical reason, why

a peak should follow the shape of an EMG [52]. It fails to fit severe cases of tailing or fronting [52]. The peak parameters determined by EMG fitting can only be as good as the fit and hence do not reflect the real peak properties when the fit is bad. Peak fitting is necessary for overlapping peaks in order to be able to deconvolute them to the individual peaks [53]. Alternatives to the EMG function have been developed, which may fit the peak better than the EMG, but are still empirical [53]. In comparison, direct numerical integration provides the most exact results [51], presuming the baseline drift is moderate and the data are smooth and without any noise.

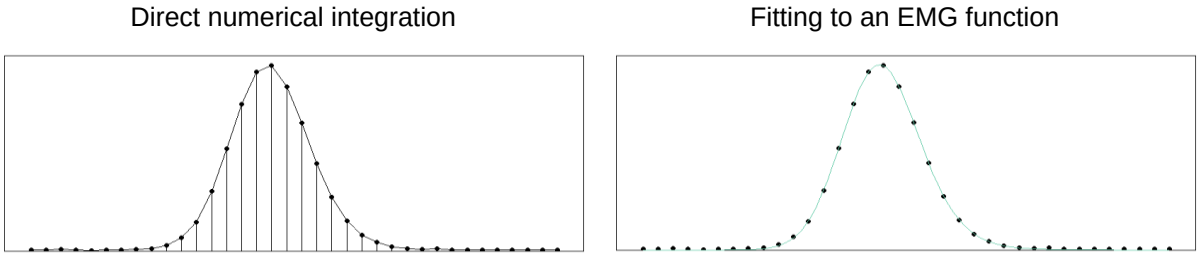

Figure 2 Schematic representation of the difference between direct numerical integration of a peak and fitting it to an EMG function.

1.3 Contributions to band broadening

1.3.1 Band broadening in the chromatography column

Ideally, solutes are introduced as finite bands onto chromatography columns and as they move along the column, the bands will broaden due to three main effects: flow path inequalities, molecular diffusion and resistance to mass transfer [54]. Many equations have been proposed to describe these effects mathematically, the most popular of which is the van Deemter equation [55]. It describes chromatographic band broadening as a sum of three variances, the A, B and C terms. All terms are additive but have different dependencies on the mobile phase velocity.

$$H = A + \frac{B}{u} + Cu \tag{10}$$

For a more general description, H is replaced by h and u by the reduced velocity v', which is calculated by

$$v' = \frac{v * d_p}{D_0} \tag{11}$$

where v is the interstitial velocity obtained from $v = u/\varepsilon$ and D_0 the solute molecular diffusivity. The resulting equation is called Generalized van Deemter equation (Figure 3).

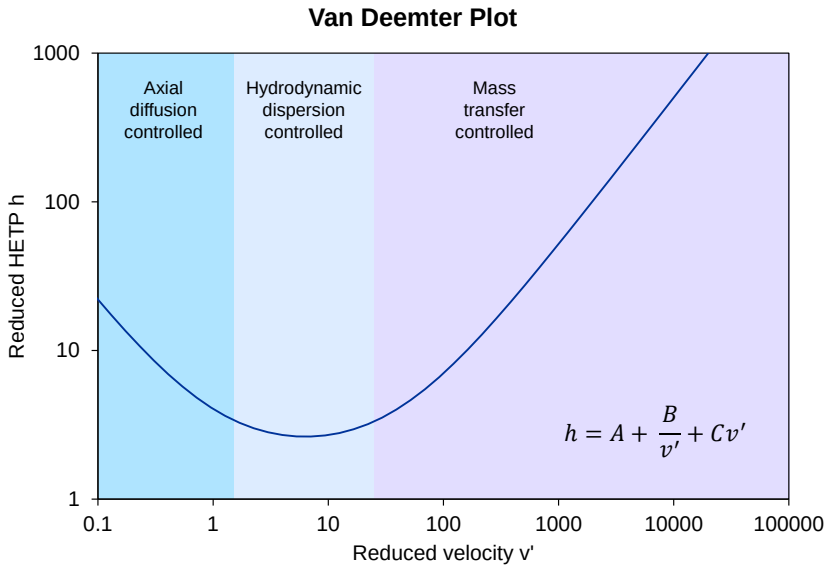

Figure 3 Generalized van Deemter plot with different regions indicating the dominant contributions to band broadening.

The A term describes band broadening due to unequal flow paths in the packed bed [56] and depends on the packing quality of the column [39]. It is also sometimes referred to as Eddy diffusion. The better the column packing, the lower the A value [57]. Eddy diffusion is caused by the availability of multiple stream paths outside of the beads, which a solute can move along. Despite, being initially assumed to be independent from flow velocity, it was later shown to depend on velocity [58]. Giddings described different forms of velocity unevenness [59,60], which were recently reviewed by Gritti and Guiochon [52]. These velocity dependencies are trans-channel velocity bias, short-range inter-channel velocity bias and trans-column velocity bias. Trans-channel velocity bias occur between adjacent beads resulting from the fact that the flow velocity is zero at the surface of the beads and twice the order of the average velocity in the center of the inter-particle space. Short-range inter-channel velocity bias occur over a distance of several particle diameters and result from local velocity variations due to random packing and size distributions of the packing. Trans-channel velocity bias range over the whole column radius and occur due to radially inhomogeneous packings. All three velocity bias increase with the flow velocity but to differing degrees. The B term represents dispersion due to axial diffusion. Diffusion is dominant when the time for a solute to travel a certain distance by pure convection is longer than by diffusing along the same distance. The C term originates from mass transfer resistances between phases or zones. Mass transfer is the time needed for equilibration between the mobile and the stationary phase. It includes diffusion of the analyte through the external film around the beads and through the porous network inside the beads, surface diffusion and adsorption-desorption kinetics [54]. Mass transfer in preparative chromatography is mainly limited by diffusion inside the beads, which depends on the solute

diffusivity and size, bead diameter, pore diameter, interconnection of the pores and pore tortuosity [54].

The validity of the van Deemter equation was questioned by many scientists later, leading to the development of further equations such as the Giddings equation, the Horvarth and Lin equation or the Knox equation. A recent study showed that all the equations fit experimental data well and no equation outperformed the others [61].

Considering evaluation of the suitability of pre-packed columns for process development and manufacturing, some of the above described effects are more important. Axial diffusion depends on the solute, the mobile phase composition and the mobile phase velocity and hardly contributes to band broadening in preparative liquid chromatography. Mass transfer occurs at the bead level and mainly depends on the solute diffusivity, the internal bead and pore structure, bead diameter, adsorption and mobile phase velocity. Since the solutes and the beads are the same for pre-packed and conventional self-packed columns at different scales, this effect is also of minor importance for demonstrating the suitability of pre-packed columns. The most important parameter is the three dimensional arrangement of the beads inside the column, which can differ between pre-packed and self-packed columns. Different bead arrangements and packing densities lead to different flow profiles, which influence Eddy diffusion. Consequently, the three dimensional structure of the packed bed needs to be evaluated in detail when different column types and scales shall be compared.

1.3.2 3D structure of the packed bed

The more homogeneously the beads are distributed in the column, the better its performance [62]. Bed heterogeneity is determined by the packing process and is assumed to be stable after packing as long as the operating mobile phase velocity is smaller than the packing velocity. Bed heterogeneity depends on several factors such as the properties of the beads (charge, roughness, diameter, size distribution, compressibility [18–20]), the packing method [16], the column hardware such as the column wall, the filter or frit [21–24] [22,23], the column dimensions [63,64], the packing solution [24,37], the slurry concentration [18,24] and the packing operator [65]. Sometimes vibration during the packing process can help to attain a homogeneous particle arrangement [66,67]. In order to get a better insight into the forces during packing, packing processes were simulated and their effect on the final 3D structure were evaluated [68,69]. Several studies on the homogeneity of packed columns were conducted with high performance liquid chromatography (HPLC) columns. Despite the packing structure in preparative chromatography columns potentially being different, certain findings are likely to be valid for preparative columns as well. The packed bed is heterogeneous in the axial and the radial direction [64,66,70]. It is generally agreed that the

inlet section of the column has the most packing non-uniformities [64,71]. Studies with columns made of stainless steel tubings which were sectioned to 5 cm pieces after packing showed that the axial variation of the column performance depends on the total bed height and is mostly better in the region of the column furthest from the inlet [64]. Besides, the packing density increases from the column inlet to the outlet. However, packing density does not necessarily correlate with good performance. It is rather suggested that the column efficiency is mainly influenced by the radial fluctuation of the packing density [63]. The column wall has a large influence on the packing density. The mobile phase velocity can be 2-8 % higher in the center of the columns [16,72,73] and nearly two times higher next to the wall [62]. The presence of two different wall effects has been demonstrated explaining these velocity differences: the geometrical wall effect and the frictional wall effect [74,75]. According to the geometrical wall effect [18], the void fraction of the packed bed increases extensively towards the wall. Since the beads cannot penetrate the wall and commonly have a round shape, the void fraction tends to 1 towards the wall. Within one particle radius, the void fraction decreases to a minimum value before it reaches a maximum at a distance of one particle diameter. The amplitude of this fluctuation continuously decreases until the void fraction reaches an average value after a few particle diameters. The frictional wall effect is caused by the friction between the bed and the column wall [16] leading to a higher packing density within approximately 30 particle diameters from the wall [66]. The thickness of the frictional wall effect depends on the column diameter [73] and also on factors like the bed porosity, particle size distribution, surface roughness of the particles or the packing method [62]. The frictional wall effect is the main source of radial packing heterogeneity [74]. Both wall effects are particularly pronounced in columns with very thin diameters [76]. Moreover, the velocity distribution and consequently also the three dimensional structure of the beads are typically not symmetrical [72]. Apart from radial bed heterogeneity, also defects in the three dimensional structure of the beds deteriorate the column performance. The presence of small void areas in columns has been demonstrated [18,75]. The presence of more than 1 % of interparticle voids largely contributes to an efficiency loss [77].Long length-scale packing defects result in multipath flow leading to column fronting [77].

1.3.3 Extra column effects

A peak will not only broaden in the chromatography column, but also in the workstation (Figure 4) [78].

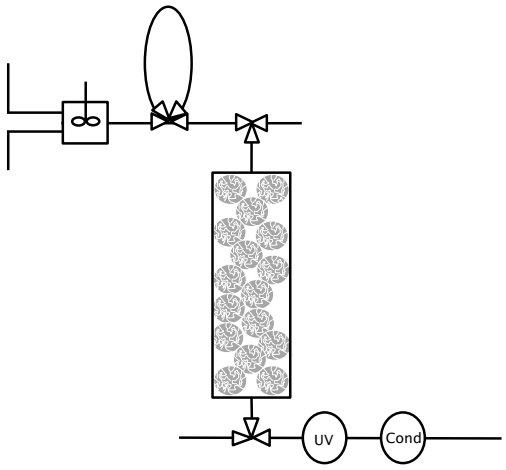

Figure 4 Schematic drawing of a chromatography column and a workstation including a mixer, an injection loop, valves for switching the column position and detectors.

The additional volume inside of the workstation will also add an additional delay to the peak retention. For an HPLC workstation with a column volume 30 times larger than the extra column volume, 60-80 % of the total band broadening of a non-retained compound occurred due to axial dispersion in the extra column volume [79]. A different study confirmed that the extra column band broadening contributes to 60 % of the total band broadening of unretained solutes [61]. Optimizing the flow path in an HPLC system allowed decreasing the peak variance by 40 % [51].

The magnitude of the extra column effects depends on the chromatographic workstation, the injection volume and system, the superficial velocity and the diffusion coefficient of the solute [51,80–82]. The column dimensions are also of importance, since the contribution of extra column band broadening to total band broadening will be less pronounced in columns with a wide diameter [51]. The less retained a compound is, the higher the influence of the extra column effects [61,79]. More retained compounds give wider peaks and therefore the extra column contribution has a smaller effect on peak width [80].

For unretained peaks, the retention volume measured at the detector will be the sum of the extra column volume and the fluid volume inside the column accessible for a solute, which can be calculated from the total porosity and the column volume, assuming that the solute has access to all pores

$$V_R = V_{ex} + \varepsilon_T * V_C \tag{12}$$

where ε_T is the total porosity. For linear chromatography, the total peak width measured at the detector is the sum of the intra and the extra column band broadening

$$\sigma_{tot}^2 = \sigma_{col}^2 + \sigma_{ex}^2 \tag{13}$$

where σ^2_{tot} is the total band broadening, σ^2_{col} the intra column band broadening and σ^2_{ex} the extra column band broadening. The extra column band broadening is the sum of the contributions of the individual parts of the workstation in linear chromatography, for example mixer, valves, injection system, heat exchanger, tubing or detectors. The influence of various parts of chromatography systems has been analyzed extensively [33,83–87]. However, peak variances are non-additive for preparative chromatography, when the sample load becomes significant compared to the column capacity [88]. The reason is that the effect of each plate on the peak profile depends on the solute concentration in that plate. Extra column contributions can be obtained by peak deconvolution, which allows extraction of the influence of extra column volumes on peak shapes [89,90]. The contribution of the injection to extra column band broadening can be calculated with the following equation assuming that the sample is distributed uniformly in the injection valve

$$\sigma_{inj}^2 = \frac{V_{inj}^2}{12} \tag{14}$$

where σ^2_{inj} is the band broadening introduced by the injection and V_{inj} is the injection volume. This equation assumes ideal rectangular shape of the injection. Lower divisors than 12 may occur due to unideal effects during injection and can be experimentally determined [91]. Recently, it was shown that σ^2_{inj} also depends on the mobile phase velocity [80]. The filter and frit as well as the volume inside the bottom and the top adapters of a column also contribute to extra column volume and band broadening and need to be considered. The importance of homogeneous flow distribution in the frit was shown by Shalliker et al. [92].

Each system component either adds an exponential or a Gaussian function to the band broadening [78,93]. Dead volumes create a type of wash out kinetics resulting in an exponential contribution to band broadening. Also finite detector volumes introduce additional symmetrical rectangular band broadening. According to Taylor [94], tubes introduce a symmetrical Gaussian-type broadening. However, the Taylor-Aris equation does not apply for most chromatography systems due to the rather short tubing lengths between the different system components. Other equations to calculate band broadening in tubings were proposed instead [95,96].

Besides, the location of a system component, before or after the column, needs to be considered for calculation of the effect of that component on the resulting peak profile for preparative chromatography [97,98]. A component introducing a Gaussian contribution that is

placed upstream of a column operated in preparative mode mainly retards the elution but hardly affects peak shape. In comparison, in linear chromatography, it would lead to additional peak broadening. If the same component was placed downstream of a column, it would broaden the chromatographic peak by smearing the sharp front by exactly the downstream spreading function of variance. The descending part and the first moment of the peak remain mostly unchanged. The upstream effect of an exponential decay function added to the peak profile is the same as for a Gaussian function. But if it is placed downstream of a column, the peak will be retarded and broadened [88].

Extra column band broadening hardly affects the determination of the mass transfer parameters, but mainly shifts the HETP curve vertically. Consequently, the extra column volume can be considered an additional constant added to the eddy diffusion term in the van Deemter equation [79].

The extra column effects, including extra column volume and extra column band broadening, can be determined by different methods:

- Theoretical calculation from the sum of the individual geometric volumes
- Pulses through a zero-dead volume (ZDV) connector
- Pulses through a zero length column
- Extrapolation from columns of different lengths
- Extrapolation from solutes with different retention factors

For theoretical calculation, the inner volumes of the individual geometric parts are summed up to give the extra column volume. The theoretical calculation of the sum of all geometrical contributions of the system parts was shown to yield systematically 30 % smaller elution volumes compared to the measured elution volumes [83].

Alternatively, a ZDV connector can be inserted into the flow path instead of the column. Pulses through a ZDV connector are the most common method to determine the extra column volume due to its fast and easy experimental design and analysis. This method is only accurate if a radial mixer unit is added to the system instead of the column, so pre- and post-column tubings are separated [89]. This ensures that band broadening in these two parts are independent of each other. If this is not done, the column-only dispersion is over-corrected. Another main drawback of this method is that the volumes inside the top and bottom adapters of the column as well as the frit and filters are not considered.

This issue can be overcome by using a zero length column instead of the column. A zero length column is a column, where the top and the bottom adapters are directly fixed on top of each other, which no beads in between. Eventually also the filters and the frits can be inserted. Despite the extra column volume determined by a zero length column is higher than measured

by a ZDV connector, the extra column band broadening is nearly the same [99]. System peaks with a ZDV or a zero length column instead of a column may give unreliable results due to lower back pressure in the pre-column volumes leading to variations in pre-column dispersion [100,101]. The variance of a peak increases linearly with the pressure in the tubing volume by about 7 % for each 100 bar pressure increase [102]. This can result in a large difference especially for HPLC columns and system variances, but will only have a minor impact on extra column band broadening for preparative systems. Peaks only going through the extra column volume are usually tailing a lot since there is only little time available for radial diffusion [79].

The extra column volume can be calculated by extrapolation from columns of different lengths [97]. These columns need to have the same diameters, frits and top and bottom adapters. Using this method, the retention volume is plotted versus the column length, which are linearly related. Extrapolation to zero column length gives the extra column volume. This method can similarly applied to calculate the extra column band broadening by plotting the total band broadening over the retention volume, which again gives a linear relation. By finding the corresponding ordinate for $V_R = V_{ex}$, the extra column band broadening can be obtained. The different pre-column pressures in columns of different length may also be a problem for the extrapolation method from columns of different lengths especially at high pressures [102]. Furthermore, the length extrapolation method requires many columns with the same top and bottom adapters and of the same packing quality [103].

Alternatively, the extra column band broadening can be determined only from one column by extrapolation from differently retained solutes [103,104]. Assuming that $V_{ex} << V_0$, HETP is related to the column dimensions, extra column band broadening and the retention factor [100]

$$H\,(k') = H_{col} + L\frac{\sigma_{col}^2}{V_0^2}\frac{1}{(1+k`)^2} \qquad (15)$$

where H_{col} is the intrinsic HETP of the column, k' is the retention factor and V_0 is the column void volume. The void volume can be obtained by multiplication of the column volume and the total porosity of the column. Consequently, a plot of H against $(1+k')^{-2}$ allows determination of intra column band broadening from the slope of a linear regression line. The extrapolation method from differently retained solutes requires method development for every different resin type, because compounds of the same diffusion coefficient but with different retention are required [100]. Besides, only the extra column band broadening can be determined independently, not the extra column volume. The advantage of the two extrapolation methods is that also the effects of the filter and the frit and the top and bottom adapters can be evaluated.

1.4 Scale-up

As mentioned already, the peak dispersion in protein chromatography is mainly influenced by the A and the C term of the Van Deemter equation. The chromatography beads are typically same on all scales leading to the assumption that the mass transfer limitations will also be the equal over all scales. The term, which is assumed to be affected most by changes in scale is the A term, which is influenced by the packing structure and density of different column sizes. But apart from the hydrodynamic dispersion inside the packed bed, additional factors can influence the outcome of a chromatography run at a different scale, for example the measurement accuracy of the workstation, the exact buffer conductivities and pH or the extra column effects [97,105,106].

The resolution and the binding capacity of a chromatography step can be kept constant at various scales by keeping the number of plates in the column constant. For protein chromatography, where HETP is mainly dominated by mass transfer, scaling at constant resolution or binding capacity requires [54]

$$\frac{D_0 L}{d_p^2 u} = constant \tag{16}$$

In the traditional scale-up approach, column bed height, superficial velocity and sample to column volume ratio are kept constant and the column volume is increased by increasing its diameter [106–108]. This scale-up approach requires bed heights in process development, which are as high as in the production, which in turn leads to high demands of buffers, samples and long run times already in the process development scale. Besides, it is hard to pack columns of very thin diameters at long bed heights. An alternative scaling approach utilizes constant height-to-diameter ratios [109]. Meanwhile it is state of the art to scale mass transfer limited chromatography by constant residence time [110]. The advantage of scaling with constant residence time is that even shorter columns can be used for scale-up studies. The effect of either increasing column diameter of bed height was investigated [111]. Hutchinson et al. used changes in transition curves to determine corrective factors for differences in dispersion and retention for prediction of scale-up [110].

For linear gradient elutions, chromatography columns are typically scaled by maintaining a constant normalized gradient slope [54]. A more advanced scaling approach developed for linear gradient elution predicts optimal gradient slope, flow velocity and column length for a desired resolution [112]. Scalability of this approach was demonstrated from 5 mL to 2.5 L columns by similar elution curves, retention times, recoveries and purities. Furthermore, the mobile phase velocity of manufacturing scale columns can be limited by bed stability [106] and consequently lower flow rates might be necessary for large scale runs. Calculations allow *a*

priori prediction of the bed stability [113] and problems in bed stability can sometimes be solved by changing the packing method [106].

Another common problem during scaling of preparative columns is the pressure drop over the column. The pressure is hardly ever a problem during laboratory scale runs since the equipment can maintain fairly high pressures. However, the maximum pressure during production scale runs is often limited to a few bars. Columns packed with rigid media can be scaled [54] by maintaining

$$\frac{\eta u L}{d_p^2} = constant \tag{17}$$

Models have been developed for compressible media, which optimize operating conditions at different scales to maximize the productivity while taking into account the maximum allowable pressure constraint [37,114].

In early phases of process development, batch binding studies or very small columns in the 96-well format are commonly used [115]. Their advantages are low requirements of buffers and samples, fast processing times and parallelization. Several studies showed that columns operated by robotic liquid handling systems can be used for prediction of modelling parameters or for directly predicting performance of small laboratory scale columns operated on a regular chromatography workstation [26–29]. The scale-up of data generated with columns operated with a manual pipet to 1 mL columns has also been shown [116].

Only a limited number of studies regarding scale-up up to production scale are available [108,117], since pharmaceutical companies tend to keep their production processes secret. These studies demonstrate the scale-up of self-packed columns of different sizes. Despite the usefulness of these studies, scalability studies on commercially available pre-packed columns would be interesting for industry, especially considering that every self-packed column is different but pre-packed columns would also be available for other users.

2 Objectives

The objective of the thesis was to get a deeper understanding of the packing quality of small pre-packed columns and of the scale-up of pre-packed columns. Process development with small pre-packed chromatography columns is already state of the art in modern bioseparation engineering. Understanding of the influencing parameters for packing quality and performance is crucial for the prediction to large scale, interpretation of results, trouble shooting of process deviations using scale down models and additional extraction of information from small scale runs. Despite their frequent usage, it has not been demonstrated that pre-packed columns are reproducibly packed at different column dimensions and with various media over time. The main focus is on evaluating the suitability of commercially available pre-packed columns for preparative protein separations at different scales.

In particular, the following objectives were determined:

- Evaluation of packing quality of pre-packed chromatographic columns over a time span of serval years
- Quantification of the column-to-column packing variation
- Comparison of the performance of pre-packed and self-packed columns and of different types of pre-packed columns
- Development of computational fluid dynamics simulation to support scaling relationships
- Development of engineering relationships for scale-up of chromatography columns
- Development of suited methods for demonstrating scalability of pre-packed columns
- Demonstration of scalability of pre-packed columns

3 Summary of the work and conclusions

The work has been published in four manuscripts. The first manuscript describes the reproducibility of the packing over longer time periods and the second manuscript covers the column-to-column packing variation and its reasons and compares pre-packed to self-packed columns. The third and the fourth manuscript describe scaling relationships of either acetone peaks or of protein separations respectively.

To test if pre-packed columns can be reproducibly packed over longer time periods, column qualification data from nearly 25,000 columns, packed with different media over a time span of 10 years, was analyzed. The packing quality, assessed in terms of reduced HETP and asymmetry, was stable over time confirming that columns can be consistently produced over a long time period (Figure 5). Moreover, correlations between medium properties and packing quality could be derived. Firstly, the lower the particle size, the higher the reduced HETP, which suggests that the difficulty of packing chromatography media increases with decreasing size. Secondly, the packing quality depends on the functional mode of the medium and its scaffold. These two parameters have a huge influence on the three dimensional structure of the packed bed since they determine the charge, the density, the compressibility and the surface roughness of the particles during packing. Additional correlations could be made regarding column dimensions. Shorter columns had a better packing quality indicated by smaller *h* values, which means that long columns are more difficult to pack than short ones. Peak tailing increased with decreasing column volume, which was attributed to increasing influence of extra column effects at a smaller scale. The conclusion from this study was that pre-packed columns can be consistently produced with a reproducible packing quality over one decade and that the columns were well packed.

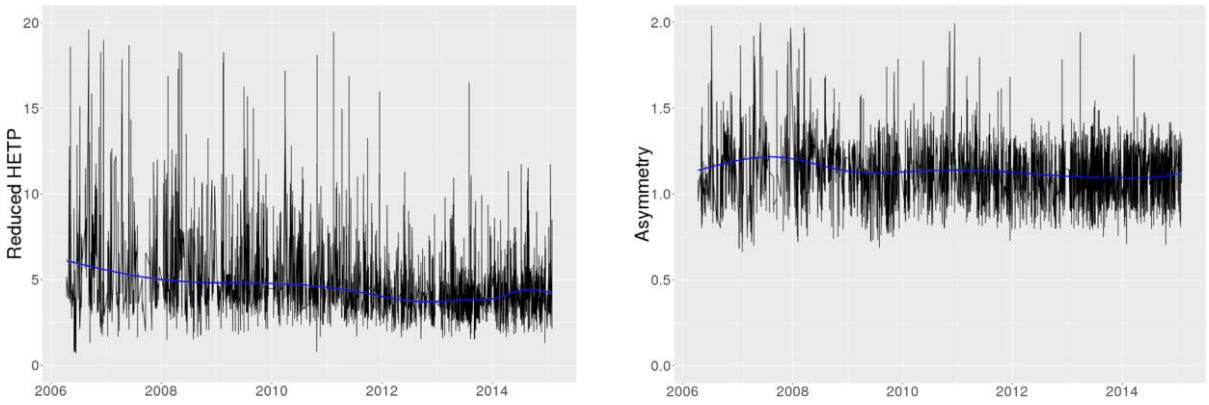

Figure 5 Trend analysis of reduced HETP and asymmetry of pre-packed columns over a time span of 10 years [Publication I].

Next, the packing quality of numerous small pre-packed columns was analyzed more deeply not only evaluating reduced HETP and asymmetry but also peak retention, peak width and peak skew. The evaluated columns were packed with 4 different media. Various column dimensions were evaluated for each medium representing the whole range of available MiniChrom columns. The resulting wide range of column efficiencies is a more representative sample for various available columns. The focus of this work was to determine the column-to-column packing variation between equally packed columns. Columns are assumed to be equally packed, when they are packed with the same medium and have the same dimensions. However, not only the different packing between columns introduces variation to the results but also the measurement precision of the workstation. Consequently, the effects of the measurement precision and the packing variation need to be separated (Figure 6). The measurement precision was derived from the individual triplicate measurements of each column. For calculation of the packing variation, one mean value was calculated from the triplicates for each column and the variation of the means of the different columns was quantified. The variations were evaluated in terms of standard deviation to the mean.

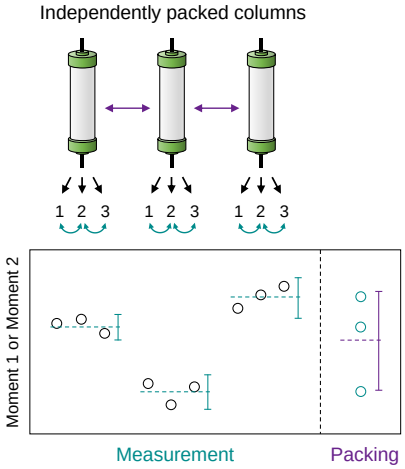

Figure 6 Schematic representation of the calculation of the measurement precision of the workstation (blue) and of the column-to-column packing variation (violet) from either the first or the second peak moment of 3 independently but equally packed columns [Publication II].

The measurement precision of the used ÄKTA pure workstation was quantified as smaller than ± 0.01 mL for the first moment and smaller than ± 0.007 mL² for the second moment for 95 % of the data points. While the measurement precision can be neglected for columns with large volumes, it definitely needs to be considered for small columns since the variation will be high compared to the performances of the packed beds. ANOVA was used to determine whether the column-to-column packing variation is a significant effect compared to the measurement precision. The variation introduced by the packing was significant for 59 of the 70 evaluated columns. The non-significant influence of the other columns was interpreted as

similar packing between the three columns or as inability to quantify the column-to-column packing variation on top of the measurement precision.

The standard deviation of the column-to-column packing variation was related to the size of its mean, so the variation of the first and the second moments was analyzed as relative standard deviation (RSD). The RSD of the first moment originating from column-to-column packing variations was smaller than 1 % of the mean for columns larger than 1 mL (Figure 7A). This small variation indicates that the column-to-column packing variation hardly influences the first moment. Moreover, the RSD of the first moment decreases with increasing mean, which indicates that columns larger than those evaluated are likely to have a smaller variation than 1 %. The RSD of the second moment is constant with respect to the mean second moment and was in a range of 10-15 % for the majority of the analyzed columns (Figure 7B). Very small columns showed very high (20-30 %) packing variation, probably because very thin columns are hard to pack. The second moment is mainly influenced by column-to-column packing variations.

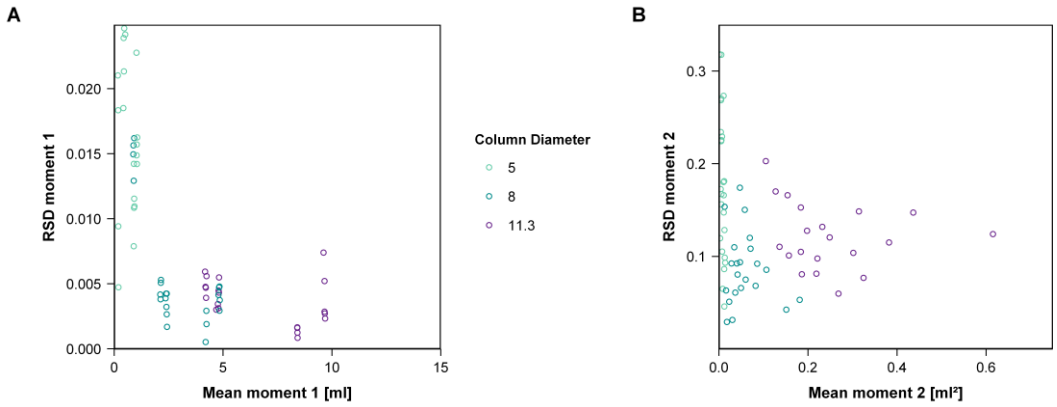

Figure 7 Influence of column-to-column packing variation on the first (A) and second (B) peak moments. The variation was analyzed as relative standard deviation (RSD) from the mean [Publication II].

The variation of HETP resulting from the variations in the first and second moment was quantified as 15 % for the pre-packed columns. This is comparable to the column efficiencies determined for semi-preparative (13.6 %) and preparative (30 %) HPLC columns [39]. Different studies determined the column-to-column variation in efficiency to be of less than 5 % for preparative HPLC columns [118] and 6.5 % for preparative LC columns using a commercially available packing system [65]. Despite the variation of the evaluated pre-packed columns is higher than these values, it is expected to be reasonably small considering that only the measurement precision alone leads to a variation of the second moment of 7.5 % for columns larger than 2 mL or even up to 25 % for columns smaller than 2 mL. Higher standards with respect to column-to-column packing variation would mean that many columns would have to be discarded, which would increase the cost of pre-packed columns immensely. It is

concluded that small pre-packed columns can be considered to be packed in the expected range.

During this study, the reasons for and implications from the column-to-column packing variations were also investigated. The column-to-column packing variation is not caused by fluctuations in the packing density but it is rather attributed to the heterogeneity in the particle structure in the column. No correlation was found between the magnitude of column-to-column packing variation and the column efficiency. Even columns with high variations in their packing can be well packed.

Additional observations could be made in the course of this study. The reduced HETP h slightly increases with the column aspect ratio L/d_c, where d_c is the diameter of the column. This means that columns with high bed heights compared to their diameter are more difficult to pack. No correlation was found between h and the bed aspect ratio d_c/d_p. Peaks were more symmetrical for columns with a large volume and displayed more tailing behavior for small columns. This was attributed to dominating extra column effects for small columns. Moreover, the reduced velocity chosen for testing the columns has a huge impact on the peak shape. The lower the reduced velocity, the more tailing occurs.

Since the peak analysis method also influences the calculated moments, two commonly used peak analysis methods were compared. Peak moments were calculated by direct numerical integration and by fitting the peaks to an EMG function. There was hardly any difference in the calculated first moments with the relative difference of the EMG fit with respect to numerical integration quantified as ± 0.9 % for 95 % of the data points. A larger variation was observed for the second moment, which varied between -36.5 % and +25.2 % for 95 % of the data points. The largest difference was observed for the peak skewness. It was already observed by Morton and Young that the error between different peak analysis methods gets larger, the higher the peak moment is [45]. As expected from the definition of the EMG function, EMG fits failed to describe fronting behavior of the peaks. This confirmed direct numerical integration as being the superior method for analyzing the peaks obtained from the pulse response experiments since it is capable to describe fronting and non-exponentially tailing peaks.

Column efficiency was compared between disposable (MiniChrom) and non-disposable (ValiChrom) pre-packed columns packed with two different media. Pre-packed non-disposable columns were found to be equally or better packed than disposable ones (Figure 8A). A comparison between pre-packed and self-packed columns should reveal whether pre-packed columns are suitable in replacing self-packed columns in terms of packing quality. The packing strategy of the self-packed columns was optimized, so the self-packed columns can be considered well packed. The packing quality of pre-packed disposable columns was found to

be better or equal compared to self-packed columns (Figure 8B). Consequently, there is no reason why pre-packed columns could not be used to replace self-packed columns.

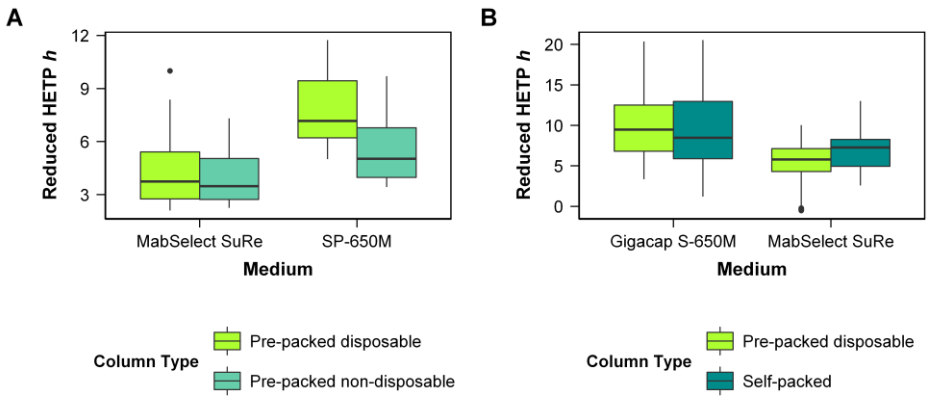

Figure 8 Comparison of the column efficiency between pre-packed disposable and non-disposable (A) and pre-packed disposable and self-packed (B) columns [Publication II].

As next step, column scalability was demonstrated for columns packed with different media at different velocities. The main focus of this work was to demonstrate the scalability of the packing quality, so non-retained acetone peaks were analyzed since they are primarily influenced by hydrodynamic dispersion. To allow reliable scale-up predictions, the extra column effects had to be quantified and subtracted in order to be able to extract the influence of the packed bed alone. Different methods for determination of the extra column effects were compared, mainly pulses through the workstation alone and the extrapolation method from different column lengths. Regarding pulses through the workstation alone, the performance of different bypass types was evaluated and found that the built-in ÄKTA pure bypass function is not suitable to accurately describe the system contribution. Any connector connecting the inlet to the outlet tubing of the column irrespective of its volume is suitable, hardly any differences were found between “normal” connectors with larger dead volumes and a ZDV connector. The length extrapolation method yielded different extra column volumes V_{ex} for different column types (MiniChrom and ValiChrom), which is reasonable since they also have different volumes inside their top and bottom adapters and inside the filters and frits. The determined V_{ex} and extra column band broadening σ^2_{ex} determined by length extrapolation differed for columns packed with different media although it should be the same, indicating that the underlying assumption that the columns are equally packed was not fulfilled. Nonetheless, the average extra column volumes determined by the length extrapolation method agreed well with the theoretical geometrical contributions from the individual parts with differences smaller than 25 µl. Furthermore, the length extrapolation method is only suitable for evaluating extra column effects if at least three different column lengths are available for extrapolation and the peaks from these columns have similar shapes. The extra column band broadening was smaller

when determined by the length extrapolation method than by injections through the workstation alone, even though it also considers band broadening in the adapters, filters and frits. This leads to the conclusion that extra column band broadening is overestimated by pulses through the workstation alone. Consequently, the length extrapolation method was superior in describing the extra column effects.

Upon investigation of the extra column band broadening correlation with the flow rate, no consistent behavior could be observed. It is constant for some columns and increasing or decreasing with flow rate for others. Other publications have also mentioned either a decrease, increase or a constant behavior with flow rate [51,52,61,79,81,86,87,99,119,120]. The dependence of the extra column band broadening with flow rate might depend on the flow-dependent behavior of the part of the workstation which contributes most to extra column band broadening.

The contribution of the extra column band broadening to total band broadening was investigated more thoroughly by comparing the ratio of extra column to total band broadening $\sigma^2_{ex}/\sigma^2_{total}$. When plotted against the column volume, the ratio $\sigma^2_{ex}/\sigma^2_{total}$ follows an exponential decay function with $\sigma^2_{ex}/\sigma^2_{total} = 1$ at a column volume of zero. This has already been described elsewhere [97]. The shape of the decline depends on the column diameter but also on geometry of the column adapters and the chosen filters and frits since different correlations were found for different column types (Figure 9).

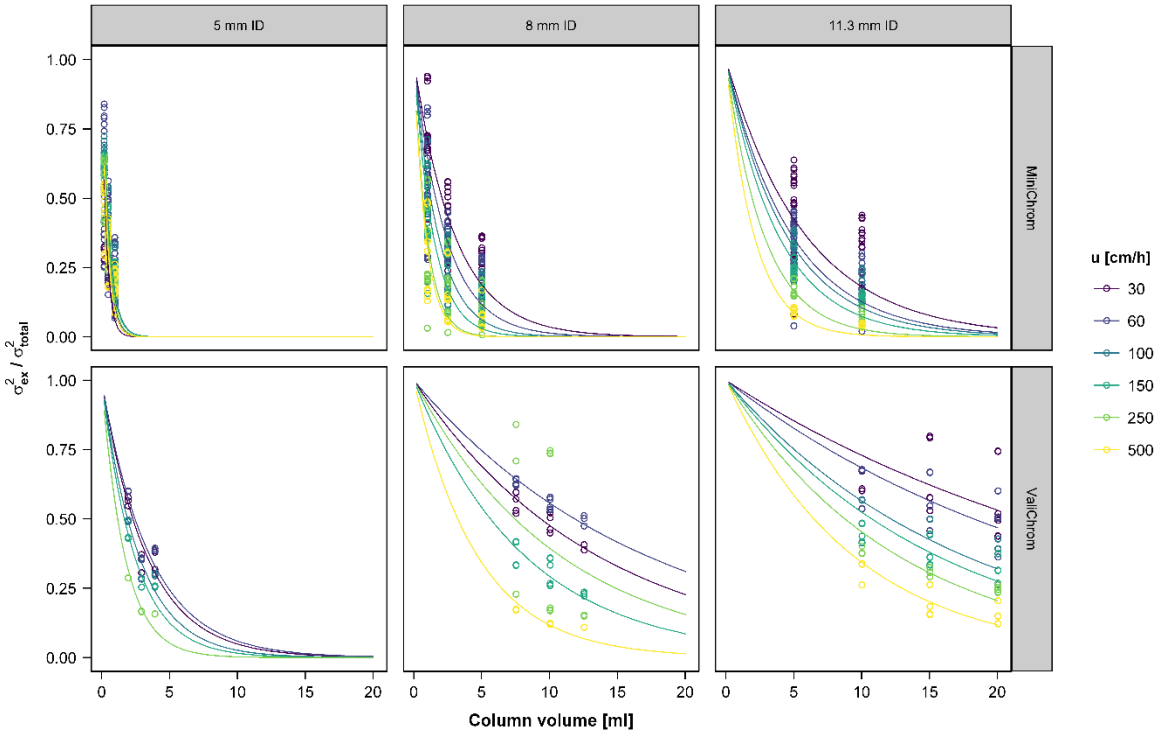

Figure 9 Ratio of extra to total column band broadening $\sigma^2_{ex}/\sigma^2_{total}$ for different column types, diameters and volumes at different superficial velocities [Publication III].

It is important that $\sigma^2_{ex}/\sigma^2_{total}$ is not only large for small column volumes but can even be more than 50 % for columns larger than 10 mL, where the V_{ex} is less than 5 % of the column volume. The lower the superficial velocity, the higher the influence of the extra column effects because intra column band broadening increases with the velocity.

For demonstration of column scalability, extra column volume and band broadening determined by the peak extrapolation method were subtracted from acetone peaks to only investigate the difference in the packing quality and not that of the system effects. The peak width of a pulse σ^2_{int} is positively linearly related with the column length. This result has been described previously [121]. But also increases in column diameter lead to increases in peak width, even for columns of the same length. This phenomenon was attributed to additional radial distribution of the pulse inside the column resulting from non-ideal design of the flow distributor, which was confirmed by computational fluid dynamics (CFD) simulations (Figure 10). Simulations showed that also the top of the packed bed is needed to homogeneously distribute the solute over the whole column cross-section.

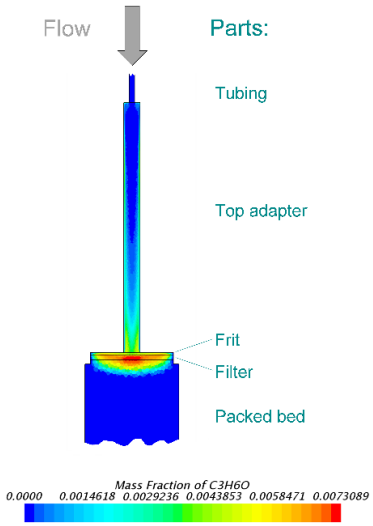

Figure 10 CFD simulation showing the top of a pre-packed MiniChrom column (8 mm ID, 10 cm long) after injection of an acetone pulse [Publication III].

For demonstration of scalability, an empirical equation was developed, which allows prediction of peak width (corrected by extra column effects) from column diameter, column length and reduced velocity (Equation 18). This is a generic equation valid for the evaluated pre-packed columns from small to medium scale irrespective of the packed medium. It confirms that pre-packed columns are packed reproducibly from 0.2 to 20 mL.

$$\frac{\sigma^2_{col}}{d_c^3} = 0.00681 * L^{0.549} + 2.31 * 10^{-5} * L * u' \quad (18)$$

Moreover, two additional empirical equations could be derived describing the influence of the extra column band broadening to total band broadening with column diameter, column length

and reduced velocity. Two different equations were necessary since the two column types had different contributions of extra column band broadening to total band broadening. Extra column effects of MiniChrom columns can be predicted with equation 19 and that of ValiChrom columns with equation 20. These equations are only valid for the used column types and the ÄKTA pure workstation.

$$\frac{\sigma_{ex}^2}{\sigma_{total}^2} = e^{-0.00801*L} * u'^{-0.210} * u'^{-0.00241*L} \quad (19)$$

$$\frac{\sigma_{ex}^2}{\sigma_{total}^2} = u'^{-0.168} * u'^{-0.00103*L} \quad (20)$$

Equations 18-20 allow the prediction of intra, extra and total column band broadening from column dimensions and reduced velocity. Consequently, the evaluated small and medium size pre-packed columns can be considered scalable over a wide range of velocities in terms of packing quality and construction of hardware even when packed with different media.

In the previous studies, peak dispersion was analyzed for non-retained peaks with small solutes giving information on the packing quality of the columns. Dispersion of retained protein peaks will also depend on additional external and internal mass transfer effects. However, these effects mainly occur on a bead level and are expected to be the same from small to large scale. Consequently, it was assumed that columns are also scalable for protein separations, when scalability can be shown for non-retained peaks with small solutes. To test this hypothesis, additional scale-up experiments were carried out over a wider range of column volumes using proteins in binding mode as well as acetone peaks to show scalability. Pre-packed columns with volumes from 1 mL to 57 L packed with a cation exchange medium were analyzed and scalability was evaluated at a constant residence time.

Firstly, packing quality and consistency was verified by non-retained acetone peaks at different velocities. A linear increase of the first peak moment with the column volume confirmed that the columns have the same packing quality and total porosity. The extra column volume was smaller than 5 % of the column volume for all columns except for the 1 mL column, where it was in a range of 20-25 % of the column volume. The second moment could also be related to the column volume.

Secondly, scalability of a protein capture step was demonstrated by breakthrough curves using lysozyme as model protein for columns up to 33 L. Superimposition of normalized (c/c_F) breakthrough curves yielded similar profiles (Figure 11A) with slopes at 50 % breakthrough in a range of 10.8 ± 0.1 CV^{-1}. The calculated equilibrium binding capacity (EBC) for lysozyme was the same for all columns with a mean EBC of 26.6 ± 0.9 mg/mL column (Figure 11B). The dynamic binding capacity was in a range of 21.3 ± 0.9 mg/mL column. The slight variations in

the binding capacities resulted from variations in the salt concentration during the loading step. A variation of the conductivity of 0.3 mS/cm resulted in a difference in EBC of 2 mg/mL. The dependency of the column capacity on the conductivity during binding was confirmed by isotherm measurements at different conductivities. Susanto et al. observed different amounts of adsorbed lysozyme (EBCs) using columns of 96-well to laboratory scale, which was attributed to fluctuations in medium quality [122]. The quality of the medium used in this study was sufficient to obtain equal binding capacities at different scales, despite different batches were used.

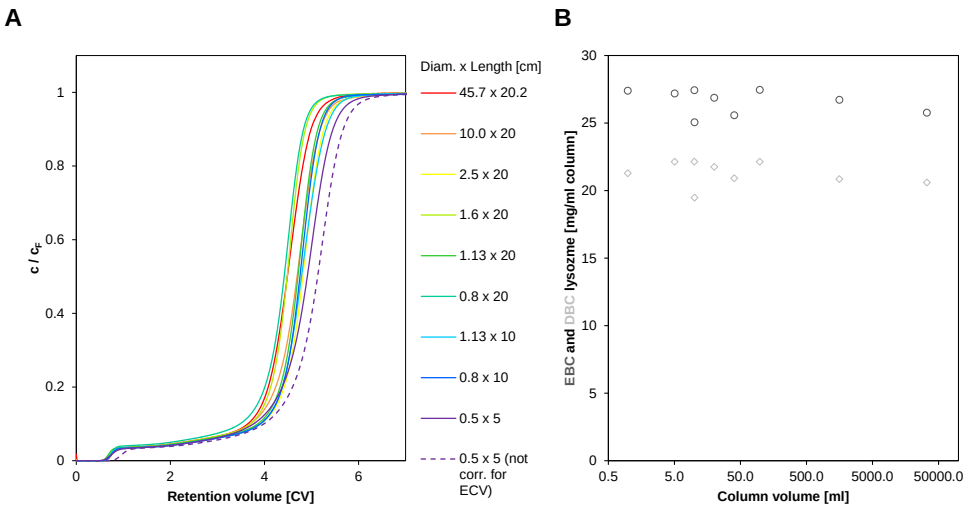

Figure 11 (A) Normalized breakthrough curves of lysozyme on pre-packed columns with volumes from 1 mL to 33 L. (B) Calculated equilibrium (EBC) and dynamic (DBC) binding capacities for lysozyme after correction for extra column volume (ECV) [Publication IV].

The scalability of pre-packed columns for polishing steps was shown by separation of a ternary protein mixture (lysozyme, cytochrome C and ribonuclease A). The separation process included a wash step, three step elutions and a regeneration step. The chromatograms from columns with volumes of 1 mL to 57 L were overlaid by normalizing the x-axis with respect to column volumes and aligning the peak profiles to the start of the conductivity rises. The developed gradient was capable of separating the three proteins in three subsequent steps (Figure 12A). Each elution step was additionally capable of separating two protein isoforms since the used model proteins were not pure. The resolution of the two isoform peaks in each elution step fluctuated and is likely to depend on the exact salt concentration in each elution step. The smaller the columns, the later and the broader the peaks eluted (Figure 12B-D). This phenomenon was explained by the shape of the gradient transitions from low to high salt. The transition was steeper for large columns which was attributed to the influence of the extra column effects, especially the mixer, on the gradient profiles. A model to describe transitions from a base to a saturation level has been developed by Kaltenbrunner and Jungbauer [123], which combines a continuous stirred tank reactor model and a logistic growth function. The

shape of the step increases of the modifier was described by fitting the conductivity curves to this model. Based on the fit, the time constant of the mixer was derived for all evaluated column volumes. An empirical relationship between the time constant and the column volume allowed to describe the variation in gradient shape for different column volumes. Consequently, column volume and the shape of gradient transitions need to be considered for scale-up predictions. The purity of the load and the eluted protein pools at each elution step was quantified by RP-HPLC. Ribonuclease A eluted in the first step with a purity of 97.9 ± 1.3 %, cytochrome C eluted in the second step with a purity of 89.3 ± 2.2 % and lysozyme eluted in the third step with a purity of 100 ± 0 %. This confirmed that the observed shifts in retention time and peak widths had no influence on protein purity. Therefore, protein binding and elution can be considered equal at all scales. The scalability study on protein separations leads to the conclusion that the evaluated pre-packed columns are packed consistently and reproducibly. Pre-packed columns are suitable for protein binding and separation from laboratory to production scale but extra column effects need to be taken into account for predictions between the different scales.

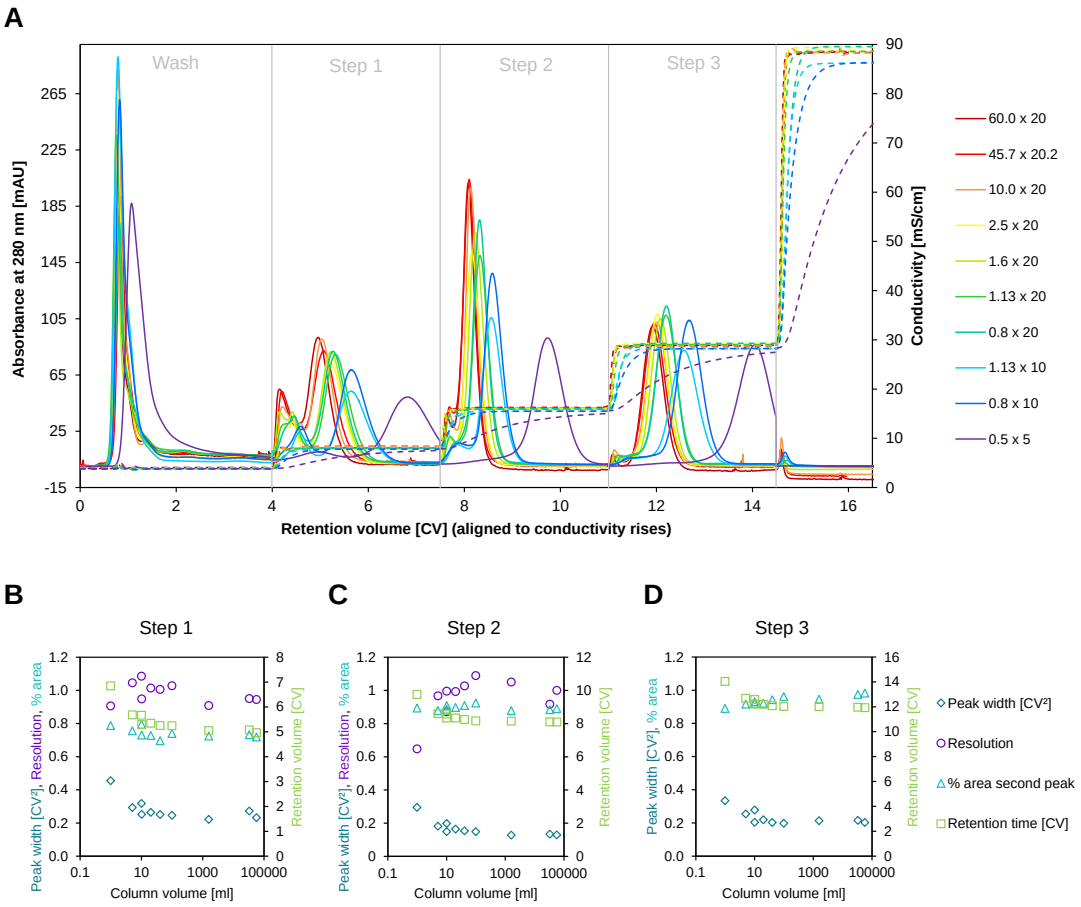

Figure 12 Step gradient separation of lysozyme, cytochrome C and ribonuclease A for column volumes from 1 mL to 57 L. (A) Chromatograms aligned to start of rises in the conductivity curves. (B-D) Retention volumes, peak widths, resolution and % area of the second peak were calculated by fitting two Gaussian peaks to each elution step and analyzing the parameters of the fitted peak [Publication IV].

The following conclusions can be made:

- The packing quality of pre-packed columns which were manufactured over a time span of 10 years was constant confirming that commercially available media can be reproducibly and uniformly packed in pre-packed columns.
- The measurement precision has a high impact for columns smaller than 2 mL.
- The column-to-column packing variation varied by 10-15 %, which is in the expected range and acceptable for the intended use.
- Pre-packed columns are of equal or better packing quality as self-packed columns. Non-disposable pre-packed columns were packed equally or better than disposable pre-packed columns.
- Extra column effects can account for more than 50 % of the total band broadening even for columns larger than 10 mL due to the additional volumes in the filter, frits, and adapters of the columns upon increases in the column diameter.
- A linear relationship between intra column band broadening and column length was found, which increased stepwise with increases in column diameter. Engineering correlations were established for scale-up allowing the prediction of intra, extra and total band broadening from column dimensions and mobile phase velocity.
- Pre-packed columns are scalable from 1 mL to 67 L scale with regards to binding capacity and protein separation. The biggest influence in the scalability are the effects of the chromatography workstation such as buffer mixing.

I concluded that pre-packed columns with current specifications adopted in industry are suitable for protein chromatography and can be used to replace conventional self-packed columns without any trade-offs in column performance from laboratory to production scale.

4 References

[1] M. Fuller, H. Pora, Introducing Disposable Systems into Biomanufacturing: A CMO Case Study, BioProcess Int. 8 (2008) 30–36.

[2] J.S. Wilson, A Fully Disposable Monoclonal Antibody Manufacturing Train, BioProcess Int. 4 (2006) 34–36.

[3] R. Jacquemart, M. Vandersluis, M. Zhao, K. Sukhija, N. Sidhu, J. Stout, A Single-use Strategy to Enable Manufacturing of Affordable Biologics, Comput. Struct. Biotechnol. J. 14 (2016) 309–318.

[4] A.A. Shukla, U. Gottschalk, Single-use disposable technologies for biopharmaceutical manufacturing, Trends Biotechnol. 31 (2013) 147–154.

[5] C. Scott, The latest single-use solutions for downstream processing, BioPharm Int. 15 (2017) 1–5.

[6] P. Rogge, D. Müller, S.R. Schmidt, The Single-Use or Stainless Steel Decision Process, BioProcess Int. 13 (2015) 10–15.

[7] R. Zheng, The game changer - Transforming the biopharmaceutical landscape through single-use technologies, Bioprocess Int. (2010) 4–9.

[8] M. Laukel, P. Rogge, G. Dudziak, Disposable Downstream Processing for Clinical Manufacturing, Bioprocess Int. (2011) 14–21.

[9] M. Hammond, L. Marghitoiu, H. Lee, L. Perez, G. Rogers, Y. Nashed-samuel, H. Nunn, S. Kline, A Cytotoxic Leachable Compound from Single-Use Bioprocess Equipment that Causes Poor Cell Growth Performance, Biotechnol. Progr. 30 (2014) 332–337.

[10] Shire, Press release: Shire announces European approval of manufacturing facility for VPRIV® (velaglucerase alfa), (2012).

[11] P. Nicholson, E. Storm, Single-Use Tangential Flow Filtration in Bioprocessing, BioPharm Int. (2011) 38–47.

[12] D. Low, R.O. Leary, N.S. Pujar, Future of antibody purification, J. Chromatogr. B. 848 (2007) 48–63.

[13] A.A. Shukla, S. Mostafa, M. Wilson, D. Lange, Vertical Integration of Disposables in Biopharmaceutical Drug Substance Manufacturing, BioProcess Int. 10 (2012) 34–47.

[14] E. Langer, 12th Annual report and survey of biopharmaceutical manufacturing capacity and production, BioPlan Associates, Dublin, Ireland, 2015.

[15] P. Millner, ed., High Resolution Chromatography: A Practial Approach, Oxford University Press, 1999.

[16] G. Guiochon, T. Farkas, H. Guan-Sajonz, J.-H. Koh, M. Sarker, B.J. Tanley, T. Yun, Consolidation of particle beds and packing of chromatographic columns, J. Chromatogr. A. 762 (1997) 83–88.

[17] R.M. Cassidy, D.S. Legay, R.W. Frei, Study of Packing Techniques for Small-Particle Silica Gels in High-Speed Liquid Chromatography, Anal. Chem. 46 (1974) 340–344.

[18] A.E. Reising, J.M. Godinho, K. Hormann, J.W. Jorgenson, U. Tallarek, Larger voids in mechanically stable, loose packings of 1.3 µm frictional, cohesive particles: Their reconstruction, statistical analysis, and impact on separation efficiency, J. Chromatogr.

A. 1436 (2016) 118–132.

[19] A. Daneyko, A. Höltzel, S. Khirevich, U. Tallarek, Influence of the particle size distribution on hydraulic permeability and eddy dispersion in bulk packings, Anal. Chem. 83 (2011) 3903–3910.

[20] H.C.H. Rumpf, A.R. Gupte, Einflusse der Porositat und Korngrösenverteilung im Widerstandsgesetz der Porenströmung, Chemie Ing. Tech. 43 (1971) 367–375.

[21] O. Kaltenbrunner, P. Watler, S. Yamamoto, Column Qualification in Process Ion-Exchange Chromatography, in: I. Endo, T. Nagamune, S. Katoh, T. Yonemoto (Eds.), Biosep. Eng., 1st editio, Elsevir, 2000: pp. 201–206.

[22] T. Takeuchi, D. Ishii, High-performance micro packed flexible columns in liquid chromatography, J. Chromatogr. A. 213 (1981) 25–32.

[23] T. Takeuchi, D. Ishii, Ultra-micro high-performance liquid chromatography, J. Chromatogr. A. 190 (1980) 150–155.

[24] J.J. Kirkland, J.J. DeStefano, The art and science of forming packed analytical high-performance liquid chromatography columns, J. Chromatogr. A. 1126 (2006) 50–57.

[25] E. Langer, Innovation in Pre-packed Disposable Chromatography Columns, 2014.

[26] A. Osberghaus, K. Drechsel, S. Hansen, S.K. Hepbildikler, S. Nath, M. Haindl, E. Von Lieres, J. Hubbuch, Model-integrated process development demonstrated on the optimization of a robotic cation exchange step, Chem. Eng. Sci. 76 (2012) 129–139.

[27] K. Treier, S. Hansen, C. Richter, P. Diederich, J. Hubbuch, P. Lester, High-Throughput Methods for Miniaturization and Automation of Monoclonal Antibody Purification Processes, Biotechnol. Progr. 28 (2012) 723–732.

[28] M. Wiendahl, P.S. Wierling, J. Nielsen, D. Fomsgaard, C.J. Krarup, A. Staby, J. Hubbuch, High Throughput Screening for the Design and Optimization of Chromatographic Processes – Miniaturization , Automation and Parallelization of Breakthrough and Elution Studies, Chem. Eng. Technol. 31 (2008) 893–903.

[29] T. Schroeder, Automated Parallel Chromatography in Downstream Process Development, Bioprocess Int. 8 (2010) 92–93.

[30] A. Rathore, R.M. Kennedy, J.K. O'Donnell, I. Bemberis, O. Kaltenbrunner, Qualification of a chromatographic column: Why and how to do it, 2003.

[31] M.A. Teeters, I. Quiñones-García, Evaluating and monitoring the packing behavior of process-scale chromatography columns, J. Chromatogr. A. 1069 (2005) 53–64.

[32] K. Yamaoka, T. Nakagawa, Moment Analysis for Isolation of Intrinsic Column Efficiencies in Gas Chromatography, Anal. Chem. 47 (1975) 2050–2053.

[33] J.J. Kirkland, W.W. Yau, H.J. Stoklosa, C.H. Dilks, Sampling and extra-column effects in high-performance liquid chromatography; influence of peak skew on plate count calculations, J. Chromatogr. Sci. 15 (1977) 303–316.

[34] R. Hahn, P. Bauerhansl, K. Shimahara, C. Wizniewski, A. Tscheliessnig, A. Jungbauer, Comparison of protein A affinity sorbents II . Mass transfer properties, J. Chromatogr. A. 1093 (2005) 98–110.

[35] N. Forrer, O. Kartachova, A. Butté, M. Morbidelli, Investigation of the porosity variation during chromatographic experiments, Ind. Eng. Chem. Res. 47 (2008) 9133–9140.

[36] J.J. Stickel, A. Fotopoulos, Pressure - Flow Relationships for Packed Beds of

Compressible Chromatography Media at Laboratory and Production Scale †, Biotechnol. Progr. 17 (2001) 744–751.

[37] E.X. Perez-Almodovar, G. Carta, IgG adsorption on a new protein A adsorbent based on macroporous hydrophilic polymers. II. Pressure-flow curves and optimization for capture, J. Chromatogr. A. 1216 (2009) 8348–8354.

[38] S. Khirevich, A. Daneyko, A. Höltzel, A. Seidel-Morgenstern, U. Tallarek, Statistical analysis of packed beds, the origin of short-range disorder, and its impact on eddy dispersion, J. Chromatogr. A. 1217 (2010) 4713–4722.

[39] B.J. Stanley, C.R. Foster, G. Guiochon, On the reproducibility of column performance in liquid chromatography and the role of the packing density, J. Chromatogr. A. 761 (1997) 41–51.

[40] D.J. Anderson, R.R. Walters, Effect of Baseline Errors on the Calculation of Statistical Moments of Tailed Chromatographic Peaks, J. Chromatogr. Sci. 22 (1984) 353–359.

[41] S.N. Chesler, S.P. Cram, Effect of peak sensing and random noise on the precision and accuracy of statistical moment analyses from digital chromatographic data, Anal. Chem. 43 (1971) 1922–1933.

[42] T. Petitclerc, G. Guiochon, Determination of the Higher Moments of a Nonsymmetrical Chromatographic Signal, J. Chromatogr. Sci. 14 (1976) 531–535.

[43] E. Grushka, M.N. Myers, P.D. Schettler, J.C. Giddings, Computer characterization of chromatographic peaks by plate height and higher central moments, Anal. Chem. 41 (1969) 889–892.

[44] R.E. Pauls, L.B. Rogers, Comparisons of Methods for Calculating Retention and Separation of Chromatographic Peaks, Sep. Sci. 12 (1977) 395–413.

[45] D.W. Morton, C.L. Young, Analysis of Peak Profiles Using Statistical Moments, J. Chromatogr. Sci. 33 (1995) 514–524.

[46] Y. Vanderheyden, K. Broeckhoven, G. Desmet, Comparison and optimization of different peak integration methods to determine the variance of unretained and extra-column peaks, J. Chromatogr. A. 1364 (2014) 140–150.

[47] H. Gao, P.G. Stevenson, F. Gritti, G. Guiochon, Investigations on the calculation of the third moments of elution peaks. I: Composite signals generated by adding up a mathematical function and experimental noise, J. Chromatogr. A. 1222 (2012) 81–89.

[48] P.G. Stevenson, F. Gritti, G. Guiochon, Automated methods for the location of the boundaries of chromatographic peaks, J. Chromatogr. A. 1218 (2011) 8255–8263.

[49] H.M. Gladney, B.F. Dowden, J.D. Swalen, Computer-Assisted Gas-Liquid Chromatography, Anal. Chem. 41 (1969).

[50] I.G. McWilliam, H.C. Bolton, Instrumental peak distortion. II. Effect of recorder response time, Anal. Chem. 41 (1969) 1762–1770.

[51] F. Gritti, G. Guiochon, Accurate measurements of peak variances: Importance of this accuracy in the determination of the true corrected plate heights of chromatographic columns, J. Chromatogr. A. 1218 (2011) 4452–4461.

[52] F. Gritti, G. Guiochon, Mass transfer kinetics, band broadening and column efficiency, J. Chromatogr. A. 1221 (2012) 2–40.

[53] J. Li, Comparison of the capability of peak functions in describing real chromatographic peaks, J. Chromatogr. A. 952 (2002) 63–70.

[54] G. Carta, A. Jungbauer, Protein Chromatography: Process Development and Scale-Up, WILEY-VCH Verlag GmbH & Co. KGaA, Weinheim, 2010.

[55] J.J. van Deemter, F.J. Zuiderweg, A. Klinkenberg, Longitudinal diffusion and resistance to mass transfer as causes of nonideality in chromatography, Chem. Eng. Sci. 5 (1956) 271–289.

[56] C.J. Giddings, The random downstream migration of molecules in chromatography, J. Chem. Educ. 35 (1958) 588–591.

[57] P.A. Bristow, J.H. Knox, Standardization of Test Conditions for High Performance Liquid Chromatography Columns, Chromatographia. 10 (1977) 279–289.

[58] C.J. Giddings, “Eddy” Diffusion in Chromatography, Nature. 184 (1959) 357–358.

[59] J.C. Giddings, Dynamics of Chromatography, Part I: Principle and Theory, Marcel Dekker, New York, NY, USA, 1965.

[60] J.C. Giddings, Nature of Gas Phase Mass Transfer in Gas Chromatography, Anal. Chem. 34 (1962) 1186–1192.

[61] K.M. Usher, C.R. Simmons, J.G. Dorsey, Modeling chromatographic dispersion: A comparison of popular equations, J. Chromatogr. A. 1200 (2008) 122–128.

[62] S. Khirevich, A. Höltzel, A. Seidel-Morgenstern, U. Tallarek, Geometrical and topological measures for hydrodynamic dispersion in confined sphere packings at low column-to-particle diameter ratios, J. Chromatogr. A. 1262 (2012) 77–91.

[63] Q.S. Yuan, A. Rosenfeld, T.W. Root, D.J. Klingenberg, E.N. Lightfoot, Flow distribution in chromatographic columns, J. Chromatogr. A. 831 (1999) 149–165.

[64] V. Wong, R.A. Shalliker, G. Guiochon, Evaluation of the Uniformity of Analytical-Size Chromatography Columns Prepared by the Downward Packing of Particulate Slurries, Anal. Chem. 76 (2004) 2601–2608.

[65] J. Moscariello, G. Purdom, J. Coffman, T.W. Root, E.N. Lightfoot, Characterizing the performance of industrial-scale columns, J. Chromatogr. A. 908 (2001) 131–141.

[66] J.H. Knox, G.R. Laird, P.A. Raven, Interaction of radial and axial disperion in liquid chromatography in relation to the “infinite diameter effect,” J. Chromatogr. Sci. 122 (1976) 129–145.

[67] C.X. Li, X.Z. An, R.Y. Yang, R.P. Zou, A.B. Yu, Experimental study on the packing of uniform spheres under three-dimensional vibration, Powder Technol. 208 (2011) 617–622.

[68] M. Dorn, D. Hekmat, Simulation of the Dynamic Packing Behavior of Preparative Chromatography Columns via Discrete Particle Modeling, Biotechnol. Progr. 32 (2016) 363–371.

[69] M. Dorn, F. Eschbach, D. Hekmat, D. Weuster-Botz, Influence of different packing methods on the hydrodynamic stability of chromatography columns, J. Chromatogr. A. 1516 (2017) 89–101.

[70] R.A. Shalliker, B.S. Broyles, G. Guiochon, Axial and radial diffusion coefficients in a liquid chromatography column and bed heterogeneity, J. Chromatogr. A. 994 (2003) 1–12.

[71] N.S. Mitchell, L. Hagel, E.J. Fernandez, In situ analysis of protein chromatography and column efficiency using magnetic resonance imaging, J. Chromatogr. A. 779 (1997) 73–89.

[72] T. Farkas, M.J. Sepaniak, G. Guiochon, Column radial homogeneity in high-performance liquid chromatography, J. Chromatogr. A. 740 (1996) 169–181.

[73] T. Farkas, G. Guiochon, Contribution of the Radial Distribution of the Flow Velocity to Band Broadening in HPLC Columns, Anal. Chem. 69 (1997) 4592–4600.

[74] R.A. Shalliker, B.S. Broyles, G. Guiochon, Physical evidence of two wall effects in liquid chromatography, J. Chromatogr. A. 888 (2000) 1–12.

[75] T.F. Johnson, P.R. Levison, P.R. Shearing, D.G. Bracewell, X-ray computed tomography of packed bed chromatography columns for three dimensional imaging and analysis, J. Chromatogr. A. 1487 (2017) 108–115.

[76] F. Gritti, G. Guiochon, Kinetic investigation of the relationship between the efficiency of columns and their diameter, J. Chromatogr. A. 1218 (2011) 1592–1602.

[77] M.R. Schure, R.S. Maier, How does column packing microstructure affect column efficiency in liquid chromatography?, J. Chromatogr. A. 1126 (2006) 58–69.

[78] J.C. Sternberg, Extracolumn contributions to chromatographic band broadening, Adv. Chromatogr. 2 (1966) 205–270.

[79] F. Gritti, A. Felinger, G. Guiochon, Influence of the errors made in the measurement of the extra-column volume on the accuracies of estimates of the column efficiency and the mass transfer kinetics parameters, J. Chromatogr. A. 1136 (2006) 57–72.

[80] P. Aggarwal, K. Liu, S. Sharma, J.S. Lawson, H. Dennis Tolley, M.L. Lee, Flow rate dependent extra-column variance from injection in capillary liquid chromatography, J. Chromatogr. A. 1380 (2015) 38–44.

[81] A.J. Alexander, T.J. Waeghe, K.W. Himes, F.P. Tomasella, T.F. Hooker, Modifying conventional high-performance liquid chromatography systems to achieve fast separations with fused-core columns: A case study, J. Chromatogr. A. 1218 (2011) 5456–5469.

[82] S.R. Bakalyar, C. Phipps, B. Spruce, K. Olsen, Choosing sample volume to achieve maximum detection sensitivity and resolution with high-performance liquid chromatography columns of 1.0, 2.1 and 4.6 mm I.D., J. Chromatogr. A. 762 (1997) 167–185.

[83] F. Gritti, G. Guiochon, On the minimization of the band-broadening contributions of a modern, very high pressure liquid chromatograph, J. Chromatogr. A. 1218 (2011) 4632–4648.

[84] A. Prüß, C. Kempter, J. Gysler, T. Jira, Extracolumn band broadening in capillary liquid chromatography, J. Chromatogr. A. 1016 (2003) 129–141.

[85] R. De Pauw, K. Shoykhet, G. Desmet, K. Broeckhoven, Understanding and diminishing the extra-column band broadening effects in supercritical fluid chromatography, J. Chromatogr. A. 1403 (2015) 132–137.

[86] K.-P. Hupe, R.J. Jonker, G. Rozing, Determination of band-spreading effects in high-performance liquid chromatographic instruments, J. Chromatogr. 285 (1984) 253–265.

[87] J.P. Grinias, B. Bunner, M. Gilar, J.W. Jorgenson, Measurement and Modeling of Extra-Column Effects Due to Injection and Connections in Capillary Liquid Chromatography, Chromatography. 2 (2015) 669–690.

[88] E. V. Dose, G. Guiochon, Effects of extracolumn convolution on preparative chromatographic peak shapes, Anal. Chem. 62 (1990) 1723–1730.

[89] Y. Vanderheyden, K. Broeckhoven, G. Desmet, Peak deconvolution to correctly assess the band broadening of chromatographic columns, J. Chromatogr. A. 1465 (2016) 126–142.

[90] Y. Vanderheyden, K. Vanderlinden, K. Broeckhoven, G. Desmet, Problems involving the determination of the column-only band broadening in columns producing narrow and tailed peaks, J. Chromatogr. A. 1440 (2016) 74–84.

[91] H.H. Lauer, G.P. Rozing, The selection of optimum conditions in HPLC I. The determination of external band spreding in LC instruments, Chromatographia. 14 (1981) 641–647.

[92] R.A. Shalliker, B.S. Broyles, G. Guiochon, On-column visualization of sample migration in liquid chromatography, Anal. Chem. 72 (2000) 323–332.

[93] S.P. Cram, T.H.J. Glenn, Instrumental contributions to band broadening in gas chromatography 1. Development of a model, J. Chromatogr. 112 (1975) 329–341.

[94] G. Taylor, Dispersion of Soluble Matter in Solvent Flowing Slowly through a Tube, Proc. R. Soc. Lond. A. 219 (1953) 186–203.

[95] K.J. Fountain, U.D. Neue, E.S. Grumbach, D.M. Diehl, Effects of extra-column band spreading, liquid chromatography system operating pressure, and column temperature on the performance of sub-2-µm porous particles, J. Chromatogr. A. 1216 (2009) 5979–5988.

[96] G. Grznárová, M. Polakovic, P. Acai, T. Görner, Extra-column dispersion of macromolecular solutes in aqueous-phase size-exclusion chromatography, J. Chromatogr. A. 1040 (2004) 33–43.

[97] O. Kaltenbrunner, A. Jungbauer, S. Yamamoto, Prediction of the preparative chromatography performance with a very small column, J. Chromatogr. A. 760 (1997) 41–53.

[98] K. Vanderlinden, K. Broeckhoven, Y. Vanderheyden, G. Desmet, Effect of pre- and post-column band broadening on the performance of high-speed chromatography columns under isocratic and gradient conditions, J. Chromatogr. A. 1442 (2016) 73–82.

[99] A. Schultze-Jena, M.A. Boon, P.J.T. Bussmann, A.E.M. Janssen, A. van der Padt, The counterintuitive role of extra-column volume in the determination of column efficiency and scaling of chromatographic processes, J. Chromatogr. A. 1493 (2017) 49–56.

[100] F. Gritti, G. Guiochon, Accurate measurements of the true column efficiency and of the instrument band broadening contributions in the presence of a chromatographic column, J. Chromatogr. A. 1327 (2014) 49–56.

[101] F. Gritti, S.J. Shiner, J.N. Fairchild, G. Guiochon, Evaluation of the kinetic performance of new prototype 2.1 mm x 100 mm narrow-bore columns packed with 1.6 µm superficially porous particles, J. Chromatogr. A. 1334 (2014) 30–43.

[102] F. Gritti, G. Guiochon, Effect of the pressure on pre-column sample dispersion theory, experiments, and practical consequences, J. Chromatogr. A. 1352 (2014) 20–28.

[103] J.F.K. Huber, A. Rizzi, Influence of the accuracy of the extra-column peak-width determination on the verification of the theoretical plate-height equations, J. Chromatogr. 384 (1987) 337–348.

[104] H.A. Claessens, C.A. Cramers, M.A.J. Kuyken, Estimation of the Band Broadening Contribution of HPLC Equipment to Column Elution Profiles, Chromatographia. 23 (1987) 189–194.

[105] F.G. Lode, A. Rosenfeld, Q.S. Yuan, T.W. Root, E.N. Lightfoot, Refining the scale-up of chromatographic separations, J. Chromatogr. A. 796 (1998) 3–14.

[106] S. Aldington, J. Bonnerjea, Scale-up of monoclonal antibody purification processes, J. Chromatogr. B. 848 (2007) 64–78.

[107] N.J. Titchener-Hooker, P. Dunnill, M. Hoare, Micro Biochemical Engineering to Accelerate the Design of Industrial-Scale Downstream Processes for Biopharmaceutical Proteins, Biotechnol. Bioeng. 100 (2008) 473–487.

[108] S. Gerontas, M. Asplund, R. Hjorth, D.G. Bracewell, Integration of scale-down experimentation and general rate modelling to predict manufacturing scale chromatographic separations, J. Chromatogr. A. 1217 (2010) 6917–6926.

[109] K. Vorauer, M. Skias, P. Schulz, A. Jungbauer, Scale-up of recombinant protein purification by hydrophobic interaction chromatography, J. Chromatogr. 625 (1992) 33–39.

[110] N. Hutchinson, S. Chhatre, H. Baldascini, T. Place, B. Road, D.G. Bracewell, M. Hoare, Ultra Scale-Down Approach to Correct Dispersive and Retentive Effects in Small-Scale Columns When Predicting Larger Scale Elution Profiles, Biotechnol. Progr. 25 (2009) 1103–1110.

[111] K.A. Kang, D.D.Y. Ryu, Studies on Scale-up Parameters of an Immunoglobulin Separation System Using Protein A Affinity Chromatography, Biotechnol. Progr. 7 (1991) 205–212.

[112] T. Ishihara, T. Kadoya, S. Yamamoto, Application of a chromatography model with linear gradient elution experimental data to the rapid scale-up in ion-exchange process chromatography of proteins, J. Chromatogr. A. 1162 (2007) 34–40.

[113] R.N. Keener III, E.J. Fernandez, J.E. Maneval, R.A. Hart, Advancement in the modeling of pressure-flow for the guidance of development and scale-up of commercial-scale biopharmaceutical chromatography, J. Chromatogr. A. 1190 (2008) 127–140.

[114] E.X. Perez-Almodovar, G. Carta, IgG adsorption on a new protein A adsorbent based on macroporous hydrophilic polymers . I . Adsorption equilibrium and kinetics, J. Chromatogr. A. 1216 (2009) 8339–8347.

[115] S. Chhatre, N.J. Titchener-Hooker, Review : Microscale methods for high-throughput chromatography development in the pharmaceutical industry, J. Chem. Technol. Biotechnol. 84 (2009) 927–940.

[116] W.R. Keller, S.T. Evans, G. Ferreira, D. Robbins, S.M. Cramer, Use of MiniColumns for linear isotherm parameter estimation and prediction of benchtop column performance, J. Chromatogr. A. 1418 (2015) 94–102.

[117] S.T. Evans, K.D. Stewart, C. Afdahl, R. Patel, K.J. Newell, Optimization of a micro-scale , high throughput process development tool and the demonstration of comparable process performance and product quality with biopharmaceutical manufacturing processes, J. Chromatogr. A. 1506 (2017) 73–81.

[118] C. Laub, Reproducible preparative liquid chromatography columns, J. Chromatogr. A. 992 (2003) 41–45.

[119] D. V. McCalley, Instrumental considerations for the effective operation of short , highly efficient fused-core columns . Investigation of performance at high flow rates and elevated temperatures, J. Chromatogr. A. 1217 (2010) 4561–4567.

[120] N. Wu, A.C. Bradley, Effect of column dimension on observed column efficiency in very

high pressure liquid chromatography, J. Chromatogr. A. 1261 (2012) 113–120.

[121] J.L. Rocca, J.W. Higgins, R.G. Brownlee, Peak variance as a function of HPLC column length and diameter, J. Chromatogr. Sci. 23 (1985) 106–113.

[122] A. Susanto, E. Knieps-Grünhagen, E. von Lieres, J. Hubbuch, High Throughput Screening for the Design and Optimization of Chromatographic Processes : Assessment of Model Parameter Determination from High Throughput Compatible Data, Chem. Eng. Technol. 31 (2008) 1846–1855.

[123] O. Kaltenbrunner, A. Jungbauer, Simple model for blending aqueous salt buffers Application to preparative chromatography, J. Chromatogr. A. 769 (1997) 37–48.

5 Publications

Publication I:

Trend analysis of performance parameters of pre-packed columns for protein chromatography over a time span of ten years

Theresa Scharl, Christian Jungreuthmayer, Astrid Dürauer, Susanne Schweiger, Tim Schröder, Alois Jungbauer (2016) Journal of Chromatography A, Volume 1465, p. 63-70

Publication II:

Column-to-column packing variation of disposable pre-packed columns for protein chromatography

Susanne Schweiger, Stephan Hinterberger, Alois Jungbauer (2017) Journal of Chromatography A, Volume 1527, p. 70-79

Publication III:

Scalability of pre-packed preparative chromatography columns with different diameters and lengths taking into account extra column effects

Susanne Schweiger, Alois Jungbauer (2018) Journal of Chromatography A, Volume 1537, p. 66-74

Publication IV:

Packing quality, protein binding capacity and separation efficiency of pre-packed columns ranging from 1 mL laboratory to 57 L industrial scale

Susanne Schweiger, Eva Berger, Alan Chan, James Peyser, Christine Gebski, Alois Jungbauer (2018) SUBMITTED to Journal of Chromatography A

Contributions to publications:

For publication I, Susanne Schweiger performed literature research on reduced HETP and velocity values for protein separations, discussed the experimental data together with the other authors and corrected the manuscript.

Susanne Schweiger designed, operated and evaluated all chromatographic experiments of publication II, evaluated the analyzed peaks, drafted and revised the manuscript.

Susanne Schweiger devised the methods and conducted the experiments, drafted and revised the manuscript of publication III.

Susanne Schweiger designed, planned and evaluated all experiments, carried out parts of the experiments and wrote the manuscript of publication IV.

PUBLICATION I

Journal of Chromatography A, 1465 (2016) 63–70

Contents lists available at ScienceDirect

Journal of Chromatography A

journal homepage: www.elsevier.com/locate/chroma

Trend analysis of performance parameters of pre-packed columns for protein chromatography over a time span of ten years

Theresa Scharl[a,b], Christian Jungreuthmayer[a], Astrid Dürauer[a,c], Susanne Schweiger[a], Tim Schröder[d], Alois Jungbauer[a,c,*]

[a] Austrian Centre of Industrial Biotechnology, Vienna, Austria
[b] Institute of Applied Statistics and Computing, University of Natural Resources and Life Sciences, Vienna, Austria
[c] Department of Biotechnology, University of Natural Resources and Life Sciences, Vienna, Austria
[d] Atoll, Weingarten, Germany

ARTICLE INFO

Article history:
Received 25 May 2016
Received in revised form 17 July 2016
Accepted 20 July 2016
Available online 21 July 2016

Keywords:
HETP
Porous media
Asymmetry
Packing
Disposable
Ready-to-use

ABSTRACT

Pre-packed small scale chromatography columns are increasingly used for process development, for determination of design space in bioprocess development, and for post-licence process verifications. The packing quality of 30,000 pre-packed columns delivered to customers over a period 10 years has been analyzed by advanced statistical tools. First, the data were extracted and checked for inconsistencies, and then were tabulated and made ready for statistical processing using the programming language Perl (https://www.perl.org/) and the statistical computing environment R (https://www.r-project.org/). Reduced HETP and asymmetry were plotted over time to obtain a trend of packing quality over 10 years. The obtained data were used as a visualized coefficient of variation analysis (VCVA), a process that has often been applied in other industries such as semiconductor manufacturing. A typical fluctuation of reduced HETP was seen. A Tsunami effect in manufacturing, the effect of propagation of manufacturing deviations leading to out-of-specification products, was not observed with these pre-packed columns. Principal component analysis (PCA) showed that all packing materials cluster. Our data analysis showed that the current commercially available chromatography media used for biopharmaceutical manufacturing can be reproducibly and uniformly packed in polymer-based chromatography columns, which are designed for ready-to-use purposes. Although the number of packed columns has quadrupled over one decade the packing quality has remained stable.

1. Introduction

Pre-packed columns or ready-to-use laboratory chromatography columns have been on the market for about one decade and have become very popular for process development and *a posteriori* evaluation of design space [1,2]. Such columns are used to reduce time for packing, which can be very tedious. Time savings is the major criterion for why pre-packed columns are widely applied in biopharmaceutical industry. It is assumed that the performance does not change over time and that consistent lots can be produced. These columns are often used to corroborate findings which have been made with automated systems either by parallel chromatography in robotics systems [3] or by adsorption measurements in microtiter plates [4–6]. For ready-to-use disposable columns, column construction must be simple and inexpensive. Adjustable pistons like adaptors are too expensive for this purpose. Therefore, a precise amount of chromatography medium must be packed into the column, which requires knowledge and skill in column packing. The performance of the packed columns is also checked by the manufacturer before sale. The customers assume that all ready-to-use columns display the same packing quality and can be applied without re-checking the packing quality. Interestingly, the quality can change to certain extent over time.

Manufacturing systems can be divided into 4 major models, transformation operations, operations of modification of structure, information operations, and transfer operations [7]. We can also assume that the same principles of manufacturing variations apply to column packing as used in other industry areas. Column packing can be considered as a transformation operation.

In principle, chromatography media can be categorized according to the backbone: (1) natural polymers such as agarose or

* Corresponding author at: Austrian Centre of Industrial Biotechnology, Vienna, Austria.
E-mail address: alois.jungbauer@boku.ac.at (A. Jungbauer).

http://dx.doi.org/10.1016/j.chroma.2016.07.054

dextran; (2) synthetic polymers such as acrylamide or polymethacrylate; and (3) inorganic materials such as silica, hydroxy apatite, or controlled pore glass [8]. Many methods have been described for column packing taking into account the nature of the backbone. The influence of packing procedures on packing quality of small columns is still not fully understood [9]. Semi-rigid chromatography material is easier to pack than rigid particles and soft material such as Sephadex G-25 or Biogel [10–12]. Slurry packing under flow (flow packing) is routinely used for packing of chromatography material based on soft natural and synthetic polymers. The column is packed under a higher flow rate and pressure than applied during separation. Rigid particles are often dry-packed, but this depends on the particle size. The beads are filled into the column and are then compressed, a process also known as axial compression [13–17]. Such axial compression can be also applied for slurry packing, but is not feasible for ready-to-use columns because a piston is not part of the construction. Vibration of the column during packing may help to improve packing density. This technique has been successfully practiced for many years [18–20].

The standard parameters for controlling the packing quality of columns on all scales are HETP (Height Equivalent to a Theoretical Plate) and asymmetry [21,22]. HETP is a parameter which is independent of column length but depends on size of the particle, pore size, pore size distribution, particle porosity, velocity and the solute which is used for the experiment. When material dedicated for protein solution is tested with a small molecule tracer then the pore, pore size, pore size distribution and particle porosity is of less concern, because the molecules have a very high effective diffusivity. Asymmetry is another very good parameter to quantify the packing quality because it indicates if the packing density close to the column wall is lower or higher than in the center of the column. It is also a measure of the exponential wash out caused by extra column volume [23]. The experimental conditions to measure HETP and asymmetry must be standardized with respect to applied solute and velocity. It is also well known that the method of peak fitting may influence the outcome, e.g., graphical peak integration, numerical integration or fitting of the peak by a model function and calculation of variance and retention time based on the model. In addition to the experimental conditions, the data evaluation must be highly standardized in order to compare packing qualities among different experiments [24,25].

In order to see trends in a material property, a simple trend analysis can be performed. A simple but very effective way is to plot the property over time to visualize changes. The variation of the data can be assessed by, e.g., principal component analysis, which may help to identify co-variances. We received the performance data of 30,000 packing experiments of ready-to-use columns. Different chromatography media designed for purification of proteins and other large biomolecules were packed under standardized conditions. For each medium, an optimal procedure was developed by the column packing company. The packing quality was tested by injection of an aliquot of acetone and the retention time and peak width were determined from the peak profiles. The same procedure was used over the entire production period of approximately ten years. The injection of a small tracer molecule was selected since due to the large pores, only the hydrodynamic dispersion was measured. This dispersion is only influenced by the packing quality and the extra-column dispersion including the dispersion by the header and adapter.

An enormous challenge of this study was the extraction of the huge quantity of experimental data obtained from column testing. A proprietary closed-source software (Eurochrom) had been used to originally test the columns and to store the corresponding results. Eurochrom stores the data in a binary format and does not provide an API (application programming interface) that enables accessing the data via another program. Consequently, the column data could only be retrieved via Eurochrom's GUI (graphical user interface). For a small number of samples, a manual export is possible. However, the manual data export of 30,000 test runs which had been stored in 550 Eurochrom databases spread over 535,000 binary files was a very time consuming and error-prone process. Therefore, a computer software program was written in the programming language Perl with the module Win32:GuiTest which emulated mouse events and key strokes of a human computer user and utilized Eurochrom's GUI to automatically retrieve the column test data that had been generated over a period of ten years. After extraction, the data were read into the statistical computing environment R (https://www.r-project.org/) where the data was further processed, summarized, and visualized. Principal component analysis [26] was used to find the directions of the largest variations of the data, to visualize present structure in the data, and to detect outliers. This paper provides a useful and practical example of how preparative chromatography with ready-to-use columns can be standardized.

2. Materials and methods

2.1. Chromatography workstation and column packing

A chromatography workstation from Knauer, Berlin, Germany was used. The workstation was controlled by the Eurochrom software, which also handled data storage and peak analysis. Columns were packed by slurry packing under vibration.

2.2. Determination of HETP

HETP was measured by injection 50 μl of acetone or sodium nitrate and the UV 218 nm response was recorded. The chromatographic workstation automatically determined the number of plates N. From retention time (t) and N ($N = 5.54^{*} (t/W_{0.5})^2$) determined from the peak width measured at half peak height ($W_{0.5}$), the peak width (σ) was calculated by

$$\sigma = \sqrt{\frac{t^2}{N}} \tag{1}$$

An effective plate number was used for the data evaluation

$$N_{eff} = \left(\frac{t - t_0}{\sigma}\right)^2 \tag{2}$$

where t is the retention time, t_0 the dead time and σ^2 the variance.

Height equivalent to one theoretical plate (*HETP*) is defined as

$$HETP = L\frac{\sigma^2}{\mu^2} \tag{3}$$

with σ^2 the variance, L the column length, and μ the first peak moment. Reduced HETP (h) is obtained by dividing HETP by the particle diameter (d_p).

$$h = \frac{HETP}{d_p} \tag{4}$$

Asymmetry (A_s) was calculated at 10% peak height [27] with

$$A_s = \frac{b}{a} \tag{5}$$

a the width of the front part of the peak divided at peak maximum and b the width of the rear part.

Reduced velocity was calculated as

$$v = \frac{u \cdot d_p}{D_0} \tag{6}$$

with u the linear velocity, and D_0 the molecular diffusivity of the tracer molecule.

2.3. Data extraction

Test runs of approximately 30,000 columns were performed over a period of ten years using the proprietary closed-source software Eurochrom by Knauer GmbH. The Eurochrom software only runs on Microsoft operating systems (Windows XP and Windows 2000) and is no longer maintained. All column data records were stored in Eurochrom databases. Eurochrom databases use binary files to persistently store and retrieve data of the tested columns. All binary files belonging to a single database are located within a single directory. The name of a directory is identical to the database name. In total, 550 databases comprised approximately 535,000 binary files. The format specification of Eurochrom's binary files was not available.

Hence, we implemented a computer tool in the programming language Perl (https://www.perl.org/) which emulates a human computer user. Perl is a freely available high-level programming language that runs on all relevant operating systems, such as Linux/Unix, Mac OS, and Microsoft Windows. We used Strawberry Perl (http://strawberryperl.com) for this study. The implemented Perl program controls the input devices (keyboard and mouse) of the computer and is, therefore, able to perform any task that a human user can do. The core element of our program was the Perl module Win32:GuiTest which is available at CPAN Comprehensive Perl Archive Network (http://www.cpan.org/). CPAN is a huge repository of Perl modules that contains more than 150,000 freely available Perl modules.

The principle workflow of our program was as follows:

- Loop over all 550 Eurochrom databases (directories on Windows file system)
  - Start Eurochrom software
  - Open current database
  - Loop over all test runs of current database
    - Retrieve data from database for current test run
    - Export general information about test run (Report)
  - Close current database
  - Stop Eurochrom

The final output of our program was 30,000 exported report files and took approximately six days to complete. The output files of our program were simple plain text files which (a) can be edited by any text editor and (b) can be easily processed by any scripting programming language, such as Perl or Python. In a post-processing step, the 30,000 data files were aggregated to a single text data file. During this aggregation process the data records were checked for plausibility and any invalid data record was removed before the statistical analysis was started.

Emulating a human user is an extremely challenging task. This is especially true if the emulator has to react to unexpected events. For instance, dialog windows which might pop up at any time to inform the user about available security updates can easily result in a malfunction that (a) stops the automatic process of data extraction and (b) in the worst case, can irreparably damage the computer system by – for instance – accidentally deleting essential files. In order to avoid any unwanted side effects, we took the following measures: (i) uninstalled any software not required for the extraction of the column data; (ii) disabled all automatic notifications; (iii) implemented a feature that tracked the successfully exported databases and allowed us to restart the extraction process at the point where an error has occurred; and (iv) ran the data extraction on a virtual machine. A virtual machine has the advantage that the entire file system of the virtual machine is a single file on the host machine. Hence, backing up and restoring a virtual machine can simply be done by copying a single file on the guest machine. We used VirtualBox (https://www.virtualbox.org/) by Oracle for our virtualization approach. The virtual machine was running Windows XP and the host machine used a Linux Ubuntu 14.04.

Table 1
Summary of top 30 chromatography material studied.

Name	Counts	Functional mode
MEP HyperCel™	1442	Mixed
HEA HyperCel™	984	Mixed
PPA HyperCel™	946	Mixed
PROSEP® Ultra Plus	828	Affinity
Q Ceramic HyperD® F	812	Hydroxapatite
Q HyperCel™	775	AIEX
S HyperCel™	749	CIEX
MabSelect SuRe™	703	Affinity
Capto™ L	614	Affinity
Fractogel® EMD SO3- (M)	598	CIEX
UNOsphere™ Q	524	AIEX
Eshmuno® A	498	Affinity
Fractogel® EMD COO- (M)	495	CIEX
CM Ceramic HyperD® F	453	CIEX
Fractogel® EMD TMAE (M)	448	AIEX
Fractogel® EMD TMAE Hicap (M)	443	AIEX
Strep-Tactin® Superflow®	428	Affinity
HyperCel™ STAR AX	422	AIEX
Fractogel® EMD DEAE (M)	421	AIEX
Eshmuno® Q	413	AIEX
Fractogel® EMD SE Hicap (M)	403	CIEX
Eshmuno® CPX	398	CIEX
Fractogel® EMD DMAE (M)	367	AIEX
MabSelect™	365	Affinity
Strep-Tactin® Superflow® high capacity	347	Affinity
Eshmuno® S	344	CIEX
Eshmuno® HCX	336	AIEX
POROS® 50 HS	262	CIEX
Macro-Prep® CHT™ Type I 40 μm	260	Hydroxapatite
ProSep® Ultra Plus	257	Affinity

2.4. Data analysis

The data were read into R where duplicate entries and entries with missing information were removed. After these polishing steps, the data contained 24,951 chromatography runs. The available variables included time, chromatography material, particle size, column diameter and length, retention time, injection time, number of plates, and asymmetry. Additional variables such as reduced HETP and reduced velocity were calculated. Particle diameters were obtained from the manufacturer's information of the individual media. The data were summarized and visualized for each particle size, backbone, functional mode, and size of the columns. The 30 most frequently used chromatography materials in this study are listed in Table 1. The Supplementary material Table sub1 shows all materials included in the data.

A mosaic plot is a graphical display that allows one to examine the relationship among two categorical variables. The mosaic plot starts as a square with unit length one. The square is divided first into horizontal bars whose widths are proportional to the probabilities associated with the first categorical variable, in this case year. Then each bar is split vertically into bars that are proportional to the conditional probabilities of the second categorical variable, i.e., backbone and functional mode of the chromatography materials.

The size of the tiles is proportional to the cell frequency, i.e., the materials per categories, which have been tested per year. The cells are shaded in proportion to standardized residuals from the log-linear model that year and category (backbone and functional mode) are independent in this dataset, which is, of course, not the case. Thus, tiles shaded in dark blue are significantly larger than

expected whereas tiles shaded in dark red are significantly smaller than expected.

2.5. Principal component analysis

In principal component analysis (PCA) [26], a set of possibly correlated variables is converted by an orthogonal transformation to a set of uncorrelated variables called principal components. The number of principal components is less than or equal to the number of original variables. The first principal component accounts for as much of the variability in the data as possible, and each succeeding component, in turn, has the highest variance possible under the constraint that it is orthogonal to the preceding components. Here PCA was used to find directions of the largest variations of the data, to visualize present structures in the data, and to detect outliers.

3. Results and discussion

After data extraction and checking for inconsistencies, exploratory data analysis was performed. A trend analysis was generated showing the reduced HETP (h) of all chromatography materials irrespective of functionalization and backbone over a period of ten years (Fig. 1). The values of h were always in the range of 5 with slight variations over time and a decrease in the year 2012 and 2013. Data collection was stopped after January 2015. To prevent the possibility that the frequency of the individual chromatography materials within a certain time period could influence h, mosaic plots were generated.

We did not observe a clear trend that a single functionality was packed particularly often (Fig. 2A). However, we were able to detect several other trends. The most material was packed in 2013 and 2014 whereas in 2007 the least amount of material was packed. In the first years, lesser amounts of AF, AIEX and CIEX materials were packed whereas more HCIC and MMC materials were packed. The mosaic plot of materials according to backbone also showed trends (Fig. 2B). Compared to the other resin types, agarose-based materials were less frequently packed in the first 4 years and in the last year. Cellulose-based resins were packed more frequently in the first 4 years and polymethacrylate and poylvinlyether-based materials were increasingly applied during later years. Inorganic material was frequently packed in the beginning and then only rarely thereafter.

We then investigated if different categories showed differences in h in order to determine if the inhomogeneous frequency of materials influenced the data. Plotting h versus particle size allowed us to evaluate the quality of packing (Fig. 3A and B). Values of h did not depend on the particle size over a wide range, because theoretically one should obtain the same value assuming the reduced velocity (ReSc) is the same for all runs. In the present study, experimental conditions for measurement of HETP were selected in a way that the results can be expected to fall within the hydrodynamic dispersion region, v < 15, and not in the mass transfer limited region, v > 100 (Fig. 4) [28]. The pore size was at least 100 times larger than the size of the tracer molecules acetone or sodium nitrate, because all tested media are intended for separations of proteins and other large biomolecules. The velocities were in a moderate range so that a low reduced velocity can be expected. The same solute was used for one resin over the entire time period and the peak integration method was always identical. Thus, two major sources of error due to varied experimental set-up or data treatment can be excluded and observed variations can be assigned to packing quality only. The obtained results indicated that the smaller particles were more difficult to pack (Fig. 3A). It is a compromise to pack small particles in a ready-to-use column. A relevant difference cannot be observed for particles larger than 50 μm although all media showed significantly different values of h. This is simply explained by the large data set and because h is a unique feature of each chromatography material (Fig. 3). Resins with a particle diameter larger than 50 μm displayed values of h smaller than 5, except for 51.5, 74.5 and 136.5 μm particles, which were all Sephadex G-25 products. Sephadex G-25 is a very soft material with a substantial bed compression. This may be an explanation for this behaviour. Slightly different packing procedure has been proposed, but this method cannot be implemented in a large scale high throughput industrial packing line [10].

For the intended purpose of protein chromatography, the columns can be considered as well packed when h is in the range between 3–15 as shown in Fig. 1. For the actual experiments with proteins and other large biomolecules the columns will be operated in the mass transfer limited regime, where reduced velocity v is >100 and reduced HETP h for this class of molecules is >100. This is exemplified in Fig. 4 where the data are plotted together with reduced HETP h for proteins. The presented data for proteins have either been taken from the literature or from our own experimental results. Although columns can be considered as well packed for the intended purpose, the trends were investigated in more detail according to the categories of chromatography media sorted by their modes of functionalization (Fig. 5). The hydrophobic or electrostatic character of the beads may prevent a full consolidation of the bed to which extent the functionaliztation has an effect is not fully understood [29]. It is well understood that tamping or vibration improves bed consolidation [19,20]. This practice has been applied for all media, but dynamic axial compression cannot be applied for these small ready-to-use columns. The ready-to-use columns are not intended for high resolution separation, most frequently they are used for confirmation of screening results obtained with even smaller columns or batch adsorption studies made, for instance, in microtiter plates. Therefore, the determined packing quality of these ready-to-use columns serves the intended purpose. To gain greater insight, the data were also categorized according to the nature of the backbone. For each category of backbone, a much more detailed picture was obtained than when all packing data were pooled and analyzed. The backbone gave the biggest contribution to the packing quality. Although not fully understood, the density and surface roughness of the chromatographic media is determined by the nature of the backbone which can be composed of inorganic material, natural polymer, and organic polymer. Analyzing media of different backbone materials but the same functionalization (Fig. 5A) provided a more heterogeneous picture as compared to media of the same backbone differing in functionalization (Fig. 5B). Hydroxy apatite (HA) is difficult to pack [30], thus the variation in reduced HETP h is large but still within an accept-

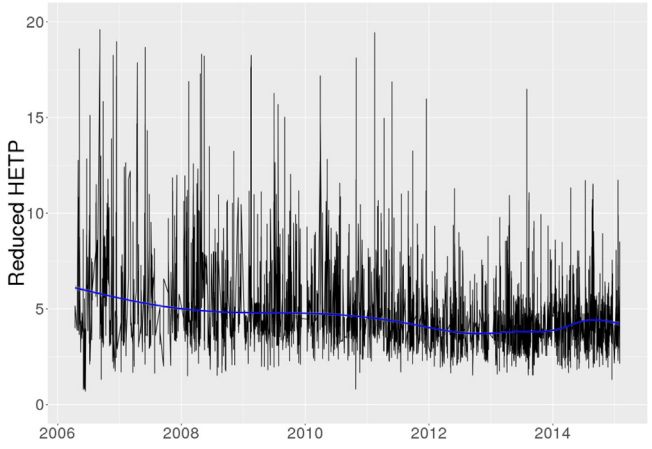

Fig. 1. Trendline of 24,626 ready-to use columns over a time span of 10 years. 325 columns with reduced HETP larger than 10 were not displayed in this figure.

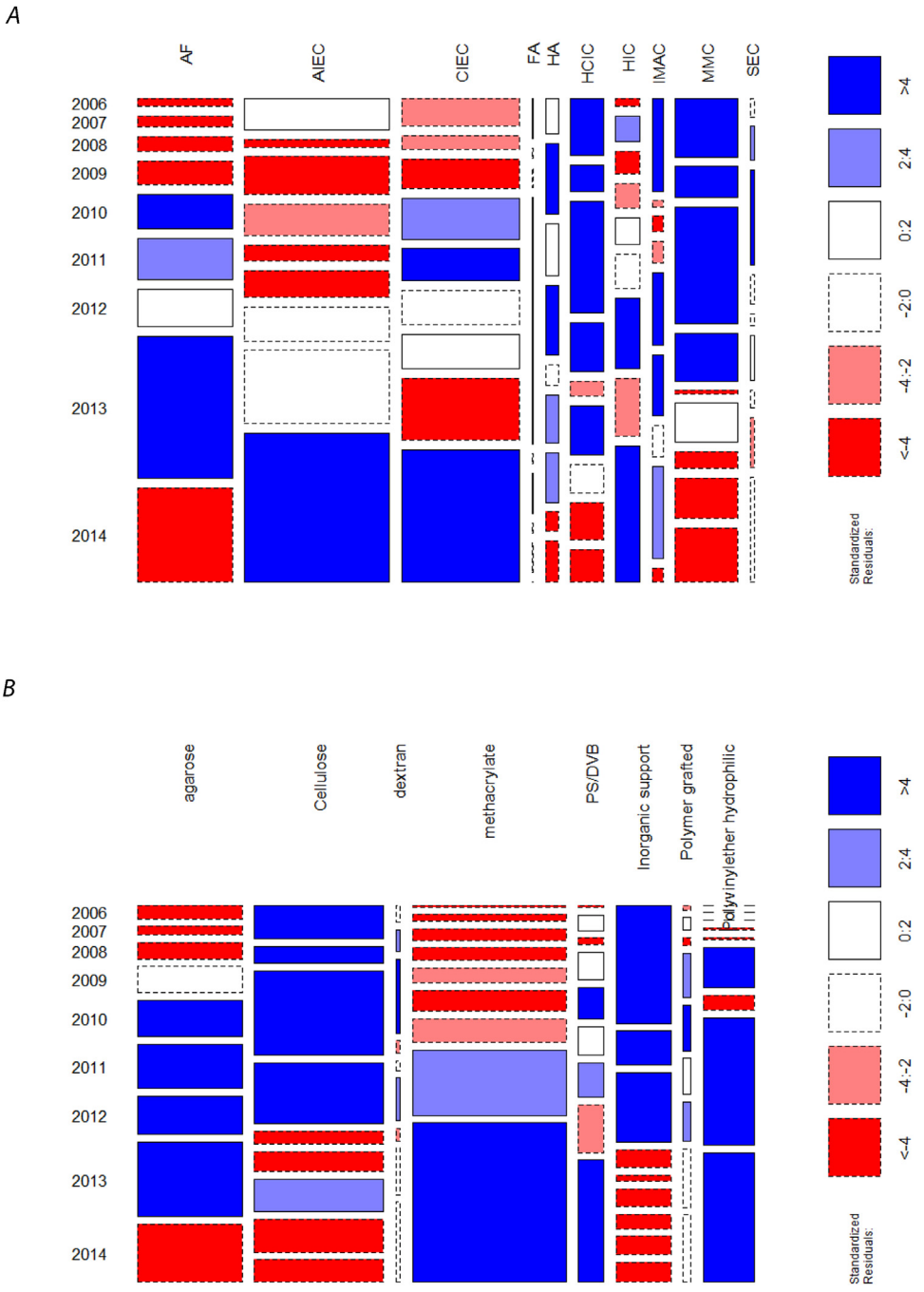

Fig. 2. Contingency table by year presented as a Mosaic plot categorized according to (A) functional chromatography modes and according to (B) composition of the backbone. The size of the tiles is proportional to the cell frequency, i.e., the materials per categories, which have been tested per year. The cells are shaded in proportion to standardized residuals. Tiles shaded in dark blue are significantly larger than expected whereas tiles shaded in dark red are significantly smaller than expected. (For interpretation of the references to color in this figure legend, the reader is referred to the web version of this article.)

able region for protein chromatography (Fig. 5A). Sorting all data by functionalization and year revealed a similar pattern for each year (Supplementary material Fig. sub2). This observation corroborated the trend-line shown in Fig. 1. We also plotted the reduced HETP (h) in relation to column volume, to examine if column size had an effect on packing quality (Fig. 6). No trend was observed; h did not change with column size.

A trend line was also generated for the asymmetry (Fig. 7) showing that this performance parameter was stable over the past ten years. The asymmetry is influenced by extra column band spreading and thus is influenced by the size of the column. The asymmetry clearly decreased with increasing column volume (Fig. 8). This effect could be caused by either extra column effects or because small columns are more difficult to pack. We have previously shown that up to 90% of the peak broadening in small columns is generated by extra column effects [23].

Principal component analysis was applied to investigate the structure of the data. In order to reduce the huge data size of almost 25,000 datapoints all (1116) unique resin-diameter-length combinations were formed and mean values for reduced HETP (h) and asymmetry were used as metric parameters in PCA together with particle size, column diameter and length. A biplot (Fig. 9) presents both the observations and variables of a matrix of the multivariate data on the same plot. The data are projected on two principal com-

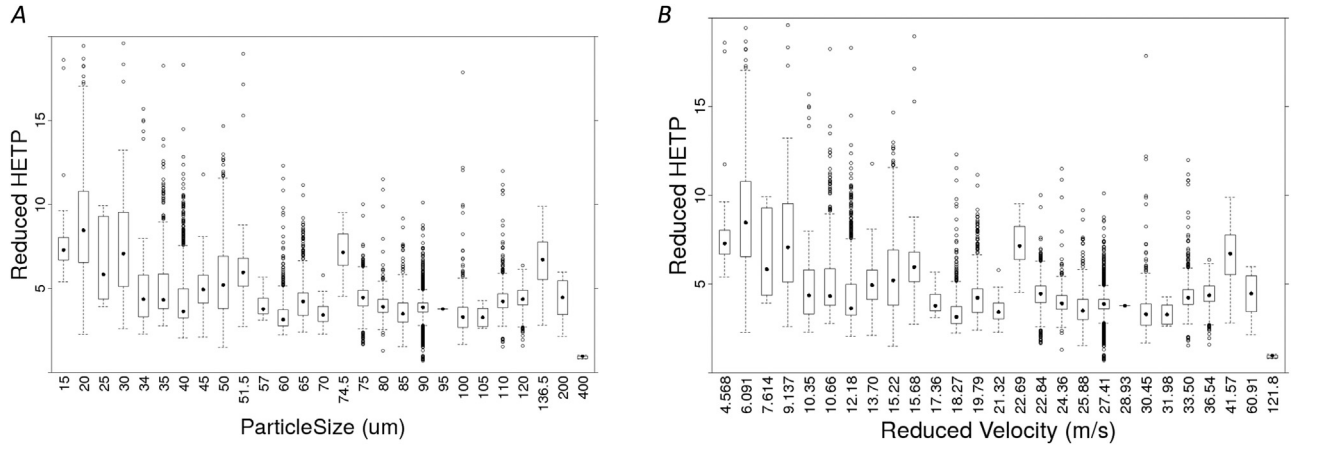

Fig. 3. Box and Whisker Plot for h versus particle size (A) and h versus reduced velocity (B); note that the distances between the particle sizes and reduced velocities are not equal.

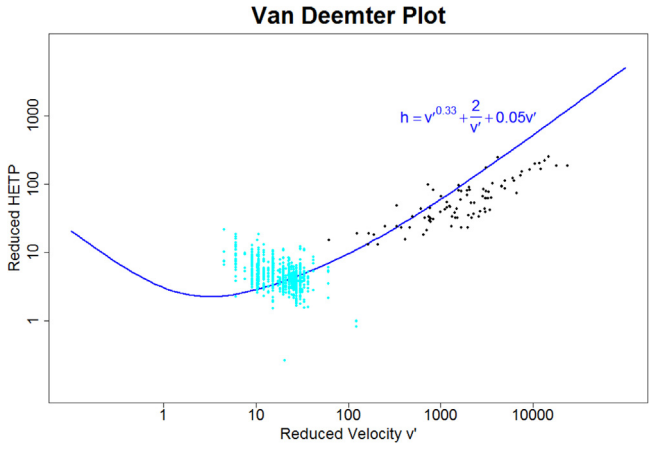

Fig. 4. Reduced HETP of acetone and selected examples for reduced HETP of proteins. The curve shown in blue is the generalized Van Deemter curve. The analyzed data set using a small molecule as tracer is shown in turquois and reduced HETP data for proteins are shown in black. These dots were reconstructed from the literature and from experiments in our laboratory and were measured for various resins (Source 30S, SP Sepharose FF, Fractogel EMD, POROS 50 HS, POROS Q/M, CaptoS and UNOSphereS) and proteins (lysozyme, bovine thyroglobulin, immunoglobulin G, myoglobulin, ovalbumin, bovine serum albumin, human serum albumin and cytochrome c). (For interpretation of the references to color in this figure legend, the reader is referred to the web version of this article.)

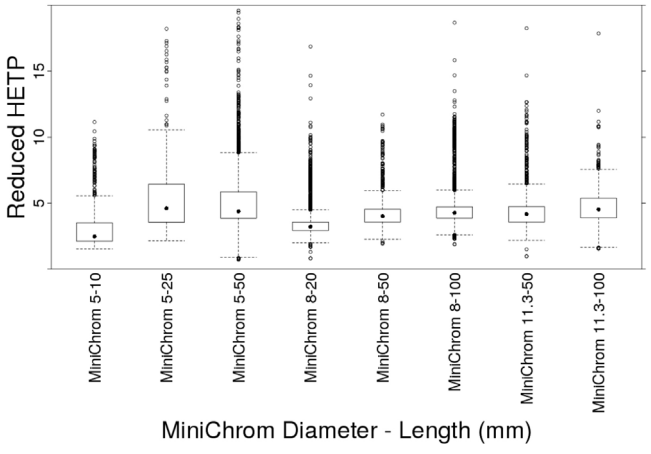

Fig. 6. Reduced HETP by the size of the columns.

ponents (PC), in this case the first and second PC are used, which accounts for 64% of the variance explained. The direction of the variables, here reduced HETP (h), asymmetry, particle size, column length, and diameter, are given by the blue arrows. The farther away from the center an observation is located, the larger the impact of the closest variable on the observation. The observations are all placed in one big cloud with single outliers in the directions of all

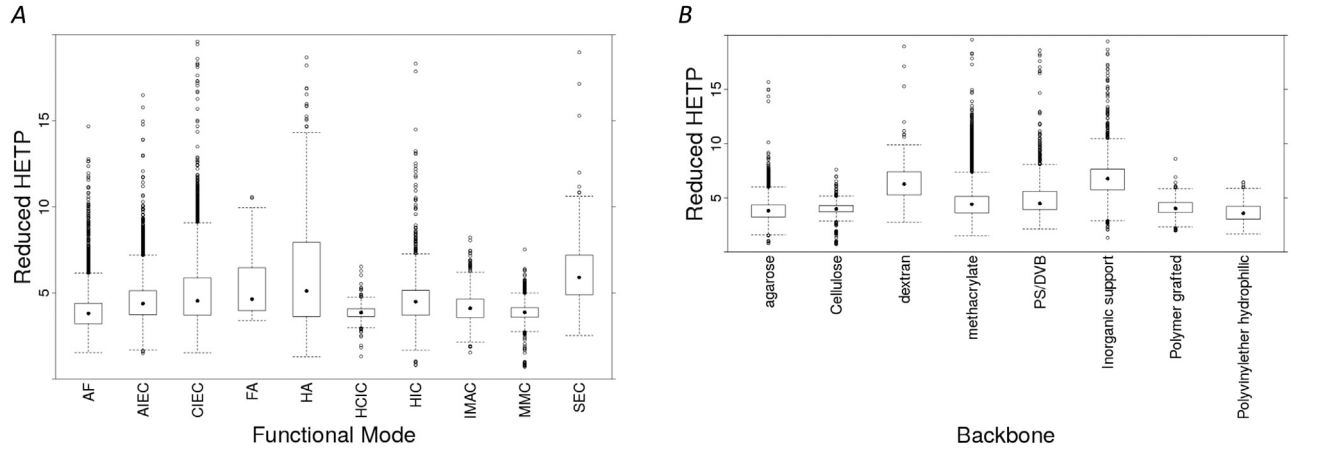

Fig. 5. Trend Analysis Boxplots of Reduced HETP by Functional Mode.

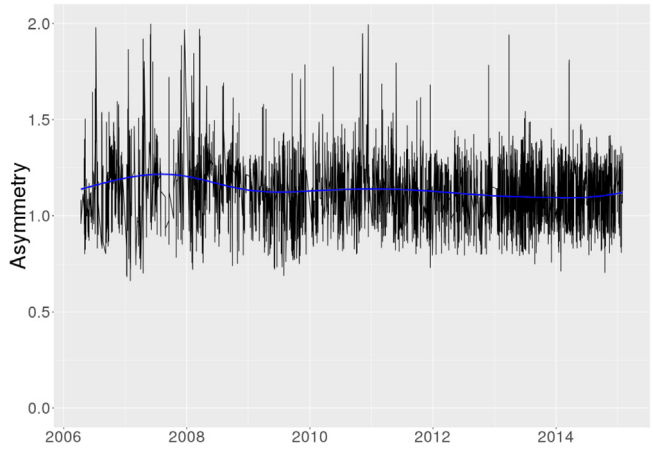

Fig. 7. Trend Analysis of Asymmetry (Tailing factor) over time.

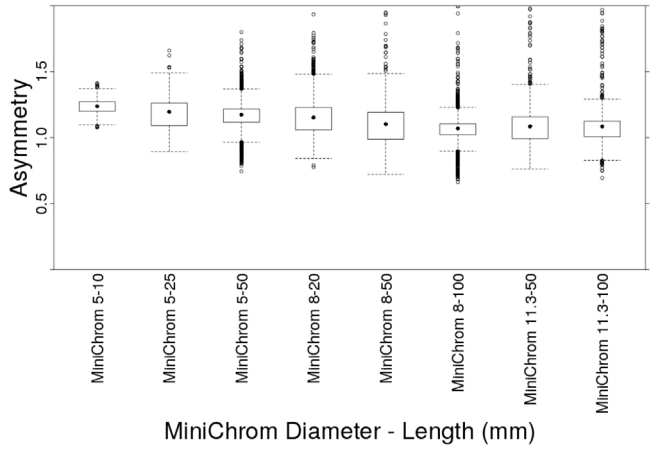

Fig. 8. Asymmetry plotted versus the size of the columns.

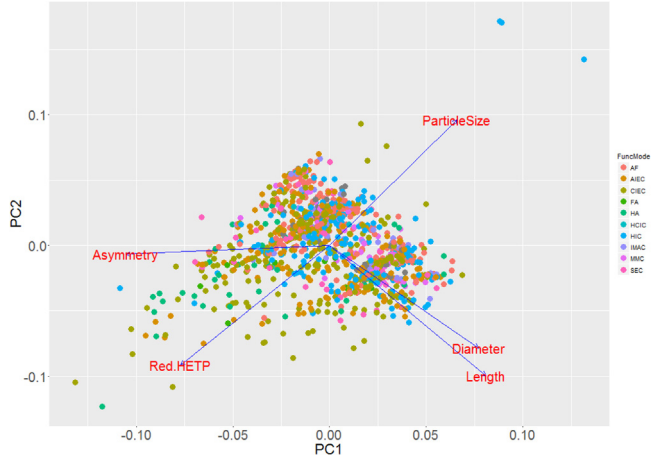

Fig. 9. PCA to identify variables influencing quality of packing. The directions of the variables reduced HETP (h), asymmetry, particle size, column length, and diameter, are given by the blue arrows. The left and bottom axis show the data projected to the first and second principal components (PC1 and PC2). (For interpretation of the references to color in this figure legend, the reader is referred to the web version of this article.)

variables. This PCA showed that all packing materials clustered very well.

Theoretical analysis from Schure and Maier [31] showed that the column packing procedure must prevent the formation of defective sites leading to inhomogeneous packing rather than aiming for the highest packing density. Guiochon and colleagues concluded that a "well packed column is not optimal packed, it is reproducible" [32]. In this respect, the investigated large number of columns were well packed over an impressively long period of time, 25,000 columns over ten years.

4. Conclusion

The statistical evaluation of the quality parameters of reduced HETP and asymmetry of 25,000 different ready-to-use columns showed they were well packed. Variations in reduced HETP were higher than variations in asymmetry, which is influenced by the column geometry and design. The functional mode did not influence the packing quality. However, we observed a connection between packing quality and the composition of the resin backbone. Asymmetry slightly decreased with increasing size of the column. For their intended purpose as ready-to-use columns, reproducible packing quality has been observed over one decade, since these types of columns became commercially available.

Acknowledgements

This work has been supported by the Federal Ministry of Science, Research and Economy (BMWFW), the Federal Ministry of Traffic, Innovation and Technology (bmvit), the Styrian Business Promotion Agency SFG, the Standortagentur Tirol, the Government of Lower Austria and ZIT – Technology Agency of the City of Vienna through the COMET-Funding Program managed by the Austrian Research Promotion Agency FFG.

Appendix A. Supplementary data

Supplementary data associated with this article can be found, in the online version, at http://dx.doi.org/10.1016/j.chroma.2016.07.054.

References

[1] V. Brenac Brochier, H. Chabre, A. Lautrette, V. Ravault, M.N. Couret, A. Didierlaurent, P. Moingeon, High throughput screening of mixed-mode sorbents and optimisation using pre-packed lab-scale columns for the purification of the recombinant allergen rBet v 1a, J. Chromatogr. B 877 (2009) 2420–2427.
[2] J. Friedle, Chromatography media scouting, Eur. Biotechnol. Sci. Ind. News 7 (2008) 41–42.
[3] T. Schroeder, Automated parallel chromatography in downstream process development, Bioprocess Int. 8 (2010) 92–93.
[4] K.M. Łacki, High-throughput process development of chromatography steps: advantages and limitations of different formats used, Biotechnol. J. 7 (2012) 1192–1202.
[5] X. Li, G. de Roo, K. Burgers, M. Ottens, M. Eppink, Self-packed filter plates: a good alternative for pre-packed filter plates for developing purification processes for therapeutic proteins, Biotechnol. J. 7 (2012) 1269–1276.
[6] N. Sanaie, D. Cecchini, J. Pieracci, Applying high-throughput methods to develop a purification process for a highly glycosylated protein, Biotechnol. J. 7 (2012) 1242–1255.
[7] I. Demongodin, N. Sauer, L. Truffet, Performance evaluation in manufacturing systems, in: M. Diaz (Ed.), Petri Nets, Fundamental Models, Verifcatrion and Applications, John Wiley & Sons, Inc., Hoboken, NJ, USA, 2009, pp. 527–578.
[8] A. Jungbauer, Chromatographic media for bioseparation, J. Chromatogr. A 1065 (2005) 3–12.
[9] V. Wong, R.A. Shalliker, G. Guiochon, Evaluation of the uniformity of analytical-size chromatography columns prepared by the downward packing of particulate slurries, Anal. Chem. 76 (2004) 2601–2608.
[10] M.B. Baru, A.V. Danilov, I.V. Vagenina, Size exclusion chromatography on soft and semi-rigid packing materials in the dynamic axial compression mode, J. Biochem. Biophys. Methods 57 (2003) 115–142.
[11] A.V. Danilov, L.G. Mustaeva, I.V. Vagenina, M.B. Baru, Size-exclusion chromatography on soft packing material under axial compression, J. Chromatogr. A 732 (1996) 17–25.
[12] I.V. Vagenina, E.A. Kozlovsky, L.G. Mustaeva, E.Y. Gorbunova, M.B. Baru, Size exclusion chromatography of polypeptides on Bio-Gel P2 in the dynamic axial compression mode, J. Chromatogr. A 840 (1999) 281–288.

[13] D.E. Cherrak, M. Al-Bokari, E.C. Drumm, G. Guiochon, Behavior of packing materials in axially compressed chromatographic columns, J. Chromatogr. A 943 (2002) 15–31.
[14] D.E. Cherrak, G. Guiochon, Phenomenological study of the bed-wall friction in axially compressed packed chromatographic columns, J. Chromatogr. A 911 (2001) 147–166.
[15] G. Guiochon, T. Farkas, H. Guan-Sajonz, J.H. Koh, M. Sarker, B.J. Stanley, T. Yun, Consolidation of particle beds and packing of chromatographic columns, J. Chromatogr. A 762 (1997) 83–88.
[16] J.H. Koh, B.S. Broyles, H. Guan-Sajonz, M.Z.C. Hu, G. Guiochon, Consolidation and column performance of several packing materials for liquid chromatography in a dynamic axial compression column, J. Chromatogr. A 813 (1998) 223–238.
[17] J.H. Koh, G. Guiochon, Effect of the column length on the characteristics of the packed bed and the column efficiency in a dynamic axial compression column, J. Chromatogr. A 796 (1998) 41–57.
[18] M. Kamiński, J. Klawiter, J.S. Kowalsczyk, Investigation of the relationship between packing methods and efficiency of preparative columns. II. Characteristics of the slurry method of packing chromatographic columns, J. Chromatogr. A 243 (1982) 225–244.
[19] S.C. Siu, C. Chia, Y. Mok, P. Pattnaik, Packing of large-scale chromatography columns with irregularly shaped glass based resins using a stop-flow method, Biotechnol. Progr. 30 (2014) 1319–1325.
[20] J. Klawiter, M. Kamiński, J.S. Kowalczyk, Investigation of the relationship between packing methods and efficiency of preparative columns. I. Characteristics of the tamping method for packing preparative columns, J. Chromatogr. A 243 (1982) 207–224.
[21] O. Kaltenbrunner, P. Watler, S. Yamamoto, Column qualification in process ion-exchange chromatography, Progr. Biotechnol. (2000) 201–206.
[22] A.S. Rathore, R.M. Kennedy, J.K. O'Donnell, I. Bemberis, O. Kaltenbrunner, Qualification of a chromatographic column: why and how to do it, BioPharm Int. 16 (2003) 30–40.
[23] O. Kaltenbrunner, A. Jungbauer, S. Yamamoto, Prediction of the preparative chromatography performance with a very small column, J. Chromatogr. A 760 (1997) 41–53.
[24] N. Dyson, Digital measurementof peak areas, in: R. Smith (Ed.), RSC Chromatography Monographs, The Royal Society of Chemistry, Hertfordshire, UK, 1990, pp. 140–192.
[25] N. Dyson, Peak distortion, data sampling errors and the integrator in the measurement of very narrow chromatographic peaks, J. Chromatogr. A 842 (1999) 321–340.
[26] K. Varmuza, P. Filzmoser, Introduction to Multivariate Data Analysis in Chemometrics, CRC Press, Boca Ranton, FL, 2009.
[27] J.J. Kirkland, W.W. Yau, H.J. Stoklosa, C.H. Dilks Jr., Sampling and extra-column effects in high-performance liquid chromatography; influence of peak skew on plate count calculations, J. Chromatogr. Sci. 15 (1977) 303–316.
[28] J.C. Giddings, Reduced plate height equation: a common link between chromatographic methods, J. Chromatogr. A 13 (1964) 301–304.
[29] J.J. Stickel, A. Fotopoulos, Pressure-flow relationships for packed beds of compressible chromatography media at laboratory and production scale, Biotechnol. Progr. 17 (2001) 744–751.
[30] J.T. McCue, D. Cecchini, K. Hawkins, E. Dolinski, Use of an alternative scale-down approach to predict and extend hydroxyapatite column lifetimes, J. Chromatogr. A 1165 (2007) 78–85.
[31] M.R. Schure, R.S. Maier, How does column packing microstructure affect column efficiency in liquid chromatography? J. Chromatogr. A 1126 (2006) 58–69.
[32] B.J. Stanley, C.R. Foster, G. Guiochon, On the reproducibility of column performance in liquid chromatography and the role of the packing density, J. Chromatogr. A 761 (1997) 41–51.

PUBLICATION II

Journal of Chromatography A, 1527 (2017) 70–79

Contents lists available at ScienceDirect

Journal of Chromatography A

journal homepage: www.elsevier.com/locate/chroma

Full length article

Column-to-column packing variation of disposable pre-packed columns for protein chromatography

Susanne Schweiger[a], Stephan Hinterberger[a], Alois Jungbauer[a,b,*]

[a] Austrian Centre of Industrial Biotechnology, Vienna, Austria
[b] Department of Biotechnology, University of Natural Resources and Life Sciences Vienna, Austria

ARTICLE INFO

Article history:
Received 9 August 2017
Received in revised form 23 October 2017
Accepted 24 October 2017
Available online 26 October 2017

Keywords:
Preparative chromatography
Peak analysis
Column qualification
Measurement precision
Packing variation
Column geometry
Aspect ratio
Column performance

ABSTRACT

In the biopharmaceutical industry, pre-packed columns are the standard for process development, but they must be qualified before use in experimental studies to confirm the required performance of the packed bed. Column qualification is commonly done by pulse response experiments and depends highly on the experimental testing conditions. Additionally, the peak analysis method, the variation in the 3D packing structure of the bed, and the measurement precision of the workstation influence the outcome of qualification runs. While a full body of literature on these factors is available for HPLC columns, no comparable studies exist for preparative columns for protein chromatography. We quantified the influence of these parameters for commercially available pre-packed and self-packed columns of disposable and non-disposable design. Pulse response experiments were performed on 105 preparative chromatography columns with volumes of 0.2–20 ml. The analyte acetone was studied at six different superficial velocities (30, 60, 100, 150, 250 and 500 cm/h). The column-to-column packing variation between disposable pre-packed columns of different diameter-length combinations varied by 10–15%, which was acceptable for the intended use. The column-to-column variation cannot be explained by the packing density, but is interpreted as a difference in particle arrangement in the column. Since it was possible to determine differences in the column-to-column performance, we concluded that the columns were well-packed. The measurement precision of the chromatography workstation was independent of the column volume and was in a range of ± 0.01 ml for the first peak moment and ± 0.007 ml^2 for the second moment. The measurement precision must be considered for small columns in the range of 2 ml or less. The efficiency of disposable pre-packed columns was equal or better than that of self-packed columns.

1. Introduction

Small scale columns of up to 20 ml are frequently used in biomanufacturing for process development, scale-down studies, exploration of the design space, and troubleshooting. For preparative separations, columns can either be bought as ready-to-use pre-packed columns or they are packed by the user himself. In the latter cases, only the bulk resin and the empty column hardware are bought from the manufacturer. Pre-packed preparative columns have become popular because the laborious column packing can be outsourced [1]. Pre-packed columns are available in non-disposable and disposable designs. Non-disposable columns are made of high quality materials such as glass walls and could be re-packed with a different medium by the customer, similar to self-packed columns. In comparison, disposable columns are made of cheaper materials such as polypropylene and cannot be re-packed. If the column lifetime is over, they are discared. Disposable columns must be simple and easy to manufacture in order to yield affordable columns. Self-packed chromatography columns are commonly tested before use to check the packing quality and to identify defects in order to ensure the reproducibility of runs. Frequently, pre-packed columns are used by customers with only limited additional qualification since the columns are assumed to have the same packing quality. However, only limited information is available to prove this assumption for preparative chromatography columns on the process development scale [2]. Differences in the column-to-column performance were investigated only for process-scale chromatography columns with diameters larger than 40 cm [3,4]. Ample of literature is also available for analytical [5–10], semi-preparative and preparative HPLC columns [11,12]. The column-to-column variation is more pronounced than the

* Corresponding author at: University of Natural Resources and Life Sciences, Department of Biotechnology, Muthgasse 18, 1190 Wien, Austria.
E-mail address: alois.jungbauer@boku.ac.at (A. Jungbauer).

https://doi.org/10.1016/j.chroma.2017.10.059

change of the column performance with time [11]. To our knowledge, a comparison of the packing quality of pre-packed columns to that of self-packed columns has not been performed.

The packed bed itself is highly heterogeneous in both the axial and radial directions [13–15]. The more homogeneous the packing, the lower the peak dispersion, measured either as height equivalent to a theoretical plate (H) or skewness [16]. It is known that the packing method [17] and the properties of the chromatography medium [2,18] influence the structure of the packed bed. Furthermore, the material [19,20] and the surface properties [21] of the column wall have an influence on column performance since they change the packing behavior. The packing density is an important factor to consider for evaluation of the column performance. It influences peak retention and width, since it is directly related to the extra particle porosity. Apart from the packed bed, the column performance also depends on the design of the column header [22] as well as on frits and filters [23].

Column performance is typically qualified by pulse response experiments of a small non-interacting solute. For small molecules, the main factor controlling column performance is hydrodynamic dispersion and not mass transfer. This allows evaluation of the column packing, which would be impossible with a biomacromolecule. It is assumed when the column is packed well enough to give good performance values for small molecules, it is also suitable for biomacromolecules. Pulse response experiments are highly dependent on the type of experimental testing set-up used and the method of peak analysis. The testing solute has an impact on the peak shape [24] and therefore must be kept constant for comparative studies. The amount of the injected sample affects the statistical moments of a peak [25] and peak analysis is also influenced by noise and baseline drift [26–29]. Proper baseline correction and setting of the integration intervals still allows the determination of higher moments with a good accuracy [30]. The two most commonly used peak analysis methods are direct numerical integration and peak fitting to a predefined function. The exponentially modified Gaussian (EMG) function [31,32] is the most popular function for peak fitting and provides robust results [33], especially for peaks with high experimental noise. The EMG was derived by convolution of a Gaussian peak with an exponential decay function. However, there is no physical reason, why a peak should follow the shape of an EMG [34]. Therefore, it fails to fit severe cases of tailing or fronting [34]. The peak parameters determined by EMG fitting can only be as good as the fit and hence do not reflect the real peak properties when the fit is bad. In comparison, direct numerical integration provides the most exact results [33], presuming the baseline drift is moderate and the data are smooth and without any noise.

In this study, we analyzed the performance of 0.2–20.0 ml pre-packed and self-packed preparative chromatography columns of different lengths and diameters that had been packed with different chromatography media in order to shed light on the scale-down of protein chromatography. The columns have been tested by injection of a non-interacting solute at different flow rates. The peak was evaluated by numerical integration and EMG fitting and the first and second peak moments and peak skewness were calculated and statistically evaluated with respect to column-to-column variation, measurement precision of the workstation, column types, and column dimensions.

2. Material and methods

2.1. Chemicals

Tris and sodium chloride were purchased from Merck Millipore and acetone was obtained from VWR chemicals. Silica particles (surface plain, size 1 μm, 50 mg/ml suspension in water) were purchased from Kisker Biotech GmbH & Co KG.

2.2. Columns

Pre-packed MiniChrom and ValiChrom columns from Repligen (previously Atoll) were used. MiniChrom columns are of disposable design while ValiChrom columns are non-disposable columns. The walls of the MiniChrom columns are made of polypropylene, while the ValiChrom columns are made of glass. The adapters of both column types are designed differently and have different volumes. The disposable columns are available at 2–3 pre-defined lengths. In contrast, the non-disposable columns are custom-made with any required length. All pre-packed columns have the same frit and filter at the top and at the bottom of the column (polypropylene/polyethylene fibre, weight 200 g/m^2, thickness 0.42 mm). The columns were packed with 4 different media: MabSelect SuRe (GE Healthcare, 85 μm particle diameter), Toyopearl Gigacap S–650 M (Tosoh, 75 μm particle diameter), Toyopearl SP–650 M (Tosoh, 65 μm particle diameter) and Toyopearl Phenyl–650 M (Tosoh, 65 μm particle diameter). MabSelect SuRe is a compressible Protein A medium with highly cross-linked agarose as backbone. Both, Toyopearl Gigacap S–650 M and Toyopearl SP–650 M media are strong cation exchange media with a methacrylate backbone. The Gigacap resin has an additional polymer linker between the backbone and the sulfopropyl functionalization. Toyopearl Phenyl–650 M has the same backbone as SP–650 M but is a hydrophobic interaction medium since it is functionalized with a phenyl ligand group. MiniChrom columns were supplied in complete sets of all available column sizes with the following diameter-length combinations (in mm): 5–10, 5–25, 5–50, 8–20, 8–50, 8–100, 11.3–50 and 11.3–100. Each of those column dimensions was delivered three times pre-packed with either MabSelect SuRe or Toyopearl Gigacap S–650 M. Three additional columns packed with MabSelect SuRe were available in the 11.3–50 dimension. Each column dimension was available once pre-packed with Toyopearl SP–650 M and Toyopearl Phenyl–650 M. ValiChrom columns packed with MabSelect SuRe and Toyopearl SP–650 M were delivered in the following diameter-length combinations (in mm): 5–100, 5–150, 5–200, 8–150, 8–200, 8–250, 11.3–100, 11.3–150 and 11.3–200. ValiChrom columns packed with Toyopearl Phenyl–650 M were available in the following diameter-length combinations (in mm): 5–100, 5–200, 8–150, 8–200, 11.3–150 and 11.3–200.

Additionally, we packed columns in our laboratory with MabSelect SuRe and Toyopearl Gigacap S–650 M using Tricorn 5 columns (GE Healthcare). They are designed as non-disposable columns with a diameter of 5 mm. Tricorn 5 filters (ethylene propylene diene/polyethylene, porosity 7 μm, thickness 1.35 mm) were used at the top and at the bottom of the columns without any frits. The columns were packed according to optimized packing protocols with bed heights in the range of 12–162 mm.

The described columns will hereafter be referred to as pre-packed disposable (MiniChrom), pre-packed non-disposable (ValiChrom), and self-packed (Tricorn) columns.

2.3. Workstation

An ÄKTA™ pure 25 M2 chromatography system (GE Healthcare) was used, which was controlled with Unicorn software 6.4. The extra column tubing between the pumps, valves, and detectors was used as provided by the manufacturer. The samples were injected via an injection loop. The injection valve has a total volume of 44 μl and the column valve of 110 μl. The detection cell of the UV detector has a volume of 15 μl. The tubing from the column valve to the column and back was varied based on the column type used. Tubings with an ID of 0.25 mm and a length of

234 mm from the column valve to the column and 179.5 mm from the column outlet to the column valve were used for pre-packed disposable columns, for pre-packed non-disposable columns with diameter-length combinations of 5–100 and 5–150 and for self-packed columns. For pre-packed non-disposable columns with the diameter-length combinations of 5–200, 8–150, 8–200, 8–250, 11.3–100, 11.3–150 and 11.3–200, the tubing from the column to the column valve was 331 mm in length.

The extra column volume and band broadening was determined by injections of acetone through the workstation including the tubing to and from the column, which was connected by a PEEK connector, 0.010" thru-hole and 0.07 μl volume. The influence of extra column volume and band broadening is shown in the Supplementary Material. For very small columns the extra column volume was even larger than the column volume and also extra column band broadening was very high.

2.4. Pulse response experiments

Column performance was evaluated in triplicate by pulse response experiments at different superficial velocities (30, 60, 100, 150, 250 and 500 cm/h). Acetone (1%, v/v) was used for the pulse. The injected pulse volumes were 10 μl for all pre-packed disposable columns, pre-packed non-disposable columns with 5 mm ID, and self-packed columns, 50 μl for pre-packed non-disposable columns with 8 mm ID, and 500 μl for pre-packed non-disposable columns with 11.3 mm ID. For pulses through the extra column volume only, 10 μl were injected at all the used flow rates. The running buffer was 50 mM Tris, 0.9% (w/v) sodium chloride pH 8.0 (pH adjusted with hydrogen chloride).

2.5. Determination of extra particle porosity

The extra particle porosity of the pre-packed disposable columns was determined by injection of silica nanoparticles (surface plain) with a diameter of 1000 nm. Silica nanoparticles (50 μl) were injected to the MabSelect SuRe columns and 10 μl to the Gigacap S–650 M columns with a concentration of 50 mg/ml. Purified water was used as a running buffer at a superficial velocity of 250 cm/h. The extra column volume was determined by injections through the workstation and the tubing ranging to and from the column at the respective flow rates. The retention volume at peak maximum was used for calculation of the extra particle porosity.

2.6. Peak analysis

The peaks were automatically analyzed with a script written in the statistical software R. The script was optimized for peaks obtained by pulse response experiments and runs stably for data with only one main peak and few smaller peaks, which were baseline separated. The peak analysis process started with a data reduction step to about 1000 data points, then several peaks were detected and were fitted to a linear baseline through non-peak data points. Another peak detection step was performed with the baseline corrected data. For peak detection, the data were smoothed and the first derivative of the data, the slope, was calculated over a window size of 30 data points. Two threshold levels were set: level ± 1 at ± 0.5% of the maximum peak height and level ± 2 at ± 5% of the maximum peak height. As soon as the derivative of the signal increased above level 2 and returned to level −2 from the negative, a peak was detected. The detected peak then started at level 1 and ended at level −1. A peak was defined to have a width of at least 30 data points to make the script more robust. For calculation of the peak maximum, the data were smoothed in order to correct for small fluctuations of the output signal, which might bias the peak maximum. The peak was integrated from the baseline between its detected start to its end points. The calculation of the peak moments is described in Section 3, Theory. For direct numerical integration, the statistical moments of the peaks were calculated as stated in [38]. The moments were corrected for the extra column contributions to peak retention and broadening considering the different tubing lengths for each column dimension. Finally, the second moment was corrected for the different injection volumes by substracting the contribution of the rectangular injection pulse.

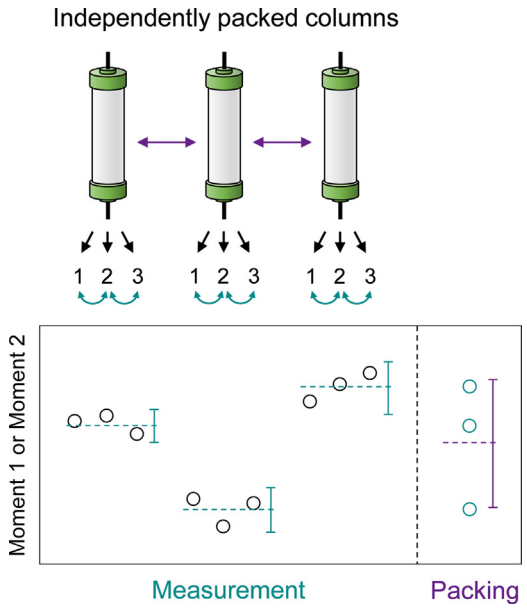

Fig. 1. Schematic distinction between measurement precision (lower left panel, blue) and the packing variation (lower right panel, violet). Every column was tested in triplicates. The variation in the triplicate measurements (blue arrows) gives information on the measurement precision. The difference between three individually packed columns gives information on the packing variation (violet arrows). Each circle represents one measurement point. The measurement precision was evaluated in terms of mean (blue dashed lines) and standard deviation (blue error bars) for each column separately. The packing variation was calculated based on the means of the triplicate measurements of the individual columns (blue circles). Again, the mean (violet dashed line) and the standard deviation (violet error bar) were considered. (For interpretation of the references to colour in this figure legend, the reader is referred to the web version of this article.)

2.7. Determination of measurement and column-to-column packing variation

Three independently packed pre-packed disposable columns were available at different dimensions packed with MabSelect SuRe and Gigacap S–650 M. All columns were packed in the same column type with the same optimized method, with the only difference being the structure of the packed bed. Every column was tested in triplicate. Considering each column separately, the mean and the standard deviation of the triplicate measurements described the measurement precision of the system (see Fig. 1). Columns were excluded for determination of the measurement precision if only duplicate or single measurements were available. The packing variation can be calculated by comparing the results of the different columns. For well-packed columns, the column-to column variation is higher than the same-column repeatability [11]. The packing variation was calculated by comparing the mean of the triplicate measurements for each column. If the means were close together, the packing was rather similar, so the results were easily reproducible. As a measure of the variance of the column means, and so for the different packings, the total mean with the respective standard deviation was determined (Fig. 1). A low standard devia-

tion indicated high column-to-column packing repeatability. This procedure was done separately for each column diameter-length combination for both media. Only columns available three times with triplicate measurements were considered for the analysis (9 data points per diameter-length combination). The calculation of the measurement precision and the column-to-column variation was made for the peaks analyzed by direct numerical integration.

2.8. Statistical testing

Statistical tests were done in the statistical software R. The data were tested for statistical significance using analysis of variance (ANOVA), Student's *t*-tests, or linear regression. The assumption of normal distribution of the residuals was confirmed using the Kolmogorov-Smirnov test. P-values smaller than 0.05 were considered significant. The *p*-values of paired *t*-tests were adjusted with the Bonferroni method. Principal component analysis was used to describe the largest variations in the data (Supplementary Material). The variables were centered and scaled for the principal component analysis.

3. Theory

The statistical moments of the peaks were determined by direct numerical integration. The first moment (M_1) is the mean retention volume of a peak. The second moment (M_2) is the variance of a peak and is a measure of peak width around its center of gravity. It is used as a measure for column efficiency. The determined first and second moments were corrected by the contributions of the extra column volume to the first and second moments. Besides, the second moment was corrected for contributions of the different injection volumes using the following equation

$$\sigma_{inj}^2 = \frac{V_{inj}^2}{12}$$

where ${\sigma_{inj}}^2$ is the peak variance arising from the injection of a rectangular sample plug and V_{inj} is the injection volume.

The third moment (M_3) is a measure for peak asymmetry. The degree of asymmetry is described by the peak skewness, which was calculated by

$$skew = \frac{M_3}{{M_2}^{3/2}} \quad (5)$$

The peak skewness is negative for fronting peaks, zero for symmetrical peaks, and positive for tailing peaks. The skewness was not corrected for contributions of the extra column volume.

The height equivalent to theoretical plate (H) was calculated by

$$H = \frac{M_2 * L}{M_1^2} \quad (6)$$

where L is the column length. Column efficiency was evaluated in terms of reduced HETP (h), which was by calculated by

$$h = \frac{H}{d_p} \quad (7)$$

where d_p is the particle diameter of the medium. The nominal particle diameters were used for the calculations as provided by the medium manufacturers. The reduced velocity u' was calculated by

$$u' = \frac{u * d_p}{D_0} \quad (8)$$

where u is the superficial velocity and D_0 is the molecular diffusivity of acetone with $1.16 * 10^{-5}$ cm^2/s.

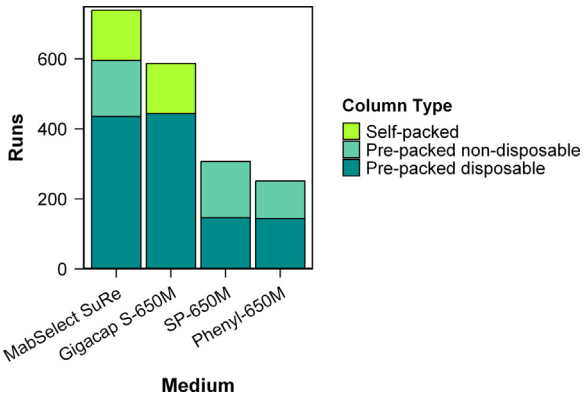

Fig. 2. Number of runs for each of the chromatography media and column types.

The column aspect ratio was calculated by

$$Column\ aspect\ ratio = \frac{L}{d_c} \quad (9)$$

where d_c is the column diameter. The bed aspect ratio was calculated by

$$Bed\ \ aspect\ ratio = \frac{d_c}{d_p} \quad (10)$$

4. Results and discussion

4.1. Data description

Column performance was evaluated by pulse response experiments in terms of first and second moment as well as reduced HETP and peak skewness. The impact of the superficial flow velocity, chromatography medium, column type, column diameter, and column length on column performance was assessed. In total, 105 columns were analyzed in 1884 runs with one run representing one pulse response experiment (Fig. 2). 1169 runs were performed with pre-packed disposable columns, 428 with pre-packed non-disposable columns and 287 with self-packed columns. Three different medium types (cation exchange, hydrophobic interaction and Protein A) were analyzed to obtain more representative results over various chromatography media and to evaluate differences between the different media types. The data structure and variability was evaluated in more detail by principle component analysis (Supplementary Material). A comparison of numerical integration and EMG fitting of the peak showed that numerical integration is more suitable for fronting and non-exponentially tailing peaks (Supplementary Material). Consequently, all the shown data were analyzed by direct numerical integration.

The Van Deemter curve shows that mass transfer is the rate limiting mechanism, since the reduced HETP increased with the reduced velocity (Fig. 3A). Consequently, especially the runs at higher reduced velocities will partly be controlled by diffusional limitations of acetone inside the beads and not only reflect the differences in the different packings. The reduced HETP widely varied within one reduced velocity, because columns of different types and dimensions were evaluated. A few reduced plate heights are negative because for some of the columns the extra column band broadening was higher than the total band broadening. This is attributed to the statistical variation of the results. The packed medium also influenced the column performance. However, the data might be biased since some media were also available in pre-packed non-disposable and self-packed format, which had longer column lengths and might have been more difficult to pack. Therefore, only the pre-packed disposable columns were considered for analyzing the impact of the packed medium on column perfor-

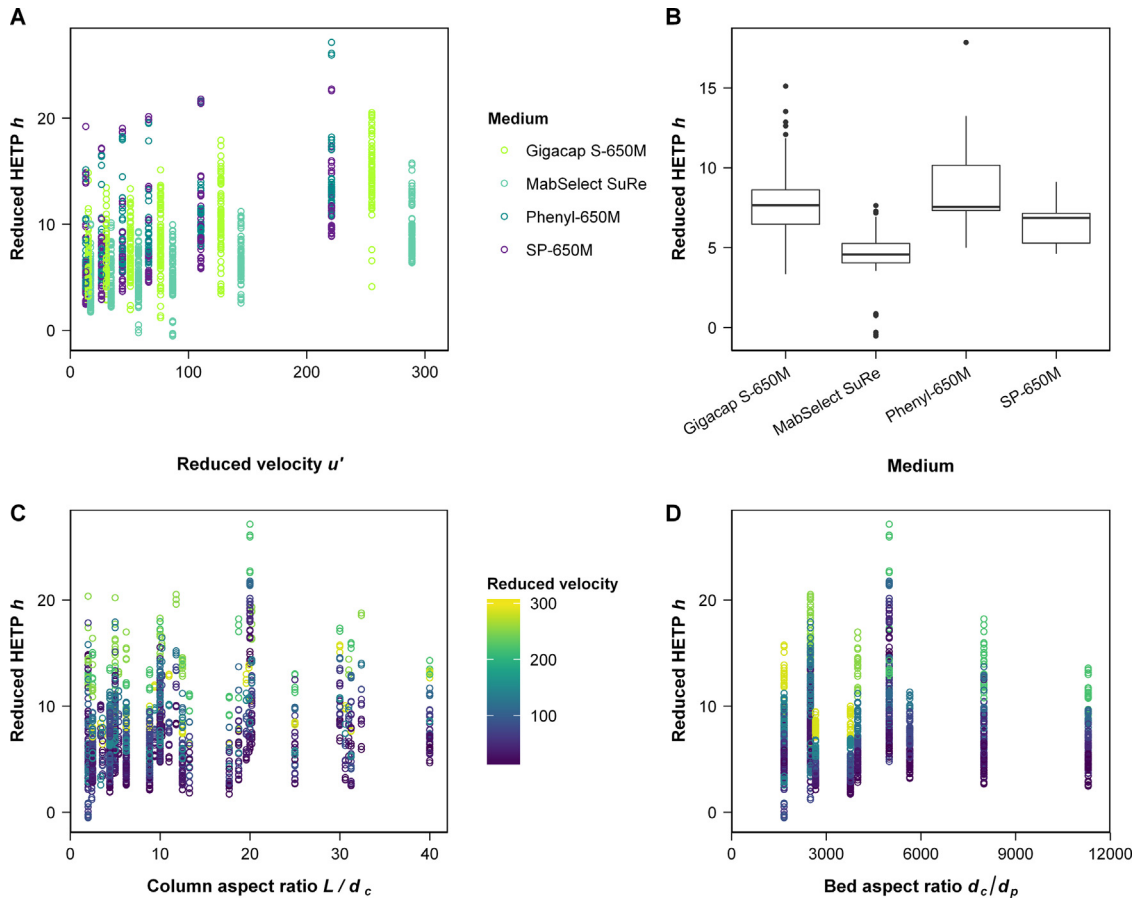

Fig. 3. Columnn performance for all columns. (A) Van Deemter plot of all runs. (B) Column performance of pre-packed disposable columns packed with the different media. Data for a superficial velocity of 150 cm/h are shown. (C) Variation of reduced HETP with column aspect ratio for all runs at all velocities. (D) Variation of reduced HETP with bed aspect ratio for all runs at all velocities.

mance (Fig. 3B). As expected, not all media were equally easy to pack, as reflected by significantly different reduced HETP values. MabSelect SuRe had the lowest reduced HETP of about 4.5. Columns packed with MabSelect SuRe are sold very frequently and therefore represent the most often packed columns of the manufacturer. It is therefore reasonable that a highly optimized packing procedure has been developed over time. Despite there is hardly any trend visisble between the reduced HETP and the column aspect ratio, a linear model gave a significant slope of 0.1 (Fig. 3C). Consequently, the reduced HETP inreases slightly with the aspect ratio. The bed aspect ratio does not change with the reduced HETP (Fig. 3D), a linear model fitted to the data gave a non significant slope.

As already shown in the Van Deemter plot, the reduced velocity affected the measured performance parameters. For more detailed analysis, the variation of the moments with reduced velocity was visualized for different column volumes. As expected from theory, the second peak moment increased with column volume and with the reduced velocity (Fig. 4A). The reduced velocity greatly influenced peak width. This confirms that pulse response experiments should always be run at the same reduced velocity in order that experiments are comparable.

The larger the column, the more symmetrical are the peaks (Fig. 4B). Peaks of columns larger than 5 ml are rather symmetrical, while columns with a volume smaller than 1 ml displayed tailing due to the dominating extra column effects. The reduced velocity used for testing has a large impact on the measured peak skewness for small columns. Consequently, the outcome of column performance tests can easily be changed by choosing a different reduced velocity. The lower the flow rate, the more tailing occurs. The same effect was observed for peaks through the workstation with no column connected (data not shown). Due to the large influence of the workstation in small columns, the peak shape was similar to peaks measured in the extra column volume.

4.2. Measurement precision of the ÄKTA pure 25 workstation

The workstation will influence every pulse response experiment since the pulse will not only broaden in the column itself but also in the extra column volume. However, apart from the additional band broadening introduced by the workstation, it will also add a certain variation to the results. A pulse response experiment done several times with the same column on the same workstation will yield slightly different results each time. Knowing the measurement precision of the workstation allows the evaluation of whether a difference in peak parameters is significant or just within the typical data variation range.

Based on the triplicate measurements of all pulse response experiments, we were able to calculate the measurement precision of the used workstation. The mean and the corresponding standard deviation of the triplicate measurements for the first and the second moment were calculated and plotted against each other. No visual trend between the absolute magnitude of the mean and its standard deviation could be observed for the first moment (Fig. 5A). A linear model fitted to the data confirmed a non-significant slope, meaning that the standard deviation of the first moment was independent of the size of the first moment and therefore could be considered constant. Consequently, even columns larger than the ones used in this study would have the same standard deviation. This is a rea-

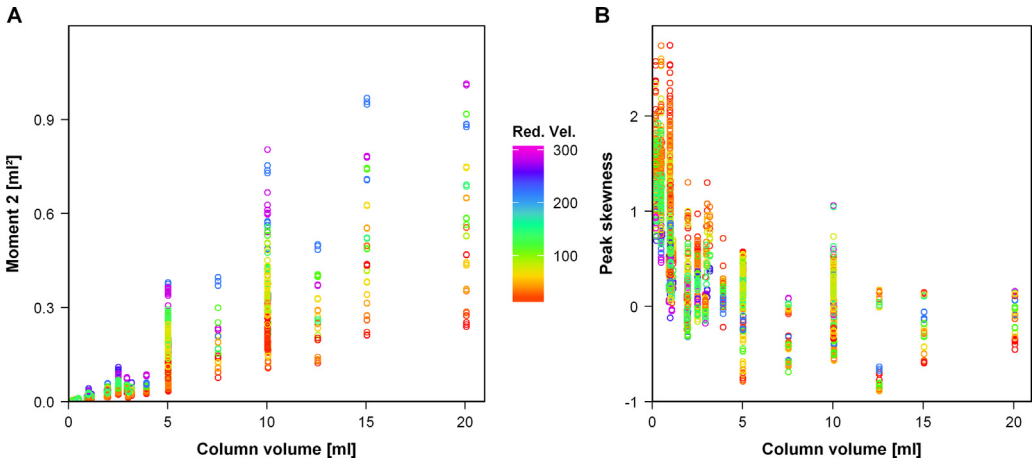

Fig. 4. Variation of column performance parameters with column volume and reduced velocity. (A) Second Moment. (B) Skewness.

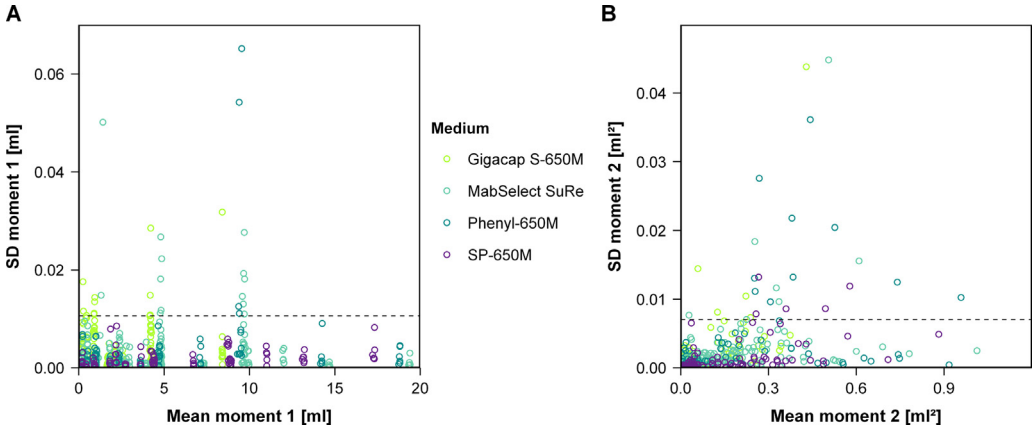

Fig. 5. Measurement precision of the ÄKTA pure 25 M2 workstation. Variation of the standard deviation (SD) with the mean of the first (A) and second (B) moment of all runs at all velocities available in triplicates (565 data points). 95% of the data points are below the black dashed line.

sonable proposal since the measurement precision originates from the workstation itself and not from the column and therefore stays constant irrespective of the column volume.

The standard deviation of the second moment depends on the size of the second moment, since the slope of a linear model fitted to the data of the second moment was significant (Fig. 5B). However, the predicted slope is small (0.014) and therefore only a slight dependence of the standard deviation with the peak width was observed. The larger the column diameter, the higher the standard deviation of the second moment. Consequently, the stated measurement precision should not be used for extrapolations to columns with an even larger diameter.

The measurement precision of the ÄKTA pure 25 workstation is smaller than ± 0.01 ml for the first moment and ± 0.007 ml^2 for the second moment for 95% of the data points, whereas the latter parameter might be higher if column volumes larger than 20 ml are used. The error ranges were given for 95% of the data points in order to give more reliable estimates representing the whole data range and not the mean. The RSD of the first moment depended on the column volume and was smaller than 0.75% for columns larger than 2 ml. The RSD of the second moment was smaller than 7.5% for columns larger than 2 ml. However, the RSD may be up to 25% for columns smaller than 1 ml. The packed medium had no effect on the measurement precision of the first and second moment.

4.3. Column-to-column packing variation

It is commonly assumed that pre-packed columns have the same packing quality, since they are packed by experts with a standardized packing method. This is especially true for columns of the same batch, which were packed simultaneously. We examined whether this assumption was valid for pre-packed disposable columns. We focused on the variation in the first and second moment caused by the packing of columns of the same size. To verify, whether the column-to-column packing variation is significant compared to the measurement precision, we made an ANOVA analysis on every column length-diameter combination at a certain velocity. The column-to-column packing variation was significant for 59 out of 70 tested length-diameter and velocity combinations. This means that the majority of the columns and velocities, the variation between the different packings was large enough to be identified as such on top of the measurement precision. For the other 11 columns and velocities, the measurement precision might either be too low to identify differences in the packing between the different columns or the column packings were the same. The calculation of the column-to-column packing variation is described in section 2.7 in more detail.

The absolute standard deviation of the first and second moment caused by the packing differences between the columns increased with the mean first and the second moment, respectively (sig-

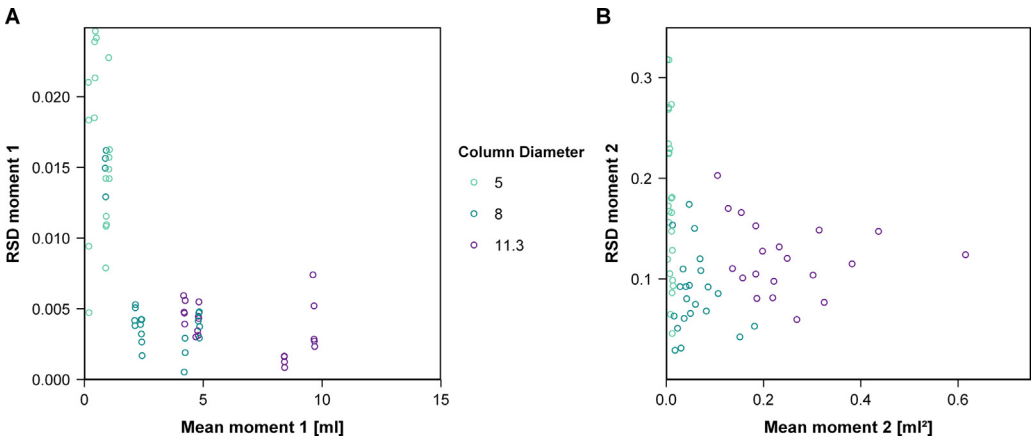

Fig. 6. Packing variation of pre-packed disposable columns. Variation of the relative SD (RSD) expressed as the % of the mean for the first (A) and the second (B) moment of all runs available for three columns of the same size (70 data points). The data are shown for all superficial velocities.

nificant slope of a linear model) (data not shown). Therefore, we considered the RSD (given in % of the mean). The RSD of the first moment was smaller than 1% of the mean for all columns larger than 1 ml (Fig. 6A), so we can conclude that the variation in packing had no impact on the first moment. The RSD of the first moment decreased with the mean, which correlates with the column volume. Consequently, this parameter should not be higher than 1% for column volumes greater than those tested. The RSD of the second moment did not increase with the mean since a linear model only gave a significant intercept and no significant slope, and can therefore be considered constant (Fig. 6B). The majority of the columns showed a RSD of around 10–15%. Compared to the first moment, the relative standard deviation of the second moment was high. This was an expected outcome since the packing quality mainly affects peak shape and width and not the position of the peak maximum. The very small columns show the highest packing variation of up to 20–30% but they also show the lowest packing variation of less than 5%. To our knowledge, it is more easy to reproducibly pack wider columns, which is the reason why the very thin columns show a higher packing variation.

When the variation in the HETP was calculated, we found a mean RSD of 15% for all data points. This value was comparable to the 14% RSD found for semi-preparative HPLC columns and 30% for preparative HPLC columns [11]. Therefore, the disposable pre-packed columns can be considered to be packed reproducibly within the expected range, despite the RSD is 1% for the first and 10–15% for the second moment. If higher standards were required by customers, for example a packing variation of less than 10% more than half of the columns would need to be discarded, which in turn would dramatically increase the costs of pre-packed columns. Considering that only the measurement precision can lead to a variation of the second moment of 7.5%, the observed column-to-column packing variation can be considered acceptable.

4.4. Influence of column geometry on packing variation

We compared the column-to-column packing variation of pre-packed disposable columns with different dimensions (diameter-length in mm: 5–10, 5–25, 5–50, 8–20, 8–50, 8–100, 11.3–50 and 11.3–100) to elucidate the influences of column volume and aspect ratio on the packing variation. We also evaluated whether one column type can be packed to the same standards of quality with various media. This factor might be important for medium screening studies, where the impact of the medium shall be evaluated instead of the packing quality. We focused on evaluating the variation in the second peak moment since this parameter is highly affected by packing differences as shown in section 4.5.

The diameter-length combination of the columns significantly influenced the column-to-column packing variation, while the medium type did not (Fig. 7A). Consequently, the columns are equally packed regardless of the medium. The RSD of the second moment varies between 7 and 20% for most diameter-length combinations. The high variation is attributed to the different velocities evaluated, since especially at high velocities also mass transfer contributes to band broadening. No trend was seen between the packing variation and the column volume or the aspect ratio. However, some diameter-length combinations were easier to pack reproducibly as illustrated by columns with 8 mm ID and 20 and 50 mm height. This observation may be attributed to different packing procedures used for different column sizes. Especially the columns with 5 mm ID show a high packing variation.

The extra particle porosity was determined (Fig. 7B) to evaluate whether column-to-column packing variation was due to different packing density. However, the packing density was not the cause for the variation of the second moment of the different columns. When the extra particle porosity varied widely, the packing can still be repeatable. For example, the variation in extra particle porosity was high for the small columns, even though they showed the same packing variation as the large ones. Hence, the reason for large column-to-column variation is explained by the particle arrangement inside the column, since all other factors could be excluded. Differences in the packing of process scale chromatography columns were also observed by [4] and the authors claimed that these differences do not have an impact on the actual separation of proteins.

When we compare the packing variation with the column performance measured as reduced HETP (Fig. 7C), no correlation between packing variation and packing quality can be seen. A high extra particle porosity does not result in low column performance, which was also shown by Stanley et al. [11] for HPLC columns. They also claimed that it is only possible to determine the column-to-column efficiency for well-packed columns. Since it was possible to determine differences in the column-to-column efficiency we can conclude that the columns are well-packed.

4.5. Influence of column type on column efficiency

Three different column types (pre-packed disposable, pre-packed non-disposable and self-packed columns) were investigated. The pre-packed disposable columns are made of polypropylene, whereas the pre-packed non-disposable columns are of higher

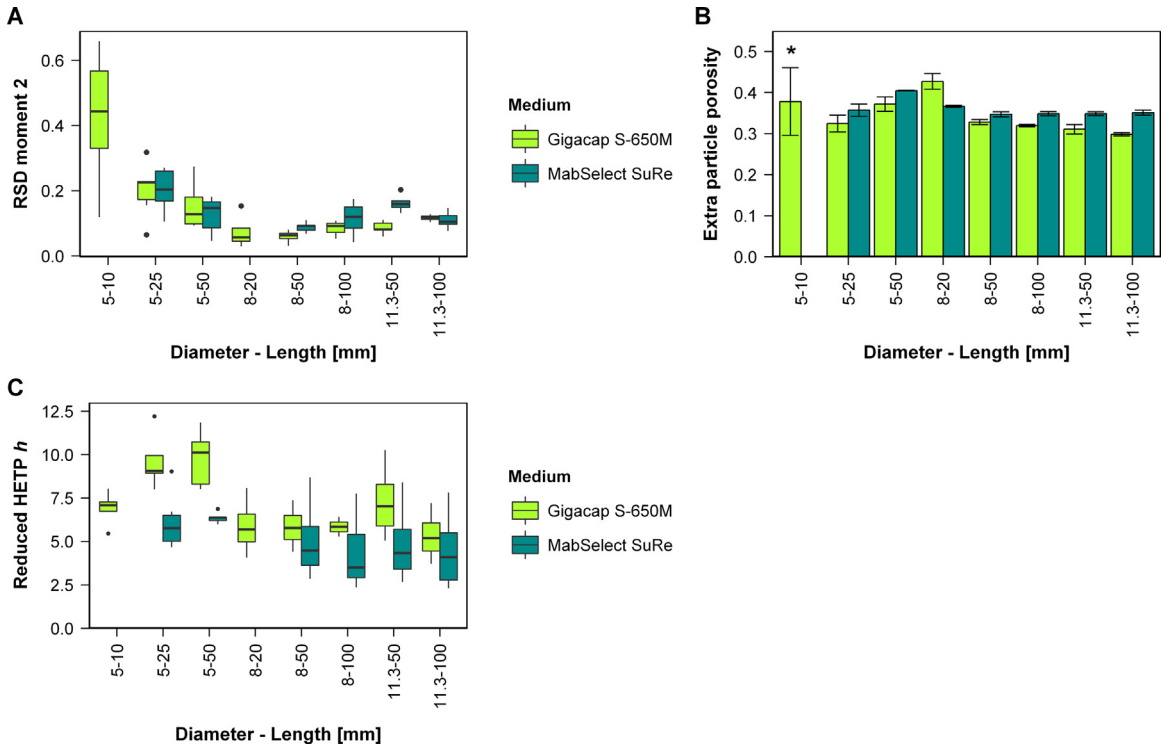

Fig. 7. Influence of column diameter and length on the column-to-column packing variation and packing quality of pre-packed disposable columns. (A) Relative standard deviation (RSD) of the second moment caused by the packing variation for the differently packed columns of various column diameter-length combinations packed with Gigacap S–650 M and MabSelect SuRe at all evaluated superficial velocities. (B) Extra particle porosity (ε) of the pre-packed disposable columns packed with MabSelect SuRe. The error bars show the standard deviation between three equally packed columns. * Standard deviation is exceptionally high because one of the three columns was treated under harsh conditions before the extra particle porosity was determined. (C) Absolute variation in reduced HETP caused by the packing variation for columns of various diameter-length combinations packed with Gigacap S–650 M and MabSelect SuRe at all evaluated superficial velocities.

quality with a column wall made of glass. Also the self-packed columns had a glass wall and were designed for re-use.

Columns with an ID of 11.3 mm and length of 100 mm were compared to elucidate the differences between pre-packed disposable and non-disposable columns since this was the only size available in both column types. We found a significant difference in the reduced HETP between the disposable and non-disposable columns packed with SP–650 M, but no difference for those packed with MabSelect SuRe (Fig. 8A). For comparison of the pre-packed with the self-packed columns, only columns with an ID of 5 mm and a maximum length of 60 mm were considered. This selection allowed us to compare columns of the same dimensions and thereby avoids biases of easier or harder to pack dimensions. Self-packed columns packed with MabSelect SuRe significantly differed from pre-packed disposable columns but showed the same efficiency when packed with Gigacap S–650 M (Fig. 8B). However, it is worth noting that the packing procedure was optimized and the column efficiency might be worse for columns which are not well packed.

The diverse effects we observed for different media may occur because of changes in the packing behavior of the media between the disposable and non-disposable columns and may be related to variations in their surface charges and roughness.

However, for HPLC columns it was shown that the column wall material does not influence column efficiency [35]. Alternatively, the packing operator might have an influence on the column efficiency since the different column types were packed by different operators. Besides, different packing solutions and procedures might have been used. Despite the differences we observed in peak shape between the different column types, these differences were also present for those media, where the efficiency of both column types was the same. The same is true considering the specific design of the top and bottom adapter and of the filter and frits in the column resulting in different extra column volumes. Furthermore, the volume of the adapters of the pre-packed non-disposable columns was larger than those of the pre-packed disposable columns and still they showed better efficiency.

In general, no clear evidence of the superiority of one column type was found. The specific combination of a certain medium and column type probably has an influence on column efficiency. For the evaluated media and columns, pre-packed non-disposable columns are better or equally packed than pre-packed disposable columns. Pre-packed disposable columns were better than or equal in efficiency to the self-packed columns. However, these results may not be applicable to columns of different dimensions or columns packed with different media.

5. Conclusions

Statistical analysis of peaks made on independently packed columns showed a significant influence of the different packings compared to the standard fluctuation introduced by the measurement precision of the workstation. The measurement precision of the ÄKTA pure 25 workstation was determined by triplicate measurements for each column and was quantified as smaller than ± 0.01 ml for the first moment and ± 0.007 ml^2 for the second moment for 95% of all data points measured. The impact of the workstation on the experiments depends on the column volume evaluated. While the measurement precision is negligible for large columns, it should definitely not be neglected for small columns, since the variation is high compared to the performance of the packed bed.

The column-to-column variation of disposable pre-packed columns depends on column volume and consequently is considered in terms of relative standard deviation (RSD). The RSD between

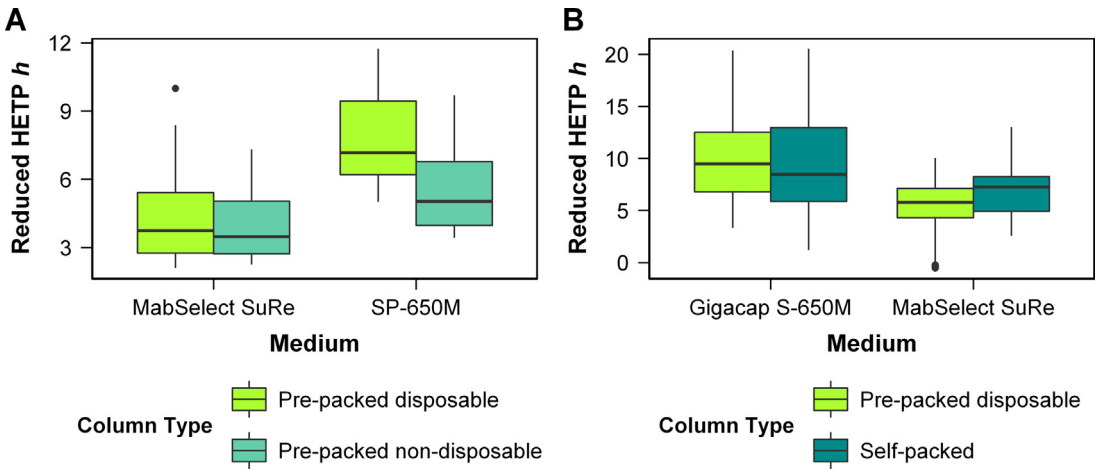

Fig. 8. Influence of column type on column efficiency. (A) Reduced HETP for pre-packed disposable and non-disposable columns with 11.3 mm ID and 10 mm bed height tested at all superficial velocities. (B) Reduced HETP for pre-packed disposable and self-packed columns with a bed height lower than 60 mm tested at all superficial velocities.

columns of the same dimensions was lower than 1% for the first moment and about 10–15% for the second moment. The only difference between the evaluated columns is the packing. We found that the variation cannot be explained by the packing density, but is rather attributed to the heterogeneity in particle structure in the column. The columm-to-column packing variation of the second moment is small, considering that the measurement precision of the workstation alone is around 7.5% for columns larger than 2 ml and up to 25% for columns smaller than 2 ml. The variation of the first and second moments leads to a resulting variation in HETP of about 15%. This is the variation for an unretained acetone pulse a user of pre-packed columns can expect if he buys two columns of the same dimensions. Considering that columns are typically used with retained solutes, which are mainly mass transfer limited, hardly any change in performance is expected. For the evaluated column dimensions and media, pre-packed disposable columns had a higher or equal column efficiency compared to self-packed columns.

Acknowledgements

This work has been supported by the Federal Ministry of Science, Research and Economy (BMWFW), the Federal Ministry of Traffic, Innovation and Technology (bmvit), the Styrian Business Promotion Agency SFG, the Standortagentur Tirol, the Government of Lower Austria and ZIT – Technology Agency of the City of Vienna through the COMET-Funding Program managed by the Austrian Research Promotion Agency FFG.

Appendix A. Supplementary data

Supplementary data associated with this article can be found, in the online version, at https://doi.org/10.1016/j.chroma.2017.10.059.

References

[1] S. Grier, S. Yakabu, Prepacked chromatography columns: evaluation for use in pilot and large-scale bioprocessing, Bioprocess Int. 14 (2016).
[2] T. Scharl, C. Jungreuthmayer, A. Dürauer, S. Schweiger, T. Schröder, A. Jungbauer, Trend analysis of performance parameters of pre-packed columns for protein chromatography over a time span of ten years, J. Chromatogr. A 2016 (1465) 63–70, http://dx.doi.org/10.1016/j.chroma.2016.07.054.
[3] J. Moscariello, G. Purdom, J. Coffman, T.W. Root, E.N. Lightfoot, Characterizing the performance of industrial-scale columns, J. Chromatogr. A 908 (2001) 131–141, http://dx.doi.org/10.1016/S0021-9673(00)01062-1.
[4] M.A. Teeters, I. Quiñones-García, Evaluating and monitoring the packing behavior of process-scale chromatography columns, J. Chromatogr. A 1069 (2005) 53–64, http://dx.doi.org/10.1016/j.chroma.2005.02.051.
[5] M. Kele, G. Guiochon, Repeatability and reproducibility of retention data and band profiles on reversed-phase liquid chromatography columns IV. Results obtained with Luna C18 (2) columns, J. Chromatogr. A 869 (2000) 181–209.
[6] M. Kele, G. Guiochon, Repeatability and reproducibility of retention data and band profiles on reversed-phase liquid chromatography columns V. Results obtained with Vydac 218TP C18 columns, J. Chromatogr. A 913 (2001) 89–112.
[7] M. Kele, G. Guiochon, Repeatability and reproducibility of retention data and band profiles on reversed-phase liquid chromatography columns I. Experimental protocol, J. Chromatogr. A 830 (1999) 41–54.
[8] M. Kele, G. Guiochon, Repeatability and reproducibility of retention data and band profiles on reversed-phase liquid chromatography columns III. Results obtained with Kromasil C18 columns, J. Chromatogr. A 855 (1999) 423–453.
[9] M. Kele, G. Guiochon, Repeatability and reproducibility of retention data and band profiles on reversed-phase liquid chromatography columns II. Results obtained with symmetry C18 columns, J. Chromatogr. A 830 (1999) 55–79.
[10] A. Felinger, M. Kele, G. Guiochon, Identification of the factors that influence the reproducibility of chromatographic retention data, J. Chromatogr. A 913 (2001) 23–48, http://dx.doi.org/10.1016/S0021-9673(00)01044-X.
[11] B.J. Stanley, C.R. Foster, G. Guiochon, On the reproducibility of column performance in liquid chromatography and the role of the packing density, J. Chromatogr. A 761 (1997) 41–51, http://dx.doi.org/10.1016/S0021-9673(96)00804-7.
[12] C. Laub, Reproducible preparative liquid chromatography columns, J. Chromatogr. A 992 (2003) 41–45, http://dx.doi.org/10.1016/S0021-9673(03)00212-7.
[13] J.H. Knox, G.R. Laird, P.A. Raven, Interaction of radial and axial disperion in liquid chromatography in relation to the infinite diameter effect, J. Chromatogr. Sci. 122 (1976) 129–145.
[14] R.A. Shalliker, B.S. Broyles, G. Guiochon, Axial and radial diffusion coefficients in a liquid chromatography column and bed heterogeneity, J. Chromatogr. A 994 (2003) 1–12, http://dx.doi.org/10.1016/S0021-9673(03)00311-X.
[15] V. Wong, R.A. Shalliker, G. Guiochon, Evaluation of the uniformity of analytical-size chromatography columns prepared by the downward packing of particulate slurries, Anal. Chem. 76 (2004) 2601–2608, http://dx.doi.org/10.1021/ac030391a.
[16] S. Khirevich, A. Höltzel, A. Seidel-Morgenstern, U. Tallarek, Geometrical and topological measures for hydrodynamic dispersion in confined sphere packings at low column-to-particle diameter ratios, J. Chromatogr. A 1262 (2012) 77–91, http://dx.doi.org/10.1016/j.chroma.2012.08.086.
[17] G. Guiochon, T. Farkas, H. Guan-Sajonz, J.-H. Koh, M. Sarker, B.J. Stanley, T. Yund, Consolidation of particle beds and packing of chromatographic columns, J. Chromatogr. A 762 (1997) 83–88 https://doi.org/10.1016/S0021-9673(96)00642-5.
[18] A. Daneyko, A. Höltzel, S. Khirevich, U. Tallarek, Influence of the particle size distribution on hydraulic permeability and eddy dispersion in bulk packings, Anal. Chem. 83 (2011) 3903–3910, http://dx.doi.org/10.1021/ac200424p.
[19] T. Takeuchi, D. Ishii, High-performance micro packed flexible columns in liquid chromatography, J. Chromatogr. A 213 (1981) 25–32, http://dx.doi.org/10.1016/S0021-9673(00)80628-7.
[20] T. Takeuchi, D. Ishii, Ultra-micro high-performance liquid chromatography, J. Chromatogr. A 190 (1980) 150–155, http://dx.doi.org/10.1016/S0021-9673(00)85524-7.
[21] J.J. Kirkland, J.J. DeStefano, The art and science of forming packed analytical high-performance liquid chromatography columns, J. Chromatogr. A 1126 (2006) 50–57, http://dx.doi.org/10.1016/j.chroma.2006.04.027.

[22] Q.S. Yuan, A. Rosenfeld, T.W. Root, D.J. Klingenberg, E.N. Lightfoot, Flow distribution in chromatographic columns, J. Chromatogr. A 831 (1999) 149–165, http://dx.doi.org/10.1016/S0021-9673(98)00924-8.
[23] R.A. Shalliker, B.S. Broyles, G. Guiochon, On-column visualization of sample migration in liquid chromatography, Anal. Chem. 72 (2000) 323–332, http://dx.doi.org/10.1021/ac990370+.
[24] O. Kaltenbrunner, P. Watler, S. Yamamoto, Column qualification in process ion-exchange chromatography, in: I. Endo, T. Nagamune, S. Katoh, T. Yonemoto (Eds.), Biosep. Eng., 1st edition, Elsevir, 2000, pp. 201–206.
[25] K. Yamaoka, T. Nakagawa, Moment analysis for isolation of intrinsic column efficiencies in gas chromatography, Anal. Chem. 47 (1975) 2050–2053.
[26] D.J. Anderson, R.R. Walters, Effect of baseline errors on the calculation of statistical moments of tailed chromatographic peaks, J. Chromatogr. Sci. 22 (1984) 353–359.
[27] S.N. Chesler, S.P. Cram, Effect of peak sensing and random noise on the precision and accuracy of statistical moment analyses from digital chromatographic data, Anal. Chem. 43 (1971) 1922–1933, http://dx.doi.org/10.1021/ac60308a005.
[28] T. Petitclerc, G. Guiochon, Determination of the higher moments of a nonsymmetrical chromatographic signal, J. Chromatogr. Sci. 14 (1976) 531–535.
[29] E. Grushka, M.N. Myers, P.D. Schettler, J.C. Giddings, Computer characterization of chromatographic peaks by plate height and higher central moments, Anal. Chem. 41 (1969) 889–892, http://dx.doi.org/10.1021/ac60276a014.
[30] H. Gao, P.G. Stevenson, F. Gritti, G. Guiochon, Investigations on the calculation of the third moments of elution peaks. I: composite signals generated by adding up a mathematical function and experimental noise, J. Chromatogr. A 1222 (2012) 81–89, http://dx.doi.org/10.1016/j.chroma.2011.12.015.
[31] H.M. Gladney, B.F. Dowden, J.D. Swalen, Computer-assisted gas-liquid chromatography, Anal. Chem. 41 (1969).
[32] I.G. McWilliam, H.C. Bolton, Instrumental peak distortion. II. Effect of recorder response time, Anal. Chem. 41 (1969) 1762–1770, http://dx.doi.org/10.1021/ac60282a002.
[33] F. Gritti, G. Guiochon, Accurate measurements of peak variances: importance of this accuracy in the determination of the true corrected plate heights of chromatographic columns, J. Chromatogr. A 1218 (2011) 4452–4461, http://dx.doi.org/10.1016/j.chroma.2011.05.035.
[34] F. Gritti, G. Guiochon, Mass transfer kinetics, band broadening and column efficiency, J. Chromatogr. A 1221 (2012) 2–40, http://dx.doi.org/10.1016/j.chroma.2011.04.058.
[35] R.J.M. Vervoort, E. Ruyter, A.J.J. Debets, H.A. Claessens, C.A. Cramers, G.J. De Jong, Influence of batch-to-batch reproducibility of Luna C18(2) packing material, nature of column wall material, and column diameter on the liquid chromatographic analysis of basic analytes, J. Sep. Sci. 24 (2001) 167–172, http://dx.doi.org/10.1002/1615-9314(20010301)24:3<167:AID-JSSC167>3.0.CO;2-9.
[38] E. Grushka, Characterisation of exponentially-modified Gaussian peaks in chromatography, Anal. Chem. 44 (1972) 1733–1738 https://doi.org/10.1021/ac60319a011.

SUPPLEMENTARY MATERIAL

PUBLICATION II

Principal component analysis

Principal component analysis is a multivariate data analysis method [1]. Based on a multidimensional data set new uncorrelated variables, also called principal components, are calculated. The principal components are linear combinations of the original variables. The first principal component describes the largest variation in the data. Every succeeding principal component describes the largest possible remaining variance, but needs to be orthogonal to the previous components. The principal component analysis for our data is shown below (see Figure 1). The first 4 principal components explain 92.8 % of the data variance, the first 2 still explain 72.9 % of the variance. The variables first and second moment as well as skewness, column diameter and length equally contribute to the first principal component, so they explain most of the data variance. All of them, except the skewness, are positively correlated. This outcome means that an increase in one of the variables leads to an increase in the others, too. The skewness points in the opposite direction and is therefore negatively correlated with the others. The second principal component mainly comprises the superficial velocity and the reduced HETP. These two variables are positively correlated, which indicates that mass transfer is the rate limiting mechanism. The pre-packed non-disposable columns were longer than the pre-packed disposable columns leading to a clustering of the pre-packed disposable columns on the left side and the pre-packed non-disposable columns on the right side of the plot. The self-packed columns clustered, since only columns of 5 mm ID and therefore of smaller volume were used.

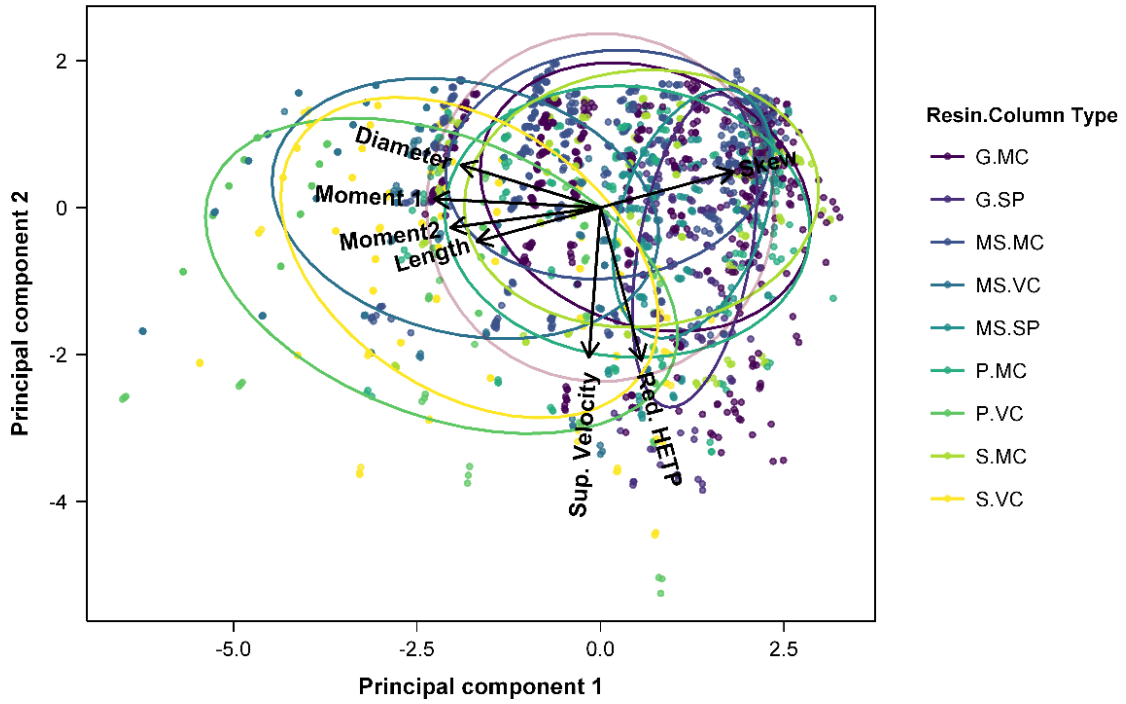

Figure 1 Principal component analysis showing the first and second principal components for each medium and column type combination. The circles represent normal data ellipses with a size of 0.68 in normal probability. G – Gigacap S-650M, MS – MabSelect SuRe, P – Phenyl-650M, SP – SP-650M, MC – MiniChrom, VC – ValiChrom, SP – Self-packed, M1 – first moment, M2 – second moment, Skew – peak skewness

References

[1] H. Abdi, L.J. Williams, Principal component analysis, WIREs Comput. Stat. 2 (2010) 433–459. doi:10.1002/wics.101.

Comparison of peak analysis methods

Various methods can be used to obtain peak parameters like the 1st and the 2nd moment or the peak skewness, but exact values for these parameters will differ depending on the chosen analysis method. We compared the two most commonly used peak analysis methods, direct numerical integration and fitting the peak to an EMG function with subsequent calculation of the parameters based on the fitted function.

The method for determination of the peak start and end points is crucial since it adds additional variation to the results, especially when peaks are detected automatically. The higher the threshold level (the percentage of the peak height at which peak analysis start and ends), the lower the determined moments. This effect becomes more pronounced for higher moments and tailing peaks [30]. Thus, our peak analysis program used the same peak start and end points for both direct numerical integration and EMG fitting.

For peak fitting, the peaks were fitted to the density function of the EMG distribution, which is defined as

$$f(x;\mu,\sigma,\lambda) = \frac{\lambda}{2} e^{\frac{\lambda}{2*(2\mu+\lambda*\sigma^2-2x)}} erfc\left(\frac{\mu+\lambda*\sigma^2-x}{\sqrt{2}\sigma}\right) \quad (1)$$

where x is the volume, μ is the mean of the Gaussian distribution, σ is the standard deviation of the Gaussian distribution and λ is the rate of the exponential distribution, which is the inverse of the exponential decay parameter τ.

The moments of the fitted EMG function were calculated by

$$M_1 = \mu + \tau \quad (2)$$

$$M_2 = \sigma^2 + \tau^2 \quad (3)$$

$$M_3 = 2\tau^3 \quad (4)$$

where M_1 is the first, M_2 the second and M_3 the third statistical moment.

The first moments determined by numerical integration and EMG fitting were very similar (see Figure 1A). The relative difference of the EMG fit with respect to the numerical integration lay between ± 0.9 % for 95 % of the data points (see Figure 1B). The first moment determined with the EMG fitting method was lower for columns smaller than 2 ml, while it was higher for larger columns. The peaks of the smaller columns show pronounced tailing, which might not be well described with the EMG function.

A larger variation between both methods was observed for the second moment (see Figure 1C). The absolute difference was smaller for narrow peaks and grew larger as the peak broadened. However, the relative difference decreased with peak width and could therefore be estimated to become very small for wide peaks (see Figure 1D). The relative difference of the second moment for 95 % of the data points fell between -36.5 % and +25.2 %. The lower second moments determined by EMG fitting of the Phenyl-650M columns may be attributed to the peak shape. The peaks were primarily fronting, which often results in poor fitting to the EMG function.

The skewness varies widely between numerical integration and EMG fits (see Figure 1E). The data set comprised mainly tailing peaks, but fronting and symmetrical peaks were measured also. Fronting peaks were obtained for pre-packed non-disposable columns packed with SP-650M and Phenyl-650M. The EMG fails to describe fronting per definition, consequently the skewness of a fronting peak determined by EMG fitting can never be smaller than 0. Many data points were located on the x-axis of the plot, which represent the fronting peaks, and which were not correctly analyzed by the EMG fitting method. The absolute error between both peak fitting methods is shown instead of the relative error (see Figure 1F). Since the data were distributed around 0, the relative error was not a good indicator for the variation between the methods since it approached infinity at 0. The peak skewness varied greatly between both methods.

As already observed by Morton and Young [1], the larger the moment, the higher the error between the different peak analysis methods. In comparison to their work, we fitted the EMG directly to the peak data instead of using only certain peak ratios to calculate the EMG function. The relative error we calculated between the two methods was smaller for the first moment, but larger for the second moment. Since our data set was larger and comprised many more variations in peak shape, we probably observed more cases with a severe discrepancy between the two peak analysis methods. Alternatively, Morton and Young's use of only some peak parameters for finding the EMG moments might be the more robust way of determining the second moment. While these authors suggest that the EMG method gives more reliable results, we also considered direct numerical integration a good option for determining the peak moments. The EMG method is a robust method as long as the EMG function fits well to the data points, but especially for fronting peaks and tailing peaks, which do not follow ideal exponential behavior, direct numerical integration is the better choice.

The relative difference in reduced HETP calculated by the EMG fitting method with respect to numerical integration is -35.9% to +24.4 %. This is in a similar range as stated by Gritti and Guiochon [2], who fitted their peaks to a EMG/GMG (Gaussian modified Gaussian) hybrid function. However,

according to their results, the peak variance observed by numerical integration was higher than for the EMG fitting method, a point which we cannot confirm.

Conclusion:

When qualifying the packing of preparative columns, the peak retention can be determined accurately independent of the peak analysis method. The difference in EMG fitting relative to direct numerical integration was < 1 % for the first moment. However, the relative difference for the second moment was high for the two methods at around 25-36 %. We suggest that direct integration is better for determination of higher moments, because fronting and non-exponential tailing behavior can also be taken into account.

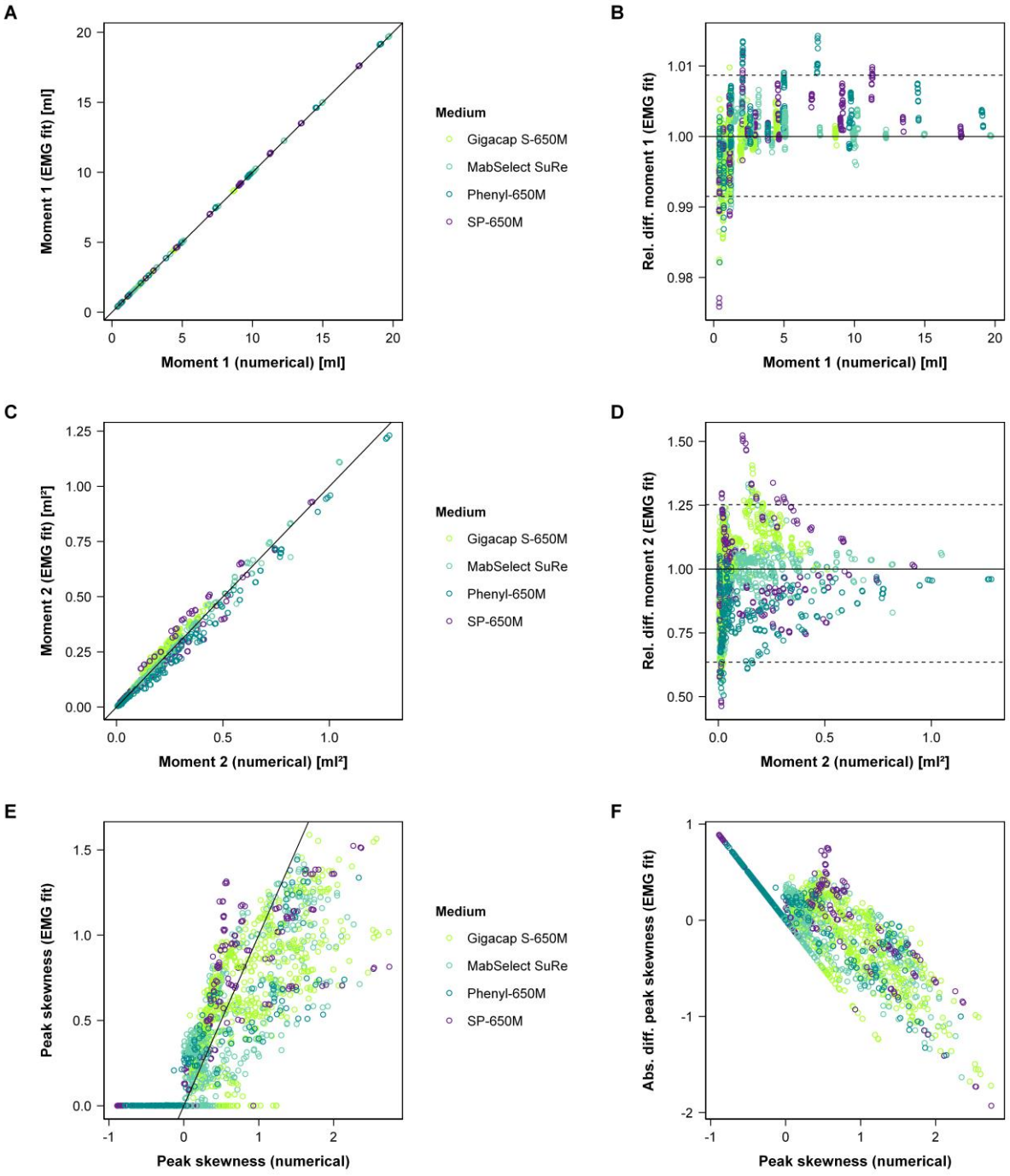

Figure 1 Comparison of peak parameters determined either by direct numerical integration or by EMG fitting. (A) First moments calculated by both methods. (B) Second moments calculated by both methods. (C) Relative error of the first moment determined by EMG fitting compared to numerical integration. (D) Relative error of the second moment determined by EMG fitting compared to numerical integration. (E) Peak skewness calculated by both methods. (F) Absolute error of the peak skewness determined by EMG fitting compared to numerical integration. The solid lines in (A-E) indicate equal values between both methods. 95 % of the data points are within the dashed lines in (B) and (D).

References

[1] D.W. Morton, C.L. Young, Analysis of Peak Profiles Using Statistical Moments, J. Chromatogr Sci. 33 (1995) 514–524.

[2] F. Gritti, G. Guiochon, Accurate measurements of peak variances: Importance of this accuracy in the determination of the true corrected plate heights of chromatographic columns, J. Chromatogr. A. 1218 (2011) 4452–4461. doi:10.1016/j.chroma.2011.05.035.

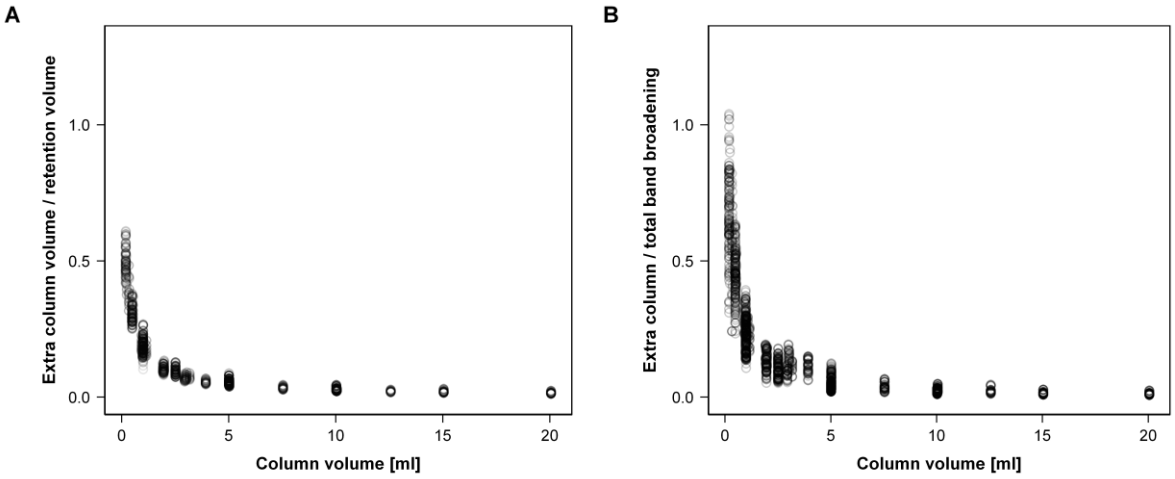
A
Extra column volume / retention volume
1.0
0.5
0.0
0
5
10
15
20
Column volume [ml]
B
Extra column / total band broadening
1.0
0.5
0.0
0
5
10
15
20
Column volume [ml]

PUBLICATION III

Journal of Chromatography A, 1537 (2018) 66–74

Contents lists available at ScienceDirect

Journal of Chromatography A

journal homepage: www.elsevier.com/locate/chroma

Scalability of pre-packed preparative chromatography columns with different diameters and lengths taking into account extra column effects

Susanne Schweiger[a], Alois Jungbauer[a,b,*]

[a] Austrian Centre of Industrial Biotechnology, Vienna, Austria
[b] Department of Biotechnology, University of Natural Resources and Life Sciences Vienna, Austria

ARTICLE INFO

Article history:
Received 6 November 2017
Received in revised form
20 December 2017
Accepted 8 January 2018
Available online 9 January 2018

Keywords:
Band broadening
Column dimension
Column performance
Column qualification
Computational fluid dynamics
Chromatography workstation

ABSTRACT

Small pre-packed columns are commonly used to estimate the optimum run parameters for pilot and production scale. The question arises if the experiments obtained with these columns are scalable, because there are substantial changes in extra column volume when going from a very small scale to a benchtop column. In this study we demonstrate the scalability of pre-packed disposable and non-disposable columns of volumes in the range of 0.2–20 ml packed with various media using superficial velocities in the range of 30–500 cm/h. We found that the relative contribution of extra column band broadening to total band broadening was not only high for columns with small diameters, but also for columns with a larger volume due to their wider diameter. The extra column band broadening can be more than 50% for columns with volumes larger than 10 ml. An increase in column diameter leads to high additional extra column band broadening in the filter, frits, and adapters of the columns. We found a linear relationship between intra column band broadening and column length, which increased stepwise with increases in column diameter. This effect was also corroborated by CFD simulation. The intra column band broadening was the same for columns packed with different media. An empirical engineering equation and the data gained from the extra column effects allowed us to predict the intra, extra, and total column band broadening just from column length, diameter, and flow rate.

1. Introduction

Small pre-packed columns are commonly used to estimate the optimum run parameters for pilot and production scale. Pre-packed columns are also widely used by the biopharmaceutical industry for preparative separations of proteins and other biomolecules. For high throughput screening, extremely small columns which can be operated by pipetting robots are commonly used. Their scalability to small benchtop columns has already been demonstrated [1–3]. However, pre-packed columns are also available in larger volumes in either disposable or non-disposable format, which are commonly used in more advanced process development stages [4,5]. To our knowledge, their performance as related to the whole available benchtop scale has not yet been demonstrated. For reliable scale-up predictions, it is necessary to consider the extra column effects, since a chromatographic peak not only broadens in the chromatography column itself, but also in the workstation as demonstrated for small molecules [6]. This peak broadening is especially important if the extra column volume is large compared to the column volume.

In HPLC, extra column effects have been studied widely, especially due to the high efficiency of the columns compared to the system performance. For example, even if the column volume is 30 times larger than the extra column volume, 60–80% of the total band dispersion of a non-retained compound occurs in the extra column volume [7,8]. However, also in preparative systems, the extra column volume has a large influence [9], especially if results made on one workstation must be compared with those made on another workstation. It was postulated that the extra column band broadening does not contribute as much to total band broadening in columns with a wider diameter [10].

The extra column effects depend on different parameters such as the configuration of the workstation, the injection volume, the linear velocity and the diffusion coefficient of the solute [10–14]. Consequently, the experimental set-up must be kept constant for

* Corresponding author at: University of Natural Resources and Life Sciences, Department of Biotechnology, Muthgasse 18, 1190 Wien, Austria.
E-mail address: alois.jungbauer@boku.ac.at (A. Jungbauer).

https://doi.org/10.1016/j.chroma.2018.01.022

the results to be comparable. Therefore, all the parts of the chromatography workstation should be considered, including valves, tubings, detectors, and the mixer. The individual parts either add a Gaussian function or an exponential decay function to the variance [15–19]. Additionally, the location of a component of the workstation (before or after the column) [9,11,15,20] affects the type of band broadening added. The contributions of the individual parts to extra column effects were investigated earlier [14,21–23]. The extra column effects are more pronounced for non-retained compounds [10]. Retained peaks are typically wider, therefore the extra column effects have a lower influence.

The experimental measurement of the extra column contribution is necessary, especially since the effect of stagnant zones at the connection between different parts is hard to model accurately [7,10,21]. There are several ways to determine the extra column volume and the extra column band broadening: (1) theoretical calculation based on the volume of the individual parts; (2) pulses through the system with tubings connected by a zero dead volume (ZDV) connector; (3) pulses through a zero-length column; (4) extrapolation from columns of different lengths; and (5) extrapolation from differently retained solutes [24]. Recently, it was shown that peak deconvolution is suitable to subtract all extra column contributions and still preserve the peak shape. Thus, the use of deconvolution allows not only the determination of the second moment of the column itself, but also of peak symmetry [25,26].

System peaks with a ZDV or a "zero-length column" instead of a column underestimate the extra column effects since the contributions of the flow distributor and column adapters are neglected. These contributions can also be accounted for using an extrapolation method with columns of different lengths, but the same filters, frits, and adapters. The length extrapolation method requires many columns with the same top and bottom adapters and of the same packing quality [28].

In this work, we measure the extra column volume and band broadening effects of the workstation and the adapters, filters, and frits of the column by extrapolation from columns of different lengths. The impact of extra column band broadening on total band broadening is evaluated for all column dimensions. Subtraction of the extra column effects allows the evaluation of the column performance alone. Scalability of the pre-packed columns is demonstrated over the whole range of tested columns for a wide range of flow rates. Based on our results, it is possible to predict extra, intra, and total column band broadening just from column dimensions and flow rate.

2. Materials and methods

2.1. Chemicals and columns

Tris and sodium chloride were obtained from Merck Millipore (Darmstadt, Germany) and acetone was purchased from VWR chemicals (Fontenay-sous-Bois, France).

Pre-packed MiniChrom and ValiChrom columns from Repligen (previously Atoll, Weingarten, Germany) were used in this study. MiniChrom columns are sold as disposable columns made of polypropylene. ValiChrom columns are non-disposable columns of a higher quality and column walls made of glass. Both column types have different designs and volumes of their top and bottom adapters. Besides, the top adapter volumes may differ between columns of the same type but of different lengths. The total adapter volumes of the top and the bottom adapters of every column dimension are given in Table 1.

The columns were packed with 4 different media: MabSelect SuRe (GE Healthcare, Uppsala, Sweden, 85 μm particle diameter), Toyopearl Gigacap S–650 M (Tosoh, Tokyo, Japan, 75 μm particle diameter), Toyopearl SP–650 M (Tosoh, Tokyo, Japan, 65 μm particle diameter) and Toyopearl Phenyl–650 M (Tosoh, Tokyo, Japan, 65 μm particle diameter). MabSelect SuRe is a compressible Protein A medium with highly cross-linked agarose as backbone. Both, Toyopearl Gigacap S–650 M and Toyopearl SP–650 M media are strong cation exchange media with a methacrylate backbone. The Gigacap medium has an additional polymer linker between the backbone and the sulfopropyl functionalization. Toyopearl Phenyl–650 M has the same backbone as SP–650 M but is a hydrophobic interaction medium since it is functionalized with a phenyl ligand group. The MiniChrom columns were used in all commercially available diameter-length combinations (in mm): 5–10, 5–25, 5–50, 8–20, 8–50, 8–100, 11.3–50, and 11.3–100. ValiChrom columns were delivered as longer columns: 5–100, 5–150, 5–200, 8–150, 8–200, 8–250, 11.3–100, 11.3–150, and 11.3–200. Every column was tested in triplicate at different superficial velocities (30, 60, 100, 150, 250 and 500 cm/h) resulting in 1597 runs. Detailed information on the data set has already been published [29].

2.2. Workstation

We used an ÄKTA™ pure 25 M2 chromatography system (GE Healthcare, Uppsala, Sweden), which was controlled with Unicorn Software 6.4. The extra column volume including the pumps, valves, detectors and tubings in between was not changed and used as provided by the manufacturer. The tubing to and from the column had an ID of 0.25 mm and the length was varied based on the column type. A length of 234 mm from the column valve to the column and 179.5 mm from the column outlet to the column valve was used for MiniChrom columns and ValiChrom columns with diameter-length combinations of 5–100 and 5–150. Since all other ValiChrom columns were significantly longer, the tubing from the column to the column valve was 331 mm long. The total volume of all parts of the workstation is 202.3 μl for the shorter tubing configuration and 209.7 μl for the longer tubing configuration.

The analysis of the extra column volume and extra column band broadening using the length extrapolation method was conducted separately for each column type because the volumes of the adapters of the MiniChrom and ValiChrom columns are considerably different. Additionally, this analysis was performed separately for every column diameter, since the volumes of the filters, frits and adapters change with the diameter. Moreover, every medium was considered separately, since we did not assume that columns with different media have the same packing quality. It was not possible to keep the adapter volume constant for columns of the same type and diameter but with different length because the supplier uses pre-defined lengths of the column outer wall and changes the length of the top adapters to give the desired bed heights. To account for these discrepancies, the measured retention volumes of the different columns were corrected with the respective volume changes for columns of different lengths. The peak widths were not corrected since it was impossible to attribute the additional volumetric increase to a certain increase in band broadening.

2.3. Pulse response experiments

Pulse response experiments were performed with acetone (1%, v/v) as a small non-interacting solute. The injected pulse volumes were 10 μl for all MiniChrom columns and ValiChrom columns with 5 mm ID, 50 μl for ValiChrom columns with 8 mm ID, and 500 μl for ValiChrom columns with 11.3 mm ID. A volume of 10 μl was injected for peaks only through the extra column volume. We used 50 mM Tris, 0.9% (w/v) sodium chloride, pH 8.0 (pH adjusted with HCl), as running buffer.

When columns were evaluated, they were tested at 6 different superficial velocities (30, 60, 100, 150, 250, and 500 cm/h). For

Table 1
Volume of the top and bottom adapters of the different column types, lengths (L) and diameters (d_c).

Column Type	d_c-L [mm]	Adapter volume [µl]	Column Type	d_c-L [mm]	Adapter volume [µl]
MiniChrom	5–10	15.7	ValiChrom	5–100	137.4
MiniChrom	5–25	15.7	ValiChrom	5–150	172.7
MiniChrom	5–50	30.4	ValiChrom	5–200	208.0
MiniChrom	8–20	38.6	ValiChrom	8–150	194.0
MiniChrom	8–50	38.6	ValiChrom	8–200	229.4
MiniChrom	8–100	38.6	ValiChrom	8–250	140.9
MiniChrom	11.3–50	55.7	ValiChrom	11.3–100	207.4
MiniChrom	11.3–100	55.7	ValiChrom	11.3–150	242.8
			ValiChrom	11.3–200	154.4

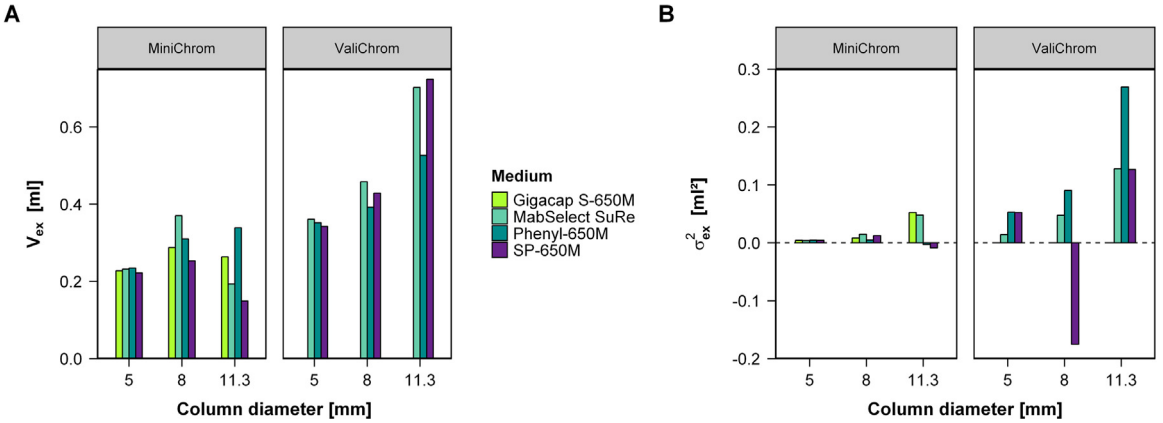

Fig. 1. Extra column effects of the workstation, column adapters, filters, and frits for MiniChrom and ValiChrom columns packed with different media run at a superficial velocity of 150 cm/h. (A) Extra column volume V_{ex}. (B) Extra column band broadening σ^2_{ex}. The data were corrected for the slightly different adapter volumes of the different lengths.

pulses through the system only, we chose 18 different flow rates, which were used for testing the columns. Each flow rate was measured in triplicate.

2.4. Data analysis

The peaks were automatically analyzed by direct numerical integration using a self-written script in the statistics software R [29]. First and second statistical moments were compared as parameters indicating peak retention and width (band broadening), respectively. The second moments were corrected for the different injection volumes by subtracting the contribution of a rectangular injection pulse.

Columns packed with different media were compared in terms of reduced velocity whenever possible. However, if columns were to be compared at one velocity this was not possible, so the superficial velocity was used instead. The corresponding reduced velocities are 4.7–6.1 for 30 cm/h, 9.3–12.2 for 60 cm/h, 15.6–20.4 for 100 cm/h, 23.3–30.5 for 150 cm/h, 38.9–50.9 for 250 cm/h and 77.8–101.8 for 500 cm/h. Comparison in terms of superficial velocity introduces an additional error. However, this error is expected to be small since the diameter of the beads is very similar (65–85 µm).

2.5. Computational fluid dynamics (CFD) simulations

We simulated a MiniChrom column with 8 mm ID and 100 mm bed height which was packed with Gigacap S–650 M. The whole column including filter, frits, adapters, and 1 cm of the tubing before and after the column was simulated. The respective dimensions were measured on a real column with a sliding caliper. We used the program Star-CCM+ (CD-Adapco, Melville, US) for CFD simulations. First, we built the geometry of the regions accessible to fluid. Based on the geometry, a surface and then a volume mesh were created. The volume mesh consisted of approximately 340 000 polyhedral cells, with 5 prism boundary layers, 1.7 million faces, and 1.2 million vertices.

The packed bed was simulated as a porous region, in which lumped parameters describe the macroscopic effect of the porous media on the fluid flow. The porosity of the porous region was set to 0.32, which is the same as the experimentally determined porosity of the respective column. Other parameters, which must be set in porous regions, are the porous viscous and the porous inertial resistance. The porous viscous resistance (3.34×10^8 kg/(m^3 × s)) and the porous inertial resistance (4.83×10^8 kg/m^4) were calculated from the porosity and the particle diameter, assuming random packing of monodisperse spheres without compression. The filter was modelled as a different porous region, with a porosity of 0.509. The porous viscous resistance of the filter was determined to be 2.05×10^{10} kg/(m^3 × s). This value was adjusted to fit to the experimentally determined pressure drop over the filter for various flow rates. The porous inertial resistance of the filter can be neglected, since laminar flow can be assumed. The frit was modelled as an empty fluid region.

The inlet was modelled as a constant velocity inlet with an applied velocity of 0.503 ml/min. The outlet surface was realized as a pressure outlet. Non-slip boundary conditions were set for all walls. A multi-component liquid was simulated with water as the first species and acetone as the second species. The fluid flow was calculated using the implicit unsteady-state laminar flow solver. The time step was 0.001 s and a maximum of 5 inner iterations was set. The simulation was started with pure water as fluid for the first 20 s to reach steady state flow conditions. Then a mass fraction of 0.798% of acetone was applied to the inlet tubing for 2.3 s. This is equivalent to an experimental injection of 1% (v/v) acetone with a volume of 10 µl. Finally, pure water was applied for the rest of the simulation. We chose constant density and non-reacting species models.

3. Theory

With the length extrapolation method, the extra column volume is determined by

$$V_R = V_{ex} + \varepsilon_T * CV \quad (1)$$

where V_R is the retention volume, V_{ex} is the extra column volume, ε_T is the total column porosity and CV is the column volume. A plot of the retention volume over the column volume will give the extra column volume as an intercept, when a linear model is fitted to the data.

Based on the definition of HETP (H), the band broadening is proportional to the retention volume for columns of different length assuming that HETP is constant:

$$\frac{L}{H} = \frac{\mu^2}{\sigma^2} \overset{L \propto \mu}{\rightarrow} \frac{1}{H} = \frac{\mu}{\sigma^2} \quad (2)$$

where L is column length, H is HETP, μ is the first statistical moment, which is equivalent to the retention time and σ^2 is the second statistical moment. Consequently, a plot of the total band broadening ${\sigma^2}_{total}$ over the retention volume will give a linear fit for columns of different length. This process differs from a previously reported approach [9], where the total band broadening ${\sigma^2}_{total}$ over the retention volume squared was used. Extrapolation of the corresponding ordinate for $V_R = V_{ex}$ gives the extra column band broadening ${\sigma^2}_{ex}$.

The total band broadening ${\sigma^2}_{total}$ measured at the detector is calculated by the sum of the intra column band broadening ${\sigma^2}_{col}$ and of the extra column band broadening [23]:

$$\sigma^2_{total} = \sigma^2_{ex} + \sigma^2_{col} \quad (3)$$

Therefore, the intra column band broadening is calculated by subtraction of the extra column band broadening from the total band broadening.

The reduced velocity u' is calculated by

$$u' = \frac{u * d_p}{D_0} \quad (4)$$

where u is the superficial velocity, d_p is the particle diameter and D_0 is the molecular diffusivity of acetone with 1.16×10^{-5} cm^2/s.

4. Results and discussion

The performance of 89 different pre-packed columns was evaluated in terms of peak retention and band broadening. The columns were packed with three different media types (cation exchange, staphylococcal Protein A and hydrophobic interaction media) in order to allow generalizations on the column performance of columns packed with different media. Out of the analyzed columns, 65 were disposable MiniChrom columns and 24 were non-disposable ValiChrom columns. The column performance was evaluated over a wide range of superficial velocities (30–500 cm/h). The Van Deemter equation states that the column performance depends on the reduced velocity of the experiments [30]. Therefore, all evaluations were done separately for each velocity. For detailed evaluation of the column performance and prediction over many different scales, the extra column effects must be considered. We investigated the extra column effects extensively, considering the contributions of the workstation alone and also of the column adapters, filters, and frits.

4.1. Extra column effects of pre-packed columns

The contribution of the workstation alone was analyzed using different bypass types (Supplementary data). In general, any connector type with a small dead volume will allow the determination of the extra column volume and extra column band broadening of the workstation alone for preparative columns. There is no need to use a ZDV connector. Moreover, the in-built bypass function of the ÄKTA pure workstation is not suitable to accurately determine the extra column effects.

The contribution of the whole extra column volume, which includes the workstation, column adapters, filters, and frits, was investigated by extrapolation from columns of different lengths using Eqs. (1)–(3). As expected, the extra column volumes differed for MiniChrom and ValiChrom columns with different diameters (Fig. 1A). Even though the extra column volume should be the same for each of the evaluated media, the extra column volumes displayed differences. The assumption that all columns packed with one medium have the same packing quality is probably not valid. The highest difference was observed for MiniChrom columns with an ID of 11.3 mm. The high difference is explained by the fact that only two column lengths were available for this diameter as opposed to 3 lengths available for all the other columns and diameters. Consequently, the extrapolation is prone to slight variations in the results. In general, the determined extra column volumes agreed well with the geometrical contributions of the workstation, the column adapters, filters, and frits (Table 2), confirming that the length extrapolation method is suitable to accurately evaluate the extra column effects. For all columns with an ID of 5 and 8 mm, the difference in extra column volume is less than 25 μl. Only the aforementioned MiniChrom columns and the ValiChrom columns, both with 11.3 mm ID, showed larger differences of 124 μl or higher.

The extra column band broadening shows a higher variation between the different media (Fig. 1B). Negative values were observed for the MiniChrom columns with 11.3 mm ID, probably because only 2 column lengths were available for extrapolation. Negative values were also observed for ValiChrom columns with 8 mm ID packed with SP-650 M, which may be attributed to the highly fronting behavior of the peaks of the longest column, which consequently had a non-proportionally large peak width. This event leads to a steeper slope in the regression line and results in the negative values for the extra column band broadening. To our knowledge, it is difficult to pack thin columns at high bed heights and the respective column was packed as high as 25 cm in height. Consequently, the packing quality may be inferior to those achieved with shorter bed heights.

The lowest extra column band broadening observed was on average 0.0043 ml^2 for the MiniChrom columns with 5 mm ID. This value is lower than the 0.0058 ml^2 determined by the injections through the workstation alone (not considering the bypass function) even though these injections did not consider band broadening in the adapters, filters, and frits. From this outcome, we conclude that the extra column band broadening is overestimated when it is determined by pulses through the workstation only, which can be explained by the marked tailing behavior of the extra column peaks.

The length extrapolation method is suitable for determination of the extra column effects, if at least 3 columns of different lengths are available for the measurements and the peak shapes are similar for all of them. We suggest using the length extrapolation method whenever possible instead of injections through a ZDV connector. More accurate determinations of the extra column broadening are possible since the frits, filters, and adapter of the column may contribute greatly to extra column band broadening.

4.2. Impact of flow rate on extra column effects

The extra column volume was determined at different superficial velocities either by injection through the workstation alone or by extrapolation from different column lengths (Fig. 2A). The extra column volume determined by the extrapolation method was

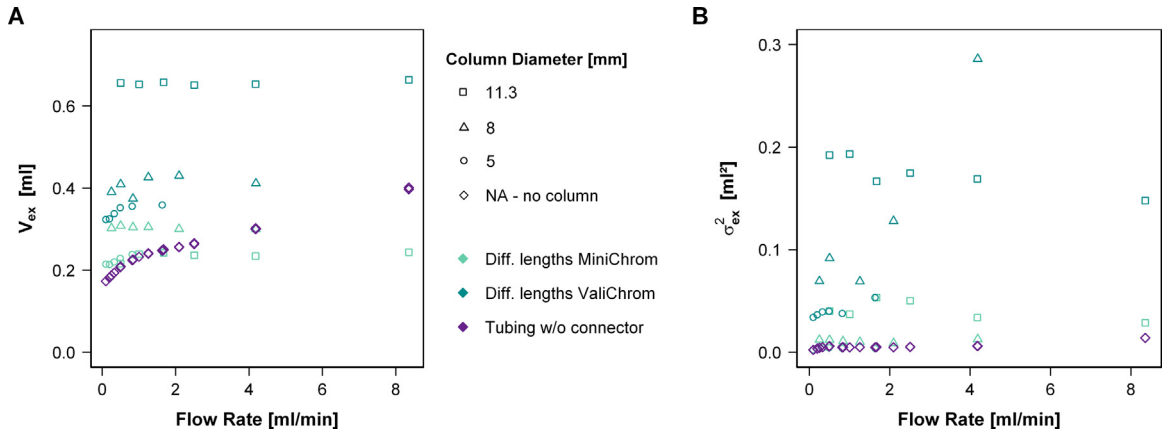

Fig. 2. Dependence of extra column volume V_{ex} (A) and the extra column band broadening σ^2_{ex} (B) on the flow rate. Data are shown for the extrapolation method of different column lengths and of pulses through the workstation only including the tubing, which was the same length as the tubing to and from the column. The extrapolation data represent the average values measured for columns packed with different resins. Negative values were not considered in calculating the means since such values are not plausible.

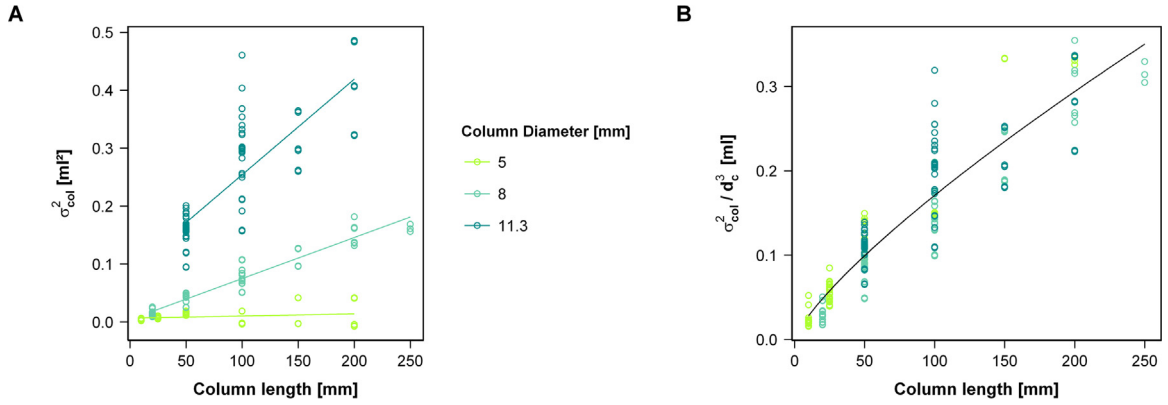

Fig. 3. Two methods to determine the variation of the intra column band broadening σ^2_{col} of the MiniChrom and the ValiChrom columns with respect to the column length and the column diameter at a fixed superficial velocity of 150 cm/h, which corresponds to reduced velocities of 23.3–30.5. (A) Intra column band broadening for different diameters. (B) Division of the intra column band broadening by the cube of the diameter allows its prediction for any column length and diameter in the used range.

Table 2
Extra column volumes determined by summing up the geometrical contributions of the individual parts and determined experimentally by extrapolation from different column lengths at a superficial velocity of 150 cm/h.

Column Type	Column diameter d_c [mm]	Geometrical contribution of V_{ex} [ml]	Experimentally determined V_{ex} [ml]
MiniChrom	5	0.242	0.229
MiniChrom	8	0.296	0.305
MiniChrom	11.3	0.376	0.236
ValiChrom	5	0.360	0.352
ValiChrom	8	0.451	0.427
ValiChrom	11.3	0.527	0.651

either constant for all flow rates or only slightly increased. However, the extra column volume determined by pulses through the workstation alone increased markedly with the flow rate. This phenomenon is well known and has already been observed previously [10,21,31]. It has been attributed to more tailing peaks at higher flow rates [7]. However, we observed decreased tailing at higher flow rates. We think this result is related to the individual design of the workstation leading to decreased total dispersion at high flow rates.

We did not observe any consistent behavior of the extra column band broadening with the flow rate. Using the length extrapolation method, the extra column band broadening is constant with flow rate for some columns, sometimes increasing with the flow rate, and sometimes decreasing (Fig. 2B). Numerous publications have reported either a decrease, an increase, or a constant behavior of extra column band broadening with flow rate [7,8,10,12,13,17,23,31–33]. From these observations, we can conclude that the workstations are apparently of very different designs. The different behaviors observed with flow rate may be related to the flow-dependent behavior of the part of the workstation which contributes most to extra column band broadening.

4.3. Prediction of peak width from column length and column diameter

The previously acquired information on extra column volume and band broadening obtained by the extrapolation method from different column lengths was used to correct the performance data of the columns. The exact extra column volume and band broadening determined for each resin was used for correction of the respective column. The correction allowed us to evaluate the per-

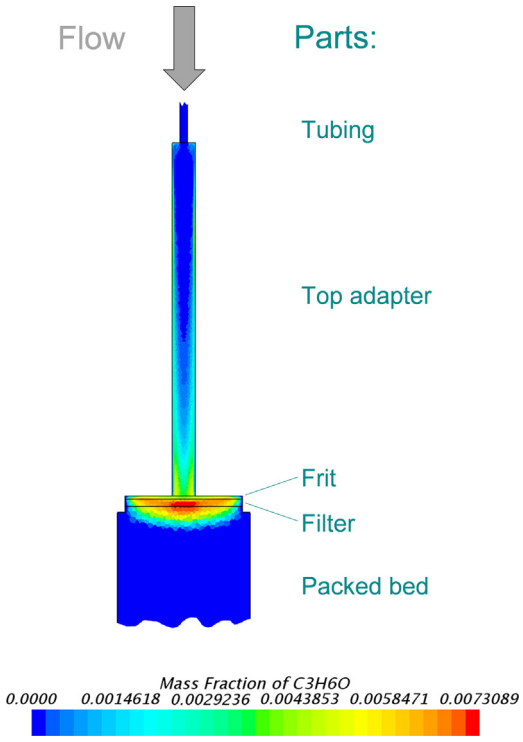

Fig. 4. CFD simulation of an acetone pulse (1% (v/v)) through a MiniChrom column with 8 mm ID and 100 mm bed height. The superficial velocity is 60 cm/h. The mass fraction of acetone at the entry of the packed bed is shown for a longitudinal cut of the column at its center.

formance of the columns themselves, independent of the used workstation.

The peak width of a pulse through a pre-packed column is positively linearly related with the column length (Fig. 3A). This result has been described previously [34]. A high variation of the intra column band broadening was especially observed for 11.3 mm ID columns of 100 mm length. We attribute this to the inaccurate determination of the extra column effects due to the use of only 2 column lengths for extrapolation. An increase in column diameter leads to an increase in peak width for columns of the same length due to the additional radial distribution of the pulse, which results from the non-ideally designed flow distributor. For columns bigger than 5 mm in diameter at low pressures, it is almost impossible to distribute the liquid homogenously over the entire cross-section within the flow distributor. This phenomenon is illustrated by CFD simulation, where not only the filter and the frit, but also the top of the packed bed is needed to homogenously distribute the solute over the entire cross-sectional area of the column (Fig. 4 and Supplementary data).

To predict the column performance, the relation between the increases in peak width with column diameter for the same length must be known. The data can be fitted with only one regression line, when the intra column band broadening is divided by the cube of the diameter (Fig. 3B). The modified data are best approximated with the following power law function:

$$\frac{\sigma^2_{col}}{d_c^3} = 0.00465 * L^{0.783} \quad (5)$$

We hypothesize that this dependence with the cube of the diameter represents an additional volume in which the solute may distribute.

Additionally, the data may not only be considered separately at every superficial velocity, but instead a three dimensional fit over all reduced velocities can be performed (Fig. 5). The intra column

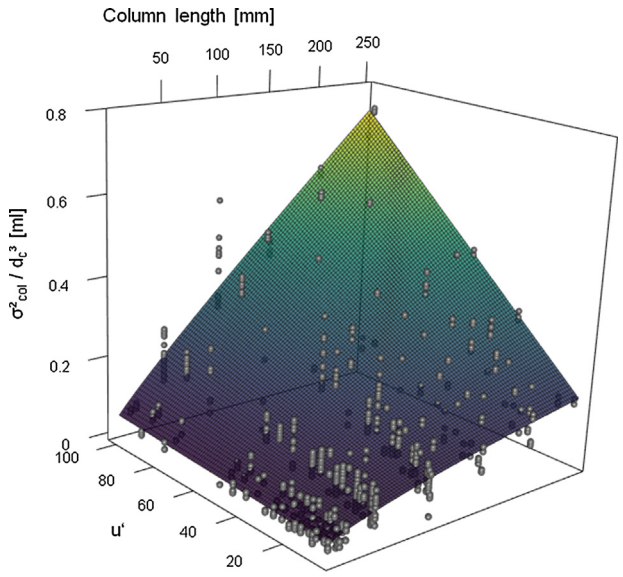

Fig. 5. Relation between intra column band broadening σ^2_{col}, column length, column diameter d_c, and reduced velocity u' for MiniChrom and ValiChrom columns. Only positive σ^2_{ex} values were included in the analysis.

band broadening increases with the superficial velocity. The fitted plane has the following equation:

$$\frac{\sigma^2_{col}}{d_c^3} = 0.00681 * L^{0.549} + 2.31 * 10^{-5} * L * u' \quad (6)$$

This equation predicts the peak width from a knowledge of the column dimensions and the superficial velocity. Therefore, the columns are scalable and packed in the same way in the tested range independent of the packed medium.

4.4. Prediction of extra column band broadening for MiniChrom and ValiChrom columns of different diameters

We investigated the influence of the extra column effects on the column performance by comparing the ratio of the extra column band broadening to the total band broadening $\sigma^2_{ex}/\sigma^2_{total}$. Since the extra column band broadening depends on the velocity, the column diameter and the column type, this analysis was conducted separately for these factors.

The change in the value of $\sigma^2_{ex}/\sigma^2_{total}$ empirically follows an exponential decay function (Fig. 6). For infinitely small column volumes, the extra column band broadening equals the total band broadening and therefore their ratio equals 1. Our data indicated that the decline of $\sigma^2_{ex}/\sigma^2_{total}$ depends on the individual construction of the column. Importantly, $\sigma^2_{ex}/\sigma^2_{total}$ can be also very high for large column volumes. The lower the superficial velocity, the higher the influence of the extra column effects because the intra column band broadening increases with the velocity, as demonstrated by CFD. Not only is the ratio of the extra column volume to the column volume important in evaluating the influence of the extra column effects, but the diameter of the columns and the design of the filter and frits/flow distributor play important roles.

Notably, the extra column volume may contribute to more than 50% of the band broadening for preparative columns with volumes larger than 10 ml, where the extra column volume is less than 5% of the column volume. This high contribution is due to the dispersion in the adapters, filters, and frits of the column.

By plotting $\sigma^2_{ex}/\sigma^2_{total}$ over the column length instead of the column volume, a simpler approximation is found (Fig. 7). The ratio $\sigma^2_{ex}/\sigma^2_{total}$ of columns with different diameters can be described with a single exponential fit. However, this estimation is only valid

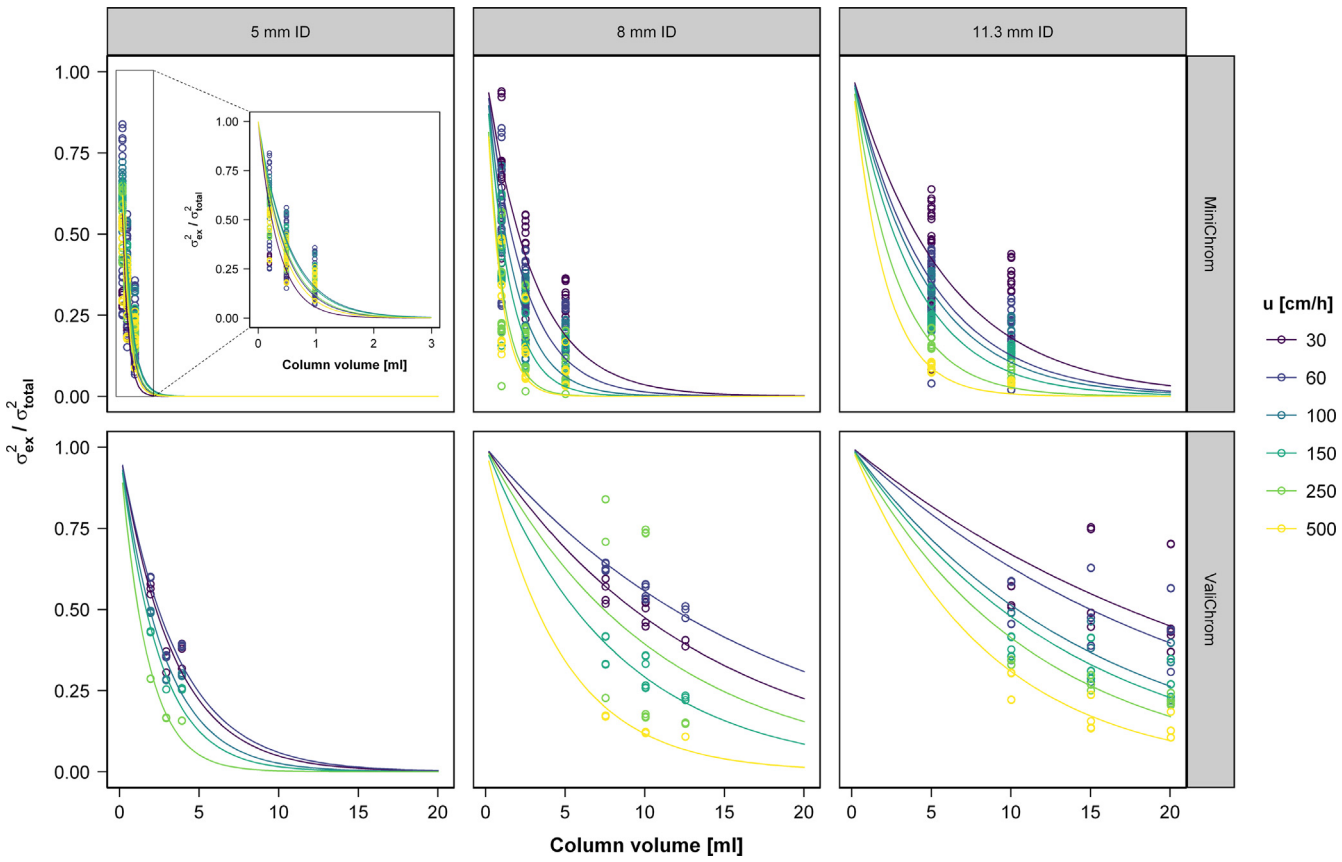

Fig. 6. Ratio of extra to total column band broadening $\sigma^2_{ex}/\sigma^2_{total}$ over the column volume for different column types, diameters, and superficial velocities u. Negative ratios were excluded as well as data from ValiChrom columns with 5 mm ID packed with SP-650 M and Phenyl-650 M since they mostly showed higher ratios than 1, which is not plausible.

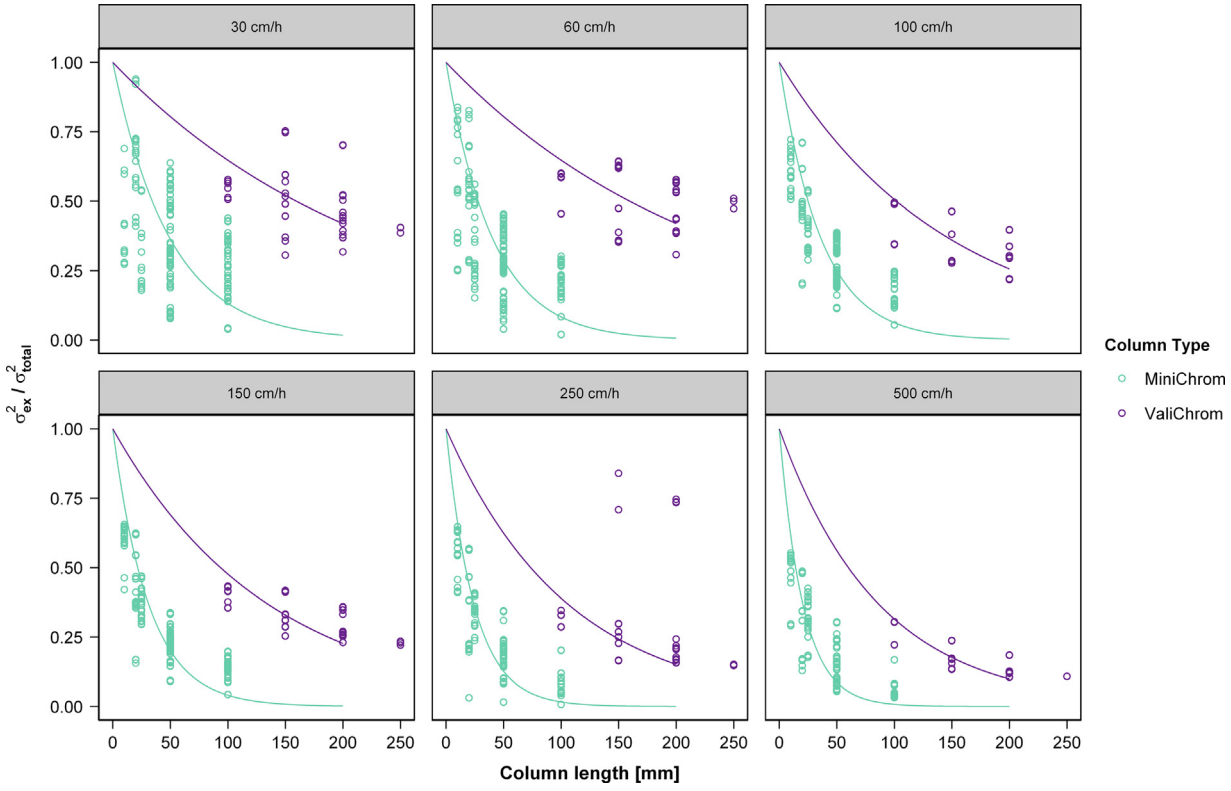

Fig. 7. Ratio of extra to total column band broadening $\sigma^2_{ex}/\sigma^2_{total}$ over the column length for different column types, diameters, and superficial velocities. Negative ratios were excluded as well as data from ValiChrom columns with 5 mm ID packed with SP-650 M and Phenyl-650 M, since they mostly showed ratios higher than 1, which is not plausible.

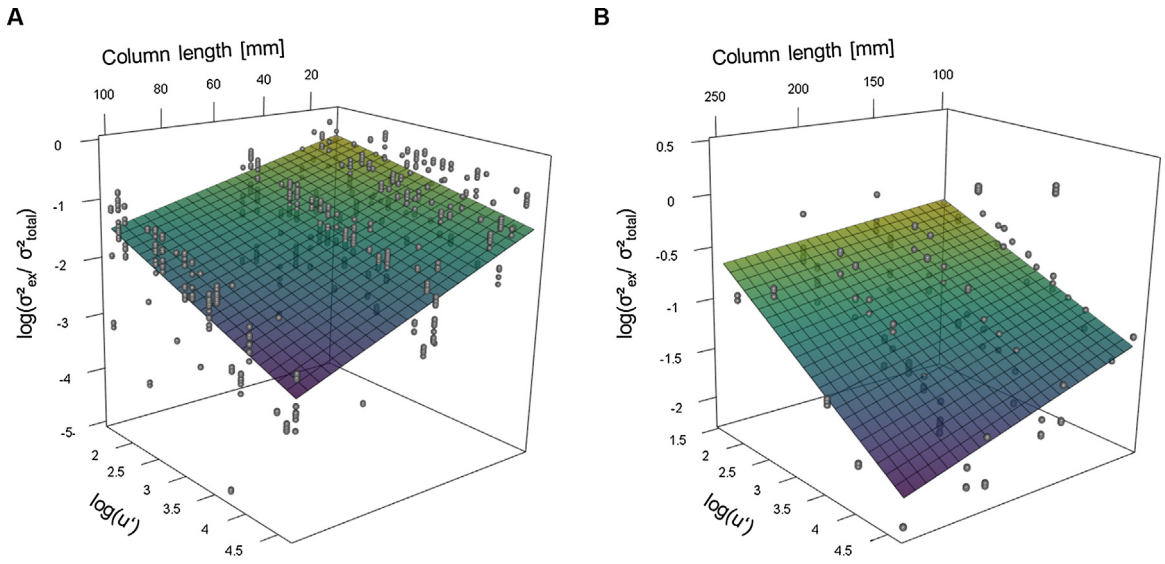

Fig. 8. Relation between extra to total column band broadening $\sigma^2_{ex}/\sigma^2_{total}$, column length, and reduced velocity u' for MiniChrom (A) and ValiChrom (B) columns. Negative ratios were excluded as well as data from ValiChrom columns with 5 mm ID packed with SP-650 M and Phenyl-650 M since they mostly showed ratios higher than 1, which is not plausible.

for superficial velocities higher than 100 cm/h. Our observation that the decline of $\sigma^2_{ex}/\sigma^2_{total}$ can be described by a single function for all column diameters can probably not be extended to other column hardware. We attribute this result to the special ratios of $\sigma^2_{ex}/\sigma^2_{total}$ for the different diameters.

The influence of the reduced velocity on $\sigma^2_{ex}/\sigma^2_{total}$ and the column length was quantified with a three-dimensional fit. The data were fitted separately for MiniChrom (Fig. 8A) and ValiChrom columns (Fig. 8B).

$\sigma^2_{ex}/\sigma^2_{total}$ of MiniChrom columns can be approximated by Eq. (7)

$$\frac{\sigma^2_{ex}}{\sigma^2_{total}} = e^{-0.00801*L} * u'^{-0.210} * u'^{-0.00241*L} \quad (7)$$

and $\sigma^2_{ex}/\sigma^2_{total}$ of ValiChrom columns with Eq. (8).

$$\frac{\sigma^2_{ex}}{\sigma^2_{total}} = u'^{-0.168} * u'^{-0.00103*L} \quad (8)$$

These equations in combination with Eq. (6) and considering that $\sigma^2_{total} = \sigma^2_{ex} + \sigma^2_{col}$ allow the calculation of the intra, extra, and total column band broadening simply by knowing the column length, diameter, and reduced velocity. This procedure allows the prediction of the column performance for any MiniChrom or ValiChrom column with a diameter smaller than 11.3 mm at any length shorter than 250 mm. This calculation is valid for all the evaluated chromatography media. The prediction of the extra column and total column band broadening is only valid for the ÄKTA pure workstation with the described configuration. The peak dispersion data were analyzed for non-retained peaks, dispersion of retained peaks will be governed by additional external and internal mass transport effects. Therefore, the equations are not applicable to predict retained protein peaks. However, from these correlations we can confirm that pre-packed columns are scalable in terms of packing quality and construction of the column hardware.

5. Conclusions

Extra column effects should not only be considered for columns of very small volume, but also for larger columns due to the additional band broadening caused by the filter, frits, and adapters of the column. The extra column band broadening may contribute more than 50% to the total band broadening even for columns with volumes of 20 ml. The higher the flow rate, the lower the contribution of the extra column band broadening. For prediction of column performance, the column diameter must be considered, since the intra column band broadening increases greatly with column diameter. This result was also confirmed by CFD simulation. An empirical relationship between the increase in band broadening and column diameter, length, and flow rate was derived, which enables the calculation of extra, intra, and total column band broadening from only the column dimensions and the flow rate. This equation can be used for all pre-packed columns with diameters up to 11.3 mm and lengths up to 20 cm, independent of the packed medium since hardly any variation in column performance with packed medium was found. The prediction of extra and total column band broadening depends on the type of chromatography workstation that is used. Herein, experiments were performed on the widespread ÄKTA pure workstation, for which these equations for prediction of column performance can be used without any adaptions.

Acknowledgements

This work has been supported by the Federal Ministry of Science, Research and Economy (BMWFW), the Federal Ministry of Traffic, Innovation and Technology (bmvit), the Styrian Business Promotion Agency SFG, the Standortagentur Tirol, the Government of Lower Austria and ZIT – Technology Agency of the City of Vienna through the COMET-Funding Program managed by the Austrian Research Promotion Agency FFG.

Appendix A. Supplementary data

Supplementary data associated with this article can be found, in the online version, at https://doi.org/10.1016/j.chroma.2018.01.022.

References

[1] T. Schroeder, Automated parallel chromatography in downstream process development, Bioprocess Int. 8 (2010) 92–93.
[2] A. Susanto, E. Knieps-Grünhagen, E. von Lieres, J. Hubbuch, High throughput screening for the design and optimization of chromatographic processes: assessment of model parameter determination from high throughput

compatible data, Chem. Eng. Technol. 31 (2008) 1846–1855, http://dx.doi.org/10.1002/ceat.200800457.
[3] W.R. Keller, S.T. Evans, G. Ferreira, D. Robbins, S.M. Cramer, Understanding operational system differences for transfer of miniaturized chromatography column data using simulations, J. Chromatogr. A 1515 (2017) 154–163, http://dx.doi.org/10.1016/j.chroma.2017.07.091.
[4] S. Grier, S. Yakabu, Prepacked chromatography columns: evaluation for use in pilot and large-scale bioprocessing, Bioprocess Int. 14 (2016).
[5] E. Langer, Innovation in Pre-packed Disposable Chromatography Columns, 2014 http://www.biopharminternational.com/innovation-pre-packed-disposable-chromatography-columns?pageID=1.
[6] J.C. Sternberg, Extracolumn contributions to chromatographic band broadening, Adv. Chromatogr. 2 (1966) 205–270.
[7] F. Gritti, A. Felinger, G. Guiochon, Influence of the errors made in the measurement of the extra-column volume on the accuracies of estimates of the column efficiency and the mass transfer kinetics parameters, J. Chromatogr. A 1136 (2006) 57–72, http://dx.doi.org/10.1016/j.chroma.2006.09.074.
[8] K.M. Usher, C.R. Simmons, J.G. Dorsey, Modeling chromatographic dispersion: a comparison of popular equations, J. Chromatogr. A 1200 (2008) 122–128, http://dx.doi.org/10.1016/j.chroma.2008.05.073.
[9] O. Kaltenbrunner, A. Jungbauer, S. Yamamoto, Prediction of the preparative chromatography performance with a very small column, J. Chromatogr. A 760 (1997) 41–53, http://dx.doi.org/10.1016/S0021-9673(96)00689-9.
[10] F. Gritti, G. Guiochon, Accurate measurements of peak variances: importance of this accuracy in the determination of the true corrected plate heights of chromatographic columns, J. Chromatogr. A 1218 (2011) 4452–4461, http://dx.doi.org/10.1016/j.chroma.2011.05.035.
[11] K. Vanderlinden, K. Broeckhoven, Y. Vanderheyden, G. Desmet, Effect of pre- and post-column band broadening on the performance of high-speed chromatography columns under isocratic and gradient conditions, J. Chromatogr. A 1442 (2016) 73–82, http://dx.doi.org/10.1016/j.chroma.2016.03.016.
[12] A.J. Alexander, T.J. Waeghe, K.W. Himes, F.P. Tomasella, T.F. Hooker, Modifying conventional high-performance liquid chromatography systems to achieve fast separations with fused-core columns: a case study, J. Chromatogr. A 1218 (2011) 5456–5469, http://dx.doi.org/10.1016/j.chroma.2011.06.026.
[13] D.V. McCalley, Instrumental considerations for the effective operation of short, highly efficient fused-core columns. Investigation of performance at high flow rates and elevated temperatures, J. Chromatogr. A 1217 (2010) 4561–4567, http://dx.doi.org/10.1016/j.chroma.2010.04.070.
[14] A. Prüß, C. Kempter, J. Gysler, T. Jira, Extracolumn band broadening in capillary liquid chromatography, J. Chromatogr. A 1016 (2003) 129–141, http://dx.doi.org/10.1016/S0021-9673(03)01290-1.
[15] E.V. Dose, G. Guiochon, Effects of extracolumn convolution on preparative chromatographic peak shapes, Anal. Chem. 62 (1990) 1723–1730, http://dx.doi.org/10.1021/ac00216a003.
[16] S.P. Cram, T.H.J. Glenn, Instrumental contributions to band broadening in gas chromatography 1. Development of a model, J. Chromatogr. 112 (1975) 329–341.
[17] J.P. Grinias, B. Bunner, M. Gilar, J.W. Jorgenson, Measurement and modeling of extra-column effects due to injection and connections in capillary liquid chromatography, Chromatography 2 (2015) 669–690, http://dx.doi.org/10.3390/chromatography2040669.
[18] O. Nilsson, On the estimation of extra-column contributions to band broadening through measurements on an authentic chroma- togram, J. HRC CC 2 (1979) 605–608.
[19] K.J. Fountain, U.D. Neue, E.S. Grumbach, D.M. Diehl, Effects of extra-column band spreading, liquid chromatography system operating pressure, and column temperature on the performance of sub-2-μm porous particles, J. Chromatogr. A 1216 (2009) 5979–5988, http://dx.doi.org/10.1016/j.chroma.2009.06.044.
[20] R.E. Pauls, L.B. Rogers, Band broadening studies using parameters for an exponentially modified Gaussian, Anal. Chem. 49 (1977) 625–628, http://dx.doi.org/10.1021/ac50012a030.
[21] F. Gritti, G. Guiochon, On the minimization of the band-broadening contributions of a modern, very high pressure liquid chromatograph, J. Chromatogr. A 1218 (2011) 4632–4648, http://dx.doi.org/10.1016/j.chroma.2011.05.024.
[22] P. Aggarwal, K. Liu, S. Sharma, J.S. Lawson, H. Dennis Tolley, M.L. Lee, Flow rate dependent extra-column variance from injection in capillary liquid chromatography, J. Chromatogr. A 1380 (2015) 38–44, http://dx.doi.org/10.1016/j.chroma.2014.12.017.
[23] K.-P. Hupe, R.J. Jonker, G. Rozing, Determination of band-spreading effects in high-performance liquid chromatographic instruments, J. Chromatogr. 285 (1984) 253–265.
[24] F. Gritti, G. Guiochon, Accurate measurements of the true column efficiency and of the instrument band broadening contributions in the presence of a chromatographic column, J. Chromatogr. A 1327 (2014) 49–56, http://dx.doi.org/10.1016/j.chroma.2013.12.003.
[25] Y. Vanderheyden, K. Vanderlinden, K. Broeckhoven, G. Desmet, Problems involving the determination of the column-only band broadening in columns producing narrow and tailed peaks, J. Chromatogr. A 1440 (2016) 74–84, http://dx.doi.org/10.1016/j.chroma.2016.02.042.
[26] Y. Vanderheyden, K. Broeckhoven, G. Desmet, Peak deconvolution to correctly assess the band broadening of chromatographic columns, J. Chromatogr. A 1465 (2016) 126–142, http://dx.doi.org/10.1016/j.chroma.2016.08.058.
[28] J.F.K. Huber, A. Rizzi, Influence of the accuracy of the extra-column peak-width determination on the verification of the theoretical plate-height equations, J. Chromatogr. 384 (1987) 337–348.
[29] S. Schweiger, S. Hinterberger, A. Jungbauer, Column-to-column packing variation of disposable pre-packed columns for protein chromatography, J. Chromatogr. A 1527 (2017) 70–79, http://dx.doi.org/10.1016/j.chroma.2017.10.059.
[30] J.J. van Deemter, F.J. Zuiderweg, A. Klinkenberg, Longitudinal diffusion and resistance to mass transfer as causes of nonideality in chromatography, Chem. Eng. Sci. 5 (1956) 271–289, http://dx.doi.org/10.1016/0009-2509(56)80003-1.
[31] N. Wu, A.C. Bradley, Effect of column dimension on observed column efficiency in very high pressure liquid chromatography, J. Chromatogr. A 1261 (2012) 113–120, http://dx.doi.org/10.1016/j.chroma.2012.05.054.
[32] A. Schultze-Jena, M.A. Boon, P.J.T. Bussmann, A.E.M. Janssen, A. van der Padt, The counterintuitive role of extra-column volume in the determination of column efficiency and scaling of chromatographic processes, J. Chromatogr. A 1493 (2017) 49–56, http://dx.doi.org/10.1016/j.chroma.2017.02.068.
[33] F. Gritti, G. Guiochon, Mass transfer kinetics, band broadening and column efficiency, J. Chromatogr. A 1221 (2012) 2–40, http://dx.doi.org/10.1016/j.chroma.2011.04.058.
[34] J.L. Rocca, J.W. Higgins, R.G. Brownlee, Peak variance as a function of HPLC column length and diameter, J. Chromatogr. Sci. 23 (1985) 106–113, http://dx.doi.org/10.1093/chromsci/23.3.106.

SUPPLEMENTARY MATERIAL

PUBLICATION III

Extra column effects of the workstation alone

The contribution of the workstation was measured by pulses through the workstation without a column connected. We analyzed different bypass types to investigate whether it is important to use a ZDV connector, or whether any connector or bypass type will give the same results. The evaluated bypass types are: (1) in-built “bypass” function in the column valve of the used ÄKTA pure workstation; (2) tubing to and from the column connected with a 70 nl connector; (3) tubing to and from the column connected with an 8 nl (ZDV) connector; and (4) long tubing with exactly the same length as the tubing to and from the column. The bypass type significantly influences the extra column volume, which was confirmed by ANOVA analysis (Figure S1A). The extra column volume was lower for the ÄKTA bypass function (212 µl) than for all the other connection types, which were approximately in the same range (239-244 µl). This is plausible since the tubing to and from the column with a volume of 20 µl was not considered using the ÄKTA bypass function. The determined extra column volumes are slightly higher than the geometrical contribution of the workstation alone, which is 202 µl with tubing to and from the column.

Additionally, the extra column band broadening was significantly influenced by the bypass type (Figure S1B). The average extra column band broadening determined by the different bypass types was in a range of 0.0054-0.0071 ml². The ÄKTA bypass function had the highest extra column band broadening, despite the extra column volume being the smallest. The reason lies probably in the design of the ÄKTA bypass valve, which has a rather wide but short flow path instead of a long and narrow one as present in all other connection types. All bypass types showed highly tailing peaks with a skew of 2.1-2.4 (Figure S1C). There were no statistical differences between the different bypass types. It is already known that peaks through the extra column volume alone tailed markedly [1–3]. The higher tailing might lead to an overestimation of the extra column band broadening. The pre-column pressure influences solute dispersion in the pre-column volume and, consequently, also affects band broadening [4]. Thus, pulses through the workstation without any column connected

represents a suboptimal method to determine the extra column band broadening of HPLC columns. However, it has been shown that the variance of a peak increases linearly with the pressure in the tubing by about 7 % for 100 bar [5]. Consequently, this dispersion can be neglected because the highest measured pre-column pressure was 11 bar. Based on these results, we can conclude that it is important to also measure the volume and band broadening inside the tubing to and from the column and that the in-built bypass function of the ÄKTA pure workstation is not suitable to accurately determine the extra column effects. It is not important to use a ZDV connector for preparative columns; any connector with a small dead volume or a single piece of tubing with the same length as the tubing to and from the column is suitable.

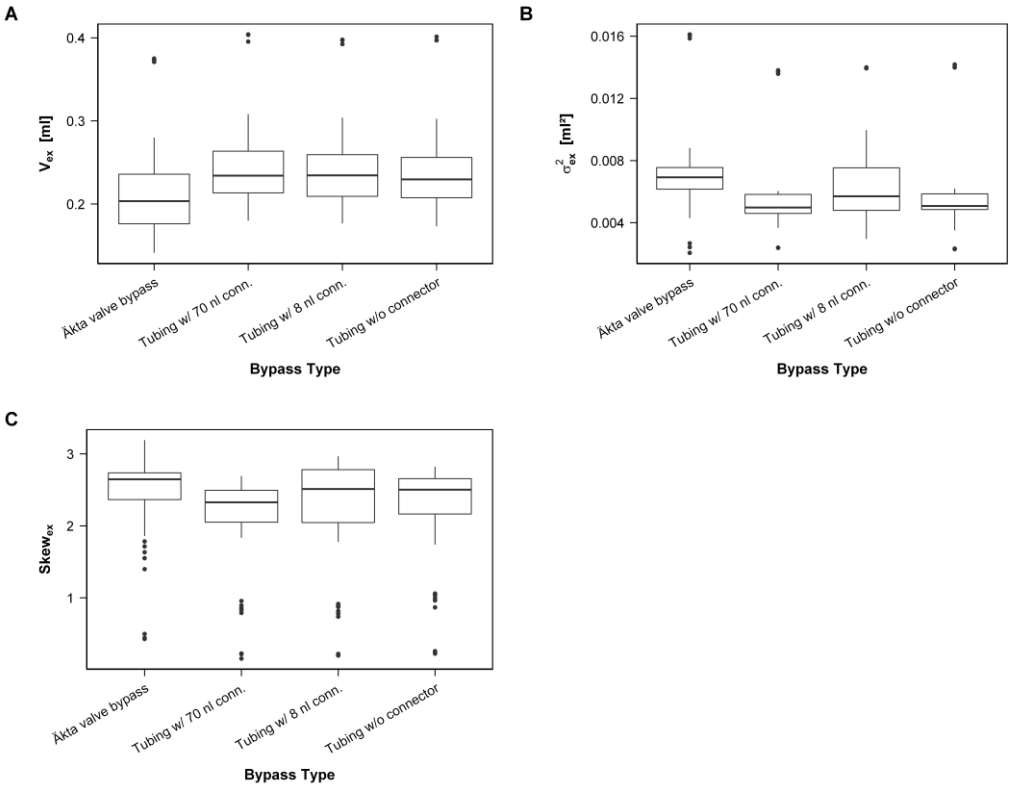

Figure S1 Differences between different connector types used to determine the performance of the workstation tested at flow rates in a range of 0.1-8.4 ml/min. (A) Extra column volume V_{ex}. (B) Extra column band broadening σ^2_{ex}. (C) Skew of extra column peaks. The shown data were measured for the shorter tubing configuration of the workstation.

References

[1] F. Gritti, A. Felinger, G. Guiochon, Influence of the errors made in the measurement of the extra-column volume on the accuracies of estimates of the column efficiency and the mass transfer kinetics parameters, J. Chromatogr. A. 1136 (2006) 57–72. doi:10.1016/j.chroma.2006.09.074.

[2] J.G. Atwood, M.J.E. Golay, Disperion of peaks by short straight open tubes in liquid chromatography systems, J. Chromatogr. 218 (1981) 97–122.

[3] M.J.E. Golay, J.G. Atwood, Early phases of the disperion of a sample injected in poiseuille flow, J. Chromatogr. 186 (1979) 353–370.

[4] F. Gritti, S.J. Shiner, J.N. Fairchild, G. Guiochon, Evaluation of the kinetic performance of new prototype 2.1mm×100mm narrow-bore columns packed with 1.6μm superficially porous particles, J. Chromatogr. A. 1334 (2014) 30–43. doi:10.1016/j.chroma.2014.01.065.

[5] F. Gritti, G. Guiochon, Effect of the pressure on pre-column sample dispersion theory, experiments, and practical consequences, J. Chromatogr. A. 1352 (2014) 20–28. doi:10.1016/j.chroma.2014.04.089.

PUBLICATION IV

Packing quality, protein binding capacity and separation efficiency of pre-packed columns ranging from 1 mL laboratory to 57 L industrial scale

Susanne Schweiger[1], Eva Berger[1], Alan Chan[2], James Peyser[2],Christine Gebski[2], Alois Jungbauer[1,3*]

[1] Austrian Centre of Industrial Biotechnology, Vienna, Austria

[2] Repligen Corporation, Waltham, MA, US

[3] Department of Biotechnology, University of Natural Resources and Life Sciences Vienna, Austria

* Corresponding author:

Alois Jungbauer

E-Mail: alois.jungbauer@boku.ac.at

Tel.: +43 1 47654 79083

Address:

University of Natural Resources and Life Sciences, Vienna

Department of Biotechnology

Muthgasse 18

1190 Wien

Austria

Abstract

Pre-packed chromatography columns are routinely used in downstream process development and scale-down studies. In recent years they have also been widely adopted for large scale, cGMP manufacturing of biopharmaceuticals. Despite columns being qualified at their point of manufacture before release for sale, the suitability of pre-packed chromatography columns for protein separations at different scales has not yet been demonstrated. In this study, we demonstrated that the performance results obtained with small scale columns (0.5 cm diameter x 5 cm length, 1 mL column volume) are scalable to production sized columns (60 cm diameter x 20 cm length, 57 L column volume). The columns were characterized with acetone and blue dextran pulses to determine the packing density and packed bed consistency. Chromatography performance was evaluated with breakthrough curves including capacity measurements and with separation of a ternary protein mixture (lysozyme, cytochrome C and RNase A) with a step gradient. The equilibrium binding capacity and dynamic binding capacity were equivalent for all columns. Slight variation was observed that could be attributed to minor conductivity differences within the sample loads. Identical buffers (± 2 mM Na^+) could not be reproduced for each scale. The step gradient separation of the ternary protein mixture displayed similar peak profiles when normalized in respect to column volume. The elution times and peak widths shifted with the slope of the gradient monitored by conductivity, but the eluted protein pools had same purity for all scales measured by RP-HPLC. A time constant of the mixer was obtained by fitting the conductivity signal with a function for logistic growth (Kaltenbrunner and Jungbauer 1997). The time constant changes dramatically when the scale is increased from 1 mL to 20 mL but then levels off to a constant value. This behavior is also reflected by the separation results, while at small-scale elution position is highly dependent on scale, whereas at large scale it is almost independent. Scalable performance of pre-packed columns is demonstrated but as with conventionally packed columns the influence of extra column

volume and system configurations, especially buffer mixing, must be taken into account when comparing separations at different scales.

Keywords

scalability, preparative chromatography; breakthrough; step gradient separation; buffer mixing; column performance

Highlights

- Scalability of pre-packed preparative chromatography column performance from 1 mL to 57 L
- Breakthrough experiments showed equal binding capacities for all column scales
- Equal level of purity for step gradient separations for all column scales
- Time constant of mixer is a simple parameter for influences of system
- Shift in relative peak position depends on mixer time constant

1 Introduction

Disposable technologies are getting increasingly popular for production of biopharmaceuticals [1–5]. Pre-packed preparative chromatography columns are commercially available in a range of sizes, from 50 µL to 85 L columns volumes, and are used for purification process development, pre-clinical, clinical and commercial manufacturing in batch and integrated continuous modes. Columns are individually qualified during manufacture, and are shown to be functional in stand-alone unit operations, but the chromatographic performance of pre-packed columns across scales has yet to be demonstrated. In the bioprocess industry, multiple theoretical and practical approaches have been described to ensure the scalable performance of chromatography columns. The most important parameter for scalability of packed beds from small to large scale is the same packing quality at all scales [6]. In addition, extra column effects must be considered to derive reliable scale-up predictions of performance [7]. Assessment of changes in buffer transition curves can be used for the determination of correction factors to more effectively predict elution behavior at a larger scale [8]. Chromatography column operation is scaled up by keeping residence time constant when mass transfer is the governing band broadening mechanism. In a conservative approach, this is achieved by maintaining a constant column bed height, increasing the column diameter and maintaining superficial velocities and the ratio of sample load volume to column volume across all scales.

It has previously been shown that small scale pre-packed columns can be manufactured over a ten year period with consistent packed bed quality [9]. The column-to-column packing variation of small scale pre-packed columns was quantified recently [10] and considered sufficiently low to perform process development and scale down studies. Moreover, pre-packed columns from 0.2-20 mL column volumes, packed with different media, are scalable [11] shown by qualification results obtained with non-retained acetone pulses. From the column qualification results, it can then be assumed that column performance with proteins will also be scalable, since extra column effects and the packing quality become less

important for retained proteins. The performance of large scale pre-packed columns has been shown to be comparable to self-packed columns [12].

Pre-packed columns designed for operation by robotic liquid handling systems were used to model separations of 1 mL laboratory scale columns [13,14] or even of larger self-packed columns [15–17]. The scalability of pre-packed columns from benchtop to production scale for protein separations has not been demonstrated yet. For demonstration of scalability over a wide range of column volumes the system contribution must be taken into account. In particular this is the contribution of the mixer forming the step gradients. It is known that system contributions are a larger percentage of total broadening at a small scale. A simple parameter for evaluating the system contribution is the time constant of the mixer. We have described it by a logistic growth function. The change of the mobile phase modifier concentration is fitted over time or volume and a constant is obtained for each scale. These data can be further correlated and used for scale-up predictions.

In this study, we investigate whether protein separations can easily be scaled up using pre-packed chromatography columns with volumes ranging from 1 mL to 57 L. Suitability of pre-packed columns over the whole range is demonstrated by comparing breakthrough curves and the resulting binding capacities. Additionally, a ternary protein mixture was separated at all column scales using a step gradient method. Effectiveness of the protein separation was determined by analyzing the purity of the individual protein fractions by RP-HPLC. Also, the relationship between relative peak positions and the slope of the gradients at each scale was established.

2 Materials and Methods

2.1 Chemicals and proteins

For all experiments with OPUS® MiniChrom and ValiChrom columns, Tris, sodium chloride, disodium hydrogen phosphate dihydrate and trifluoroacetic acid were obtained from Merck Millipore (Darmstadt, Germany), acetone was purchased from VWR chemicals (Fontenay-sous-Bois, France) and acetonitrile was obtained from Avantor Performance Materials (Deventer, Netherlands).

For all experiments with OPUS® large scale 10-60cm diameter columns, Tris was purchased from AmericanBio (Natick, US), sodium chloride was obtained from Amresco (Solon, US), sodium phosphate dibasic anhydrous was obtained from Fisher Chemical (Hampton, US) and acetonitrile, trifluoroacetic acid and acetone were purchased from EMD (now Merck Millipore, Darmstadt, Germany). For all columns, blue dextran was obtained from Sigma (St. Louis, US).

Lysozyme was obtained from Henan Senyuan Biological Technology (Henan, China). The purity of the lysozyme was determined to be 87 % by size exclusion-HPLC (SEC-HPLC). Cytochrome c and ribonuclease A were purchased from Xi'an Health Biochem Technology Co. (Xi'an, China). The purities of cytochrome c and ribonuclease A were determined to be 93 % and 70 %, respectively, by size exclusion-HPLC.

2.2 Pre-packed columns and chromatography systems

We used pre-packed OPUS® MiniChrom, OPUS® ValiChrom and OPUS® 10-60cm ID (Repligen Corp, Waltham, US and Ravensburg, Germany) for the experiments. All were packed with the 65 µm cation exchange medium Toyopearl SP-650M (Tosoh, Tokyo, Japan). Information on the column lengths, diameters and volumes are given in Table 1.

Table 1 Properties of the OPUS® pre-packed chromatography columns evaluated

TYPE	INNER DIAMETER [CM]	BED HEIGHT [CM]	VOLUME [L]
MiniChrom	0.5	5.0	0.001
MiniChrom	0.8	10.0	0.005
MiniChrom	1.13	10.0	0.01
ValiChrom	0.8	20.0	0.01
ValiChrom	1.13	20.0	0.02
ValiChrom	1.6	20.0	0.04
ValiChrom	2.5	20.0	0.1
OPUS 10	10.0	20.0	1.57
OPUS 45	45.7	20.2	33.1
OPUS 60	60.0	20.0	56.5

MiniChrom and ValiChrom columns were operated with an ÄKTA™ pure 25 M2 chromatography system (GE Healthcare, Uppsala, Sweden), which was controlled with Unicorn Software 6.4. The OPUS 10 cm column was run on an ÄKTA pilot chromatography system (GE Healthcare). All other OPUS columns were operated with QuattroFlow 1200S pumps (PSG, Oakbrook Terrace, US) to deliver the running buffer and the load material, and a peristaltic pump 520SN/R2 (Watson Marlow, Wilmington, US) to inject the pulses. The maximum achievable flow rate of the peristaltic pump was 3.2 L/min, resulting in lower flow rates during injection for the 45.7 cm and 60 cm ID columns. A split flow path after the column allowed for UV and conductivity detection on the ÄKTA pilot.

2.3 Acetone pulses

Pulse response experiments were performed with acetone (1%, v/v) as a small non-binding solute. The injected pulse volumes were 10 µl for all 0.5 cm ID MiniChrom and ValiChrom columns, 50 µl for all ValiChrom columns with 0.8 cm ID, and 500 µl for all ValiChrom columns with 1.13 cm ID. For all larger columns, 1 % of the column volume was injected. The running buffer was 50 mM Tris, 0.9 % (w/v) sodium chloride, pH 8.0 (pH adjusted with HCl). Pulse response experiments were performed at superficial velocities of 60, 100, 150

and 250 cm/h. The chromatograms from the acetone pulses were analyzed by direct numerical integration.

2.4 Breakthrough experiments

Lysozyme was loaded on all columns up to 45.7 cm ID until full breakthrough. The formulation of the loading buffer was designed to reduce the binding capacity of the media so as to minimize the amount of lysozyme required for the analysis. The running buffer was 25 mM Na_2PO_4, 170 mM NaCl, pH 7.5. Lysozyme at 6 mg/mL in running buffer was loaded at an 8 minute residence time onto the column until 100% breakthrough was observed. After washing with running buffer, the bound lysozyme was eluted with 25 mM Na_2PO_4, 1 M NaCl, pH 7.5. Between each process step, the chromatography system tubing was primed from the buffer inlet to the injection valve with the required solution, so as to minimize extra column effects. EBC (equilibrium binding capacity) and DBC (dynamic binding capacity) were determined by direct numerical integration of the breakthrough curves. The breakthrough curves were integrated from $0 < c/c_F < 1$ for determination of the total EBC. The EBC of the impurities was determined by integration of the breakthrough curve to the height of the first plateau after early impurity breakthrough. The EBC of the lysozyme was calculated by subtracting the impurity EBC from the total EBC. DBC was determined similarly by integration until $c/c_F = 0.1$ after deduction of the height of the impurity plateau. The same was done for determination of the slopes at 50 % of the lysozyme breakthrough, which is equivalent to a total height of $c/c_F = 0.517$. Values within 10 % above and below that point were used for linear fitting to calculate the slope.

2.5 Step gradient experiments

The separation of lysozyme, ribonuclease A and cytochrome c was investigated using a multi-step gradient. We used 25 mM Na_2PO_4 pH 6.5 as running buffer and 25 mM Na_2PO_4, 1 M NaCl pH 6.5 as the elution buffer. A mixture of 5 mg/mL lysozyme, 7.13 mg/mL cytochrome c and 12.56 mg/mL ribonuclease A was formulated in running buffer. The columns were loaded with a 5 % CV injection at an 8 minute residence time. After washing

with at least 4 CVs of running buffer, the three proteins were eluted with three separate steps of 4 %, 12 % and 26 % buffer B. Each step was held until the UV signal returned to the baseline level. The amount of buffer required for each step varied with column size, but in each instance at least 3.5 CV for each elution steps was used. The residual protein bound following the third elution step was stripped with 100 % B buffer. During each of step gradient elutions, 0.5 CV fractions were collected. Fractions containing protein according to the 280 nm UV signal were pooled and analyzed by reversed phase-HPLC. For peak analysis, the two peaks of each elution step were fitted to two Gaussian peaks. The respective peak retention times, widths, areas and the resolution was calculated from the fitted Gaussian functions.

2.6 Reversed-phase HPLC analysis

The purity of the load material and fractions collected during each elution step gradient was determined by RP-HPLC using a Discovery BIO Wide Pore C5 column (Supelco, Bellefonte, US) with 5 µm particles, 4.6 mm ID and 15 cm length. For the analytics of the MiniChrom and ValiChrom columns, all runs were made on a Waters Alliance HPLC system with an e2695 Separations Module (Milford, US). The samples collected from the larger columns were analyzed on an Agilent HPLC system 1100 series (Santa Clara, US).

The column was operated at a flow rate of 1 mL/min at a temperature of 25 °C. Solvent A was 0.1 % TFA in water and solvent B was 0.1 % TFA in acetonitrile. The column was equilibrated for 2 min at 25 % B and then 10 µl of sample containing 0.1 % TFA was injected. A linear gradient from 25-75 % B was run for 15 minutes. Peaks were detected at a wavelength of 214 nm. After 17 minutes the column was regenerated followed by re-equilibration at 25 % B for 13 minutes. Peaks with a retention time between 5.35 and 12 min were integrated using the respective software of the HPLC systems. Peak areas were considered for the purity determinations.

2.7 Extra particle porosities

For determination of the extra particle porosity, a 5 % CV pulse of 2 mg/mL blue dextran dissolved in 1 M NaCl was injected into the columns at a linear velocity of 250 cm/h. The mobile phase was 1 M NaCl. The pulses were corrected for the contributions of the extra column volume for calculation of the extra particle porosity. Only the position of the peak maximum was considered for determination of the extra particle porosity.

2.8 Isotherms

Isotherms were prepared in a 96-well format on a MultiScreen-HV 0.45 µm filter plate (Merck Millipore, Burlington, US). Slurries (5 %) of the SP-650M medium were prepared in three different buffers (25 mM Na_2PO_4, ~ 160 mM NaCl, pH 7.5) which were adjusted with 2 M sodium chloride to different final conductivities (20.61, 20.75 and 20.90 mS/cm). These conductivities represent the whole range of measured conductivities for the lysozyme breakthrough buffer. Despite only one formulation being used, some inaccuracies during buffer preparation, especially at larger scale, resulted in slight variations in final buffer conductivities Into each well, 200 µl slurry was added and buffer was removed by applying vacuum. The medium was then incubated with different concentrations of lysozyme in the respective buffers. After 23 h of equilibration at 24 °C and 300 rpm shaking on a ThermoMixer (Eppendorf, Hamburg, Germany), the liquid phase was transferred to a 96-well UV-Star Microplate (Greiner Bio-One, Kremsmünster, Austria) and the absorbance at 280 nm was measured with an Infinite M200 PRO plate reader (Tecan, Männedorf, Switzerland) to determine the lysozyme concentration. Each isotherm was measured in triplicate.

3 Theory

The statistical moments of the acetone peaks were determined by direct numerical integration. The first moment (M_1) is the mean retention volume of a peak. The second moment (M_2) is the variance of a peak and is a measure of peak width around its center of gravity. The determined first moment was corrected by the contributions of the extra column volume. The height equivalent to theoretical plate (H) was calculated by

$$H = \frac{M_2 * L}{M_1^2} \quad (1)$$

where L is the column length.

The peak asymmetry is commonly calculated at 10 % peak height by

$$As = \frac{b}{a} \quad (2)$$

where b is the width from peak maximum to the rear part of the peak and a is the width from the front part of the peak of the peak maximum. Alternatively, the peak skew can be used for description of the peak shape, which is calculated by

$$Skew = \frac{M_3}{M_2{}^{3/2}} \quad (3)$$

where M_3 is the third moment. The peak skew is negative for fronting peaks, zero for symmetrical peaks, and positive for tailing peaks.

The logistic dose-response function describes a transition from a base to a saturation level and is therefore excellently suited to describe chromatography gradients [18]. The volume of the mixer in relation to the chromatography system and column determines the shape of the gradient. The deviation from the ideal gradient is more dominant on small scale rather than on large scale. Mixers in chromatography systems can be described with a continuous stirred tank reactor (CSTR) model, which is modified to include logistic growth with the following equation [19]:

$$C_M = \frac{C_M^0 * C_M^{max} * \exp(\frac{t}{a})}{C_M^0 * \exp(\frac{t}{a}) + C_M^{max} - C_M^0} \quad (4)$$

where t is the retention time or volume – in our case the retention volume in CV, a is the time constant of the mixer, $C_M{}^0$ is the modifier concentration at the start of the step increase and

248 C_M^{max} is the modifier concentration at the end of the step increase. The shape of step

249 gradient increases can be described with the time constant by fitting them to equation 4.

4 Results and Discussion

4.1 Evaluation of the packed bed

The packing quality and consistency of all tested pre-packed columns with volumes from 1 mL to 57 L was verified by acetone pulses performed at different velocities. The first moments were corrected by the extra column volumes before plotting versus scale. The first moments increase linearly with the column volume indicating a similar packing quality and same total porosity for all column scales (Figure 1A). The extra column volume is less than 5 % of the CV for all columns except for the 1 mL, where it is 20-25 % (Figure 1B). Consequently, the extra column effects will affect the retention volume and peak width for the 1 mL column. The second peak moment is related to the column volume [11]. This was corroborated for a larger range of columns (Figure 1C). The variation in the data is explained by extra column band broadening effects which were not considered, since it was experimentally not possible to determine extra column band broadening in the flow distributors. Acetone peaks in the 1 mL column tailed significantly more than other column formats. This result is most probably due to the large extra column volume in the 1mL format and therefore dominance of extra column effects. Acetone peaks on all other columns were symmetric with asymmetries below 1.43 (Table 2). The calculated HETP values varied in a range of 0.027 to 0.098 cm across all scales. Moreover, the determined extra particle porosities were in a range of 0.36 to 0.49. Previously, we hypothesized that columns are scalable for protein separations when the first and second moments of non-retained peaks with small solutes such as acetone correlate with the column size, or when expressed in respect to column volume they are identical over all scales, except for the very small columns [11]. To prove this assumption, additional scale-up experiments with proteins in a binding mode were carried out.

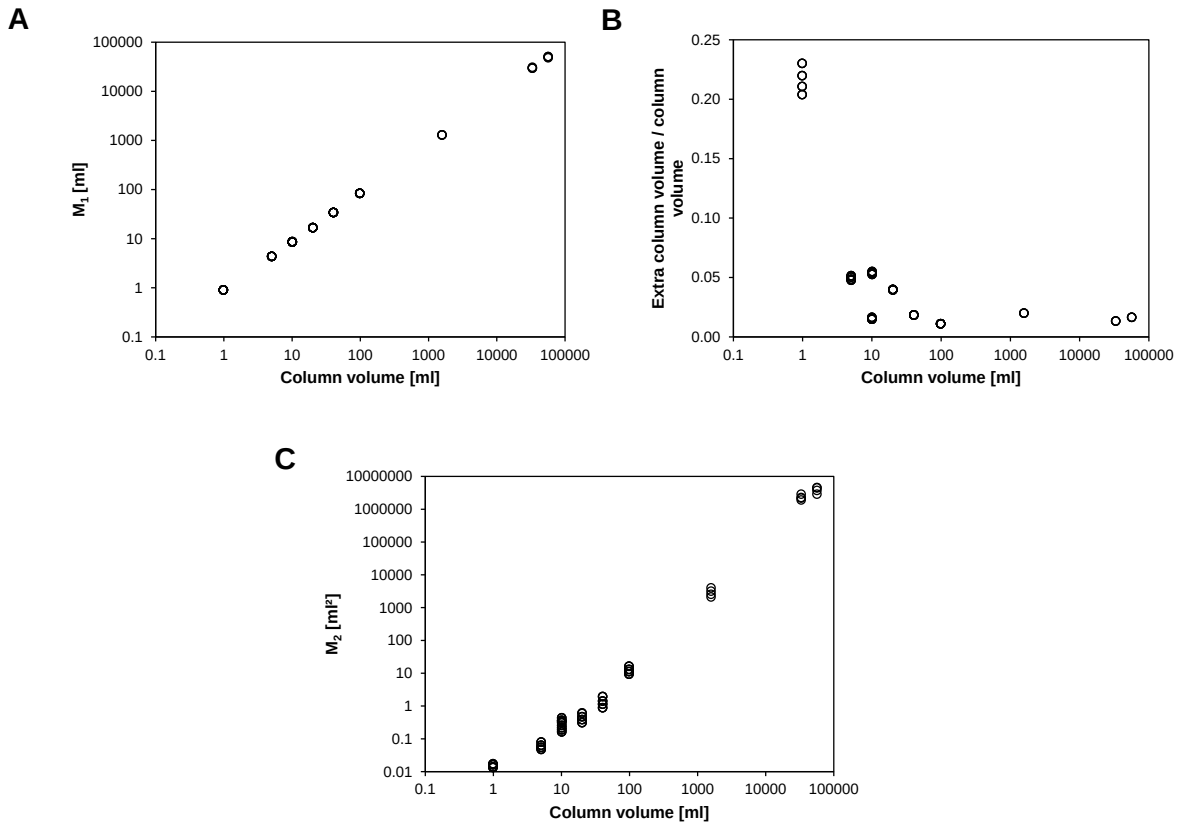

Figure 1 Peak moments of acetone peaks from multiple columns performed at 4 different superficial velocities. (A) First peak moment corrected for extra column volumes (B) Ratio of extra column volume to column volume (C) Second peak moment (D) Third peak moment for all scales

Table 2 HETP and asymmetries determined from acetone pulses at superficial velocities of 150 cm/h.

TYPE	VOLUME [L]	HETP [CM]	ASYMMETRY AT 10 % PEAK HEIGHT	EXTRA PARTICLE POROSITY (ε)
MiniChrom	0.001	0.098	1.27	0.49
MiniChrom	0.005	0.033	1.15	0.41
MiniChrom	0.01	0.048	1.43	0.38
ValiChrom	0.01	0.059	0.64	0.43
ValiChrom	0.02	0.033	1.00	0.36
ValiChrom	0.04	0.024	1.06	0.38
ValiChrom	0.1	0.036	1.20	0.39
OPUS 10	1.57	0.037	1.09	0.36
OPUS 45	33.1	0.050	1.02	0.43
OPUS 60	56.5	0.035	1.08	0.37

4.2 Binding capacity for lysozyme

Lysozyme breakthrough curves were performed on all columns except for the 60 cm ID column. We operated all columns at a constant residence time of 8 minutes, so small columns have been run at much lower superficial velocity than the larger ones. In order to minimize the amount of lysozyme protein required for the analysis, we selected a loading buffer with elevated conductivity and pH to reduce the chromatography media binding capacity. The normalized breakthrough curves (C/C_F) have been superimposed (Figure 2A) and the profiles are very similar for all columns. A small breakthrough of non-binding impurities can be observed after 1 CV. Due to the high influence of the extra column volume on the 1 mL column, the breakthrough curve is shifted (dashed line) resulting in an inaccurate, artificially higher binding capacity. Therefore, the data of this column were corrected for the extra column volume. The slightly different shape of the breakthrough curve for this column is also attributed to dominating extra column band broadening effects. However, the slope at 50 % of breakthrough is very similar for all scales with a slope of 10.8 ± 0.13 CV^{-1} (Table 3).The EBC for lysozyme was the same for all columns with an average EBC of 26.6 ± 0.9 mg/mL column. The DBC at 10 % breakthrough for lysozyme was 21.3 ± 0.9 mg/mL across the range of columns tested indicating similar column performance for all scales.

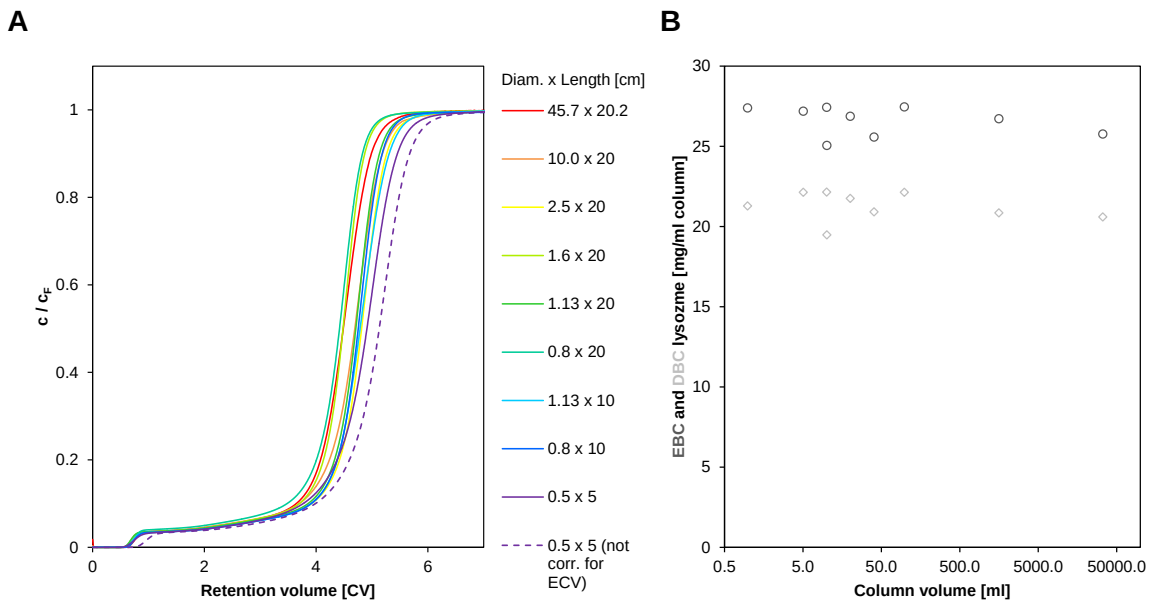

Figure 2 Lysozyme breakthrough and calculated binding capacities at a residence time of 8 min. (A) Breakthrough profiles on all columns. Data for the smallest column were corrected with the extra column volume. (B) Equilibrium binding capacities (EBC) and dynamic binding capacities (DBC) for lysozyme. The binding capacities of the impurities were subtracted from the total binding capacity to get the binding capacity of pure lysozyme.

Table 3 Calculated slopes at 50 % lysozyme breakthrough for different column scales.

TYPE	VOLUME [L]	SLOPE AT 50 % LYSOZYME BREAKTHROUGH
MiniChrom	0.001	0.89
MiniChrom	0.005	1.17
MiniChrom	0.01	0.97
ValiChrom	0.01	1.14
ValiChrom	0.02	1.18
ValiChrom	0.04	1.29
ValiChrom	0.1	1.13
OPUS 10	1.57	0.98
OPUS 45	33.1	1.00

We explain the minimal differences in the EBC and DBC by slight variations in the salt concentration of the buffer during loading. A slight variation of 0.3 mS/cm resulted in a difference in EBC of 2 mg/mL (Figure 3A).The capacity is extremely sensitive to salt and protein concentration as shown by the isotherms (Figure 3B). Isotherms were measured at

three different conductivities covering the whole experimental range. The isotherms were linear due to the less favorable binding condition and confirmed that even slight variations in the salt concentration lead to large differences in binding capacity.

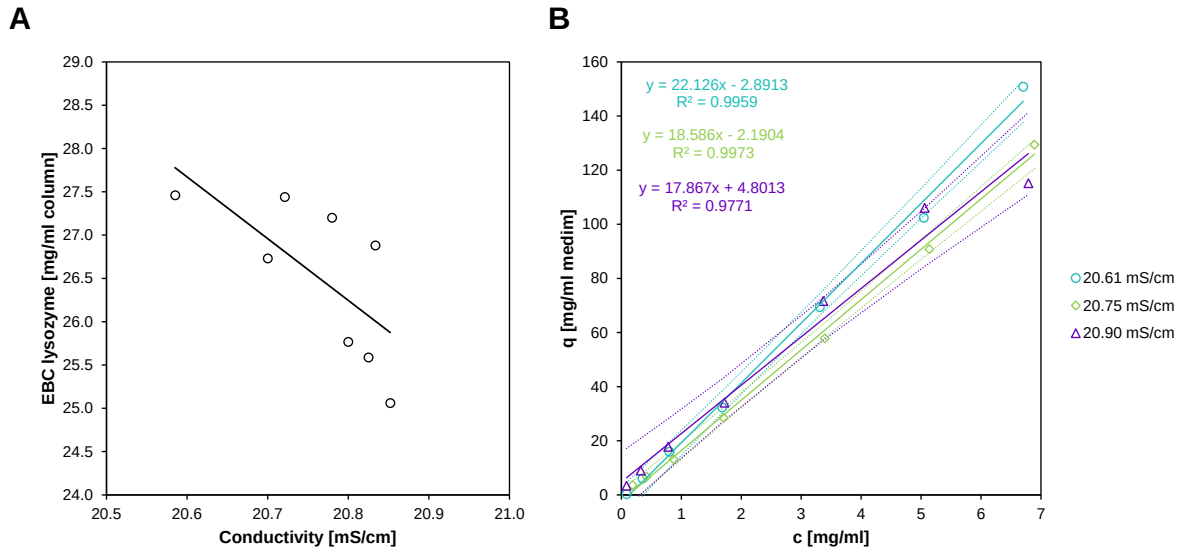

Figure 3 Influence of buffer conductivity on binding capacity (A) Equilibrium binding capacity (EBC) depends on the conductivity during the loading step. Data for the 1 mL column were omitted due to dominating extra column effects. (B) Isotherms at three different conductivities, which were in the range of the experimentally measured conductivities during breakthrough. 95 % confidence intervals of the linear fits are shown by dotted lines

4.3 Separation performance of a protein mixture using a step gradient

For all columns in the study, a ternary mixture of proteins (lysozyme, cytochrome C and ribonuclease A) was separated by a stepwise gradient. After loading the protein mixture, columns were washed with the loading buffer. The proteins were then eluted in three subsequent steps, each at a different salt concentration followed by regeneration with high salt. Figure 4A shows an overlay of the chromatograms of all scales with the retention volume provided in column volumes for normalization. The chromatograms were aligned with respect to the onset of step gradient at the column outlet indicated by rise of conductivity. They were also aligned to the largest column which had the shortest duration of the individual steps. The curves of the small columns were cut off in the figure, despite being longer in duration in the real runs. A large peak eluted in the wash step which contained unbound impurities. This wash peak eluted at a similar column volume for each of the

different scale columns, only the peak of the 1 mL column eluted later due to the large influence of the extra column effects. The developed gradient was capable of separating the three proteins. However, in each elution step, two protein isoforms could be resolved, because we did not use completely pure model proteins. When the individual fractions for each peak were analyzed by reversed phase HPLC, the co-eluting peak only had a slightly shifted retention time compared to the main peak (data shown in supplementary material), indicating degraded or modified protein forms. With increasing column size the normalized retention volumes decreased and normalized peaks became narrower (Figure 4B-D), which can be explained by the shape of the gradient. With larger scale columns, the transition from low to high salt is steeper than with small scale columns. The same gradient shape cannot be maintained over all scales due to different influences of the extra column volume especially the mixer on the gradient profiles. The relative area of the two protein isoforms at each elution step stayed the same indicating a constant ratio between the two isoforms. The resolution between the two peaks varied for the different scales but no clear trend was observed. The resolution is likely dependent on the exact salt concentration within the different steps. By comparison of the peak profiles at the different scales, we found that only slight changes in the conductivity can lead to different elution patterns confirming that step gradients are very sensitive to variations in buffer composition.

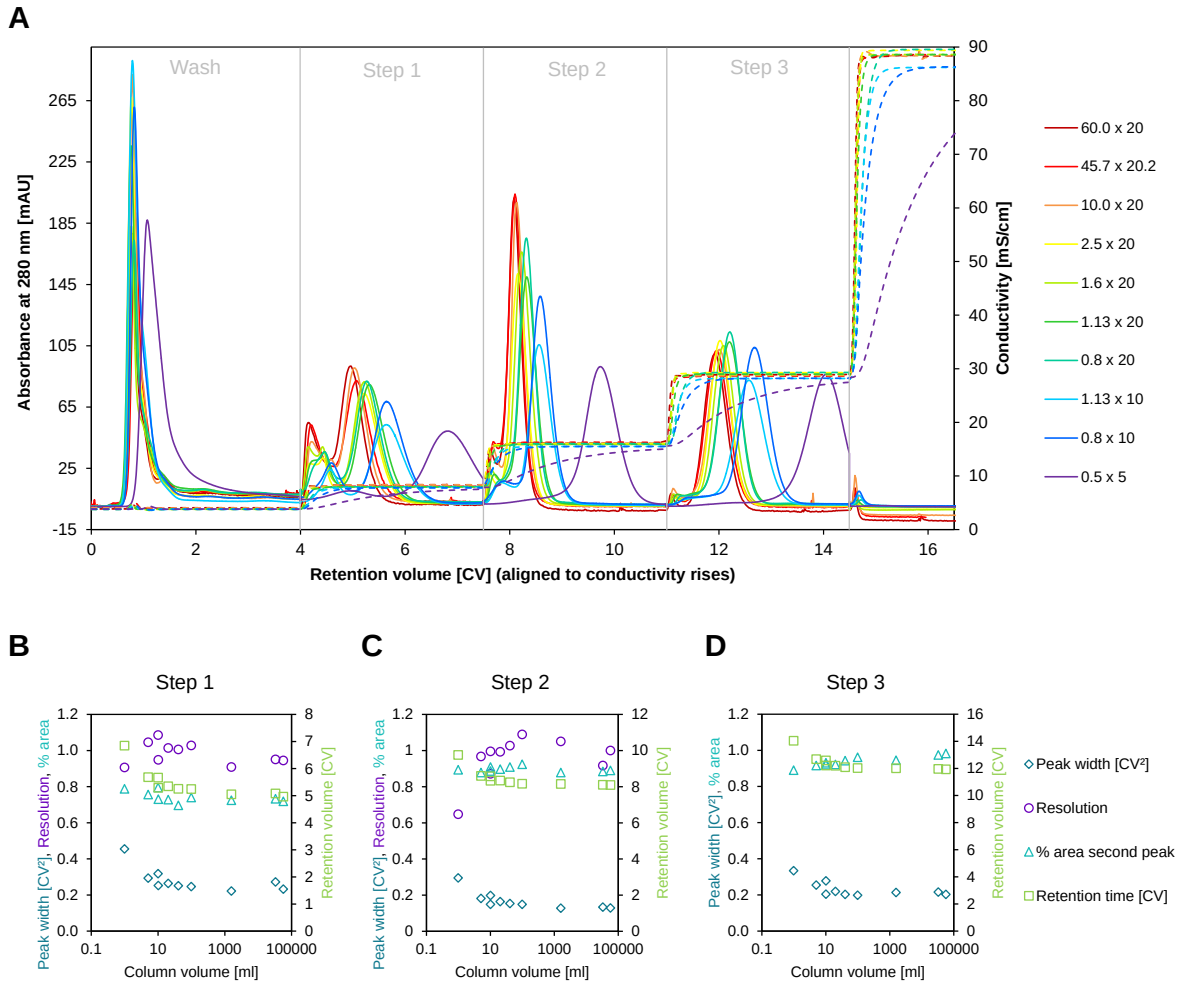

Figure 4 Step gradient separation of a mixture of lysozyme, cytochrome c and ribonuclease A with a residence time of 8 min. (A) Chromatogram of all columns, solid lines show the UV signal and dashed lines the conductivity. Each step was held until the baseline UV was reached, which lasted longer for smaller columns. For the overlay, the UV signals were aligned to the start of the rises in the conductivity signals for the largest column. Therefore the runs with the smaller columns are cut off, despite they lasted longer in reality. (B-D) Peaks of the three individual elution steps were fitted to Gaussian functions. Retention volume and peak width of the larger peak, resolution (if applicable) and the % area of larger of the two fitted peaks were calculated from the fits.

The conductivity rises of the three elution buffer step increases were fitted to equation 4 to quantify the mixer time constant *a* for the different column volumes. The mixer time constant decreases with increasing column volume and levels off between 0.03 and 0.04 CV^{-1} for columns larger than 100 mL (Figure 5). Considering only one column, the determined time constant is almost the same for the three step increases. An empirical relationship between the mixer time constant and the column volume was determined by fitting of the data points. The empirical values of the function depend on the chromatography columns and workstations especially for very small column volumes. This function reveals the importance

of also considering column volume and the shape of the conductivity curve for scale-up predictions.

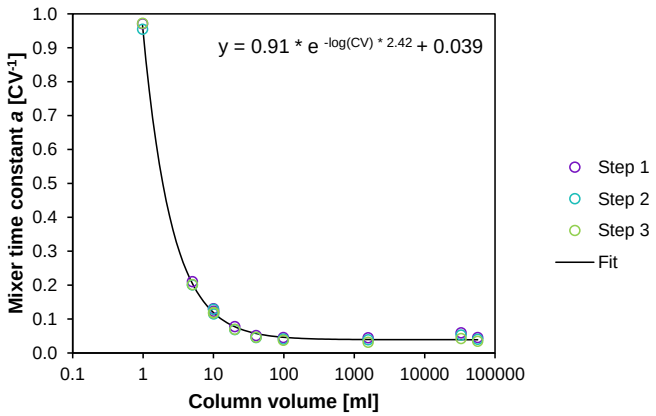

Figure 5 Mixer time constants for different column volumes, which were determined by fitting the conductivity increases to equation 4. Each color represents one step increase.

The purity of the loaded material and of the pools of the three steps were analyzed by reversed phase-HPLC. Despite some fluctuations in the concentration of the loaded material (Figure 6A), the purity of the elution pools from each of the different column volumes were comparable for all three steps (Figure 6B-D). RNase purity in the first elution step was 97.9 ± 1.3 %, cytochrome C purity was 89.3 ± 2.2 % in the second elution step and lysozyme purity was 100 ± 0 % in the last elution step. This indicates that the observed shifts in retention times, peak widths and impurities, do not influence the elution behavior and ultimately the protein purity of each elution pool. There are still some non-target protein contaminants within the pools of the first and second step, but the aim of this study was not to achieve perfection in purity but to show comparability of chromatographic performance across column scales. The data set confirms chromatographic performance of the evaluated pre-packed chromatography columns from 1 mL (0.5 x 5 cm) to at least 57 L (60 x 20 cm), indicating that packed bed consistency and pack quality across this range of column sizes is consistent.

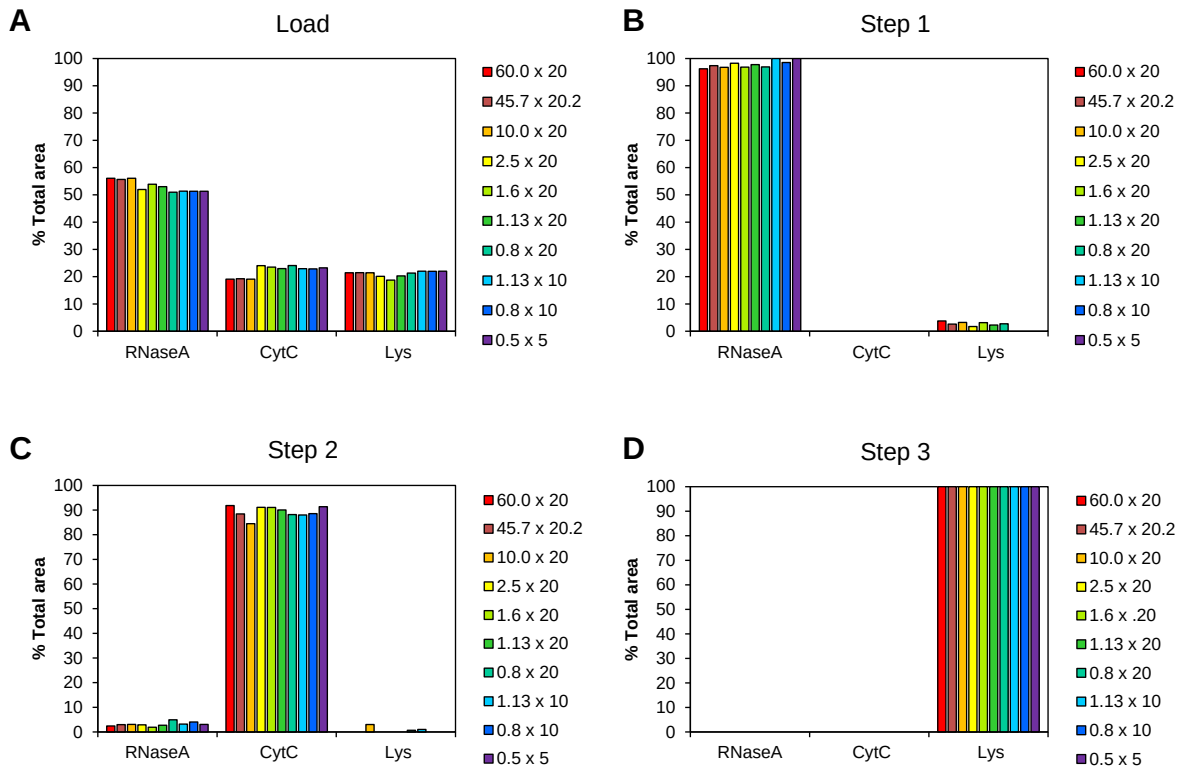

386

387 *Figure 6 Quantification of the purity by RP-HPLC of the loads and the three step gradient elution pools from the*
388 *separation of lysozyme, cytochrome c and ribonuclease A for all pre-packed columns assessed.*

389

5 Conclusions

The successful scale-up of industrial protein chromatography with pre-packed chromatography columns from laboratory scale for process development up to large scale for cGMP manufacturing was demonstrated. The uniformity of the column packing across the range of column sizes was confirmed with acetone pulses, which are very susceptible to changes in the packing structure. The acetone pulse injections provided conformation that all columns for each scale were packed to the same quality attributes measured by HETP and asymmetry. To prove that columns were acceptable for practical protein separation processes, we performed breakthrough curves as well as protein separation experiments using a stepwise gradient approach. Equilibrium and dynamic binding capacities for a model protein showed only slight variations with scale. These variations are explained by small changes in the salt concentration of the loading buffer. A mixture of three proteins was separated by step gradient method utilizing the same conditions at each column scale. The purity of the elution pool, from each of the three gradient steps, was equivalent across all column scales despite retention time and peak width differences. These differences were due to variance in the sharpness of the conductivity change attributed to mixing and extra column effects more prominent with small scale columns. In conclusion, the evaluated pre-packed preparative chromatography columns are packed consistently and reproducibly across all scales, from 0.5 cm x 5cm (1 mL) to 60 cm x 20 cm (57 L) packed bed volume. They can be used to develop and scale protein separation process from lab to production scale.

Acknowledgements

This work has been supported by the Federal Ministry of Science, Research and Economy (BMWFW), the Federal Ministry of Traffic, Innovation and Technology (bmvit), the Styrian Business Promotion Agency SFG, the Standortagentur Tirol, the Government of Lower Austria and ZIT - Technology Agency of the City of Vienna through the COMET-Funding Program managed by the Austrian Research Promotion Agency FFG.

References

[1] D. Low, R.O. Leary, N.S. Pujar, Future of antibody purification, J. Chromatogr. B. 848 (2007) 48–63. doi:10.1016/j.jchromb.2006.10.033.

[2] P. Rogge, D. Müller, S.R. Schmidt, The Single-Use or Stainless Steel Decision Process, BioProcess Int. 13 (2015) 10–15.

[3] R. Jacquemart, M. Vandersluis, M. Zhao, K. Sukhija, N. Sidhu, J. Stout, A Single-use Strategy to Enable Manufacturing of Affordable Biologics, Comput. Struct. Biotechnol. J. 14 (2016) 309–318. doi:10.1016/j.csbj.2016.06.007.

[4] C. Scott, The latest single-use solutions for downstream processing, BioPharm Int. 15 (2017) 1–5.

[5] E. Langer, Innovation in Pre-packed Disposable Chromatography Columns, 2014. http://www.biopharminternational.com/innovation-pre-packed-disposable-chromatography-columns?pageID=1.

[6] F.G. Lode, A. Rosenfeld, Q.S. Yuan, T.W. Root, E.N. Lightfoot, Refining the scale-up of chromatographic separations, J. Chromatogr. A. 796 (1998) 3–14. doi:10.1016/S0021-9673(97)00872-8.

[7] O. Kaltenbrunner, A. Jungbauer, S. Yamamoto, Prediction of the preparative chromatography performance with a very small column, J. Chromatogr. A. 760 (1997) 41–53. doi:10.1016/S0021-9673(96)00689-9.

[8] N. Hutchinson, S. Chhatre, H. Baldascini, T. Place, B. Road, D.G. Bracewell, M. Hoare, Ultra Scale-Down Approach to Correct Dispersive and Retentive Effects in Small-Scale Columns When Predicting Larger Scale Elution Profiles, Biotechnol. Progr. 25 (2009) 1103–1110. doi:10.1021/bp.172.

[9] T. Scharl, C. Jungreuthmayer, A. Dürauer, S. Schweiger, T. Schröder, A. Jungbauer, Trend analysis of performance parameters of pre-packed columns for protein chromatography over a time span of ten years, J. Chromatogr. A. 1465 (2016) 63–70. doi:10.1016/j.chroma.2016.07.054.

[10] S. Schweiger, S. Hinterberger, A. Jungbauer, Column-to-column packing variation of disposable pre-packed columns for protein chromatography, J. Chromatogr. A. (2017). doi:10.1016/j.chroma.2017.10.059.

[11] S. Schweiger, A. Jungbauer, Scalability of pre-packed preparative chromatography columns with different diameters and lengths taking into account extra column effects, J. Chromatogr. A. (2018). doi:https://doi.org/10.1016/j.chroma.2018.01.022.

[12] S. Grier, S. Yakabu, Prepacked Chromatography Columns: Evaluation for Use in Pilot and Large-Scale Bioprocessing, BioProcess Int. 14 (2016).

[13] K. Treier, S. Hansen, C. Richter, P. Diederich, J. Hubbuch, P. Lester, High-Throughput Methods for Miniaturization and Automation of Monoclonal Antibody Purification Processes, Biotechnol. Progr. 28 (2012) 723–732. doi:10.1002/btpr.1533.

[14] A. Osberghaus, K. Drechsel, S. Hansen, S.K. Hepbildikler, S. Nath, M. Haindl, E. Von Lieres, J. Hubbuch, Model-integrated process development demonstrated on the optimization of a robotic cation exchange step, Chem. Eng. Sci. 76 (2012) 129–139. doi:10.1016/j.ces.2012.04.004.

[15] S.T. Evans, K.D. Stewart, C. Afdahl, R. Patel, K.J. Newell, Optimization of a micro-scale , high throughput process development tool and the demonstration of comparable process performance and product quality with biopharmaceutical manufacturing processes, J. Chromatogr. A. 1506 (2017) 73–81.

doi:10.1016/j.chroma.2017.05.041.

[16] A. Susanto, E. Knieps-Grünhagen, E. von Lieres, J. Hubbuch, High Throughput Screening for the Design and Optimization of Chromatographic Processes : Assessment of Model Parameter Determination from High Throughput Compatible Data, Chem. Eng. Technol. 31 (2008) 1846–1855. doi:10.1002/ceat.200800457.

[17] S. Gerontas, M. Asplund, R. Hjorth, D.G. Bracewell, Integration of scale-down experimentation and general rate modelling to predict manufacturing scale chromatographic separations, J. Chromatogr. A. 1217 (2010) 6917–6926. doi:10.1016/j.chroma.2010.08.063.

[18] A. Jungbauer, K. Graumann, The logistic dose-response function: A robust fitting function for transition phenomena in life sciences, J. Clin. Ligand Assay. 24 (2001) 270–274.

[19] O. Kaltenbrunner, A. Jungbauer, Simple model for blending aqueous salt buffers Application to preparative chromatography, J. Chromatogr. A. 769 (1997) 37–48.

SUPPLEMENTARY MATERIAL

PUBLICATION IV

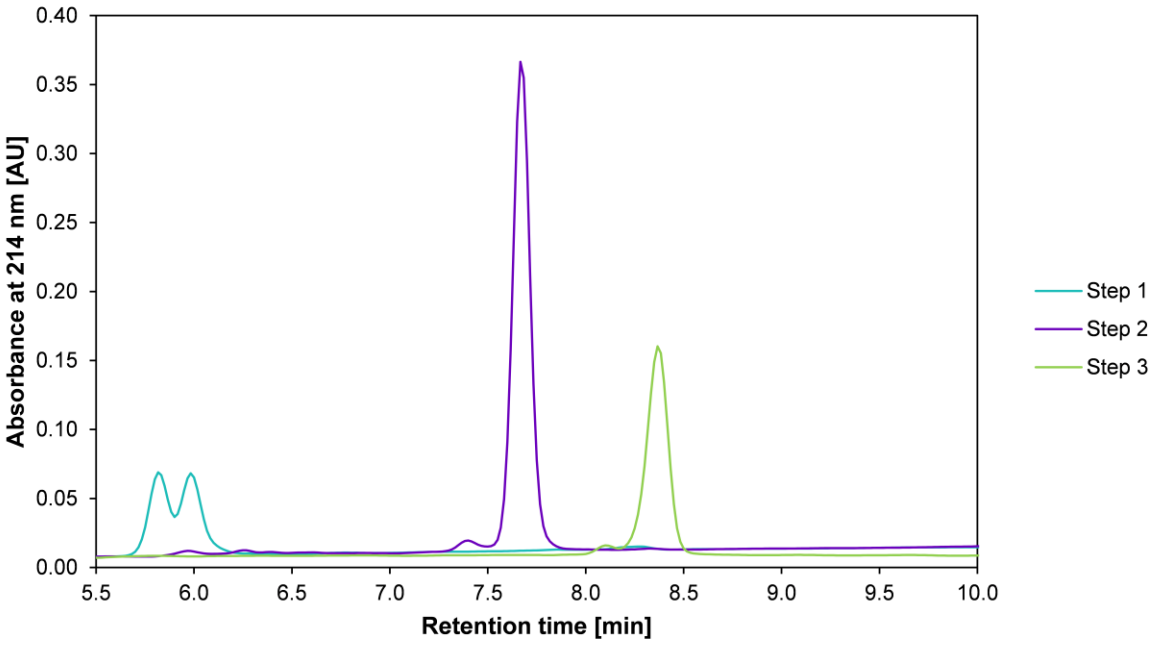

Fig. 1. Supplementary Material RP-HPLC chromatograms of one fraction of each of the steps, which contained the two protein isoforms. Ribonuclease A eluted in the first step, cytochrome C in the second and lysozyme in the third step, which also the order they elute from the HPLC columns. Each of the steps contained hardly any impurities of the other proteins, but some isoforms eluting close to the main peak.